Remediation of Cellulose Acetate Gas Separation Membranes Contaminated by Heavy Hydrocarbons

by

Charlie José Ulloa

A thesis
presented to the University of Waterloo
in fulfillment of the
thesis requirement for the degree of
Master of Applied Science
in
Chemical Engineering

Waterloo, Ontario, Canada, 2012

Author's Declaration

I hereby declare that I am the sole author of this thesis. This is a true copy of the thesis, including any required final revisions, as accepted by my examiners.

I understand that my thesis may be made electronically available to the public.

Abstract

Polymeric membranes have been essential to increasing the efficiency of membrane separation processes. The viability of membrane systems for industrial gas applications lies in the tolerance of such membranes to contamination. While membrane contamination from volatile species can be addressed using purge streams and heat treatment, contamination from non-volatile hydrocarbons can cause a significant decline in membrane permselectivity. This study was focused on the characterization and remediation of cellulose acetate (CA) hollow fibre membranes contaminated by heavy hydrocarbons.

CA membranes have a moderate resistance against performance decline from hydrocarbons found in natural gas. Hollow fibre CA membranes were coated with motor oil lubricant to simulate heavy hydrocarbon contamination from large-scale gas compressors and industrial feed streams, and remediation of the CA fibres was conducted using solvent extraction methods. The permeabilities of the membranes to carbon dioxide, helium, hydrogen, methane, nitrogen and oxygen were measured at pressures 300 – 1500kPa and at temperatures 25° – 50°C.

It was shown that even a thin layer of oil on the membrane surface can result in substantial losses in membrane performance, with faster permeating gases (e.g. He and H_2) suffering the worst losses. Solvent exchange, in which the membrane was washed using a series of solutions of varying organic content, was unable to remediate the membrane effectively, while the removal of the heavy hydrocarbons by a direct cyclohexane rinse was found to work well to restore the membrane performance.

Acknowledgements

I would like to sincerely thank Professor Xianshe Feng for his dedication to my supervision, his guidance throughout my research and his enthusiasm for what the field of membrane research has to yet to accomplish. I would also like to thank Dr Aiping Yu and Dr. Ali Elkamel for taking their time to review my thesis.

To Dr. Gil Francisco, for his practical manner and useful advice. To Shahabedin Eslami, whom I could always rely on for a helping hand. To the members of the Membrane Research Group, whose dedication and curiosity are to be admired; it has been a pleasure.

To Feng-Xuan Choo, for his technical insight and deadpan humour. To my graduate friends at Waterloo, for their unique perspectives on the place of science in this world.

To my dearest friend Yiyi Shangguan, whose inquiring mind and endless encouragement has been a gift to work with. Despite never finding that eclipse together, I'd say that searching for it was far more valuable.

I would like to thank my family for their encouragement and open-mindedness during the completion of this degree. I am especially grateful to my brother Michael, to whom I dedicate this thesis.

I would like to gratefully acknowledge the funding from the Natural Sciences and Engineering Research Council (NSERC), the Department of Chemical Engineering at the University of Waterloo and the Government of Ontario through the Queen Elizabeth II Graduate Scholarship in Science and Technology (QEII-GSST).

Table of Contents

List of Figures

List of Tables

Nomenclature

A	Effective membrane area [cm^2]
B	Bunsen coefficient
C	Concentration [mol/L]
D	Diffusion coefficient [m^2/s]
d	Diameter [cm]
E_A	Activation energy of diffusion [kJ/mol]
E_P	Activation energy of permeation [kJ/mol]
G	Overall solubility [mg/kg]
H	Henry's law constant [MPa·mol/mol]
ΔH_S	Enthalpy of dissolution
J	Flux [cm^3(STP)/cm^2·s]
L	Length [cm]
l	Total membrane thickness [μm]
L_O	Ostwald coefficient
M	Molar mass [g/mol]
N	Number of hollow fibres
P	Permeability [Barrer]
p	Feed pressure [kPa]
p_{baro}	Barometric pressure [kPa]
p_v	Vapour pressure [kPa]
Q	Permeance [GPU]
R	Resistance [Pa·s/mol]

R_G Gas constant [J/mol·K]

S Solubility coefficient [cm^3(STP)/cm^3·cmHg]

T Temperature [K]

t Time [s]

T_{amb} Ambient temperature [K]

T_C Critical temperature [K]

T_g Glass transition temperature [K]

V Volume [mL]

V_C Critical volume [mL]

V_{STP} Volumetric flowrate at STP [mL(STP)/s]

$\dot{V}$ Flowrate [mL/s]

X Mole fraction [mol/mol]

Greek lettering

α Ideal selectivity

ν kinematic viscosity [cSt, mm^2/s]

ρ Density [kg/m^3]

μ Chemical potential [J/mol]

δ Solubility parameter [$MPa^{1/2}$]

Acronyms

ASTM American Society for Testing and Materials

BTX Benzene, toluene, xylene

CA Cellulose acetate

STP Standard temperature and pressure (273.15K, 101.325kPa)

Chapter 1

Introduction

The application of membrane technology to industrial gas separation is currently a subject of intense research. Polymeric membranes are becoming more competitive with traditional cryogenic and absorption processes for gas separations, gaining greater acceptance in natural gas processing (Baker, 2008), hydrogen recovery (Kerry, 2007) and nitrogen production (Bernardo, 2009). Despite these advances, polymeric membranes remain susceptible to damage caused by high operating temperatures, harsh chemical conditions and contaminants in feed streams. Because of such limitations, of the hundreds of membranes developed in laboratories, only eight types of polymers are used industrially (Baker, 2008).

Hydrocarbon contaminants are present in a variety of industrial gas streams and can negatively affect the performance of a membrane. One of the largest applications of membrane gas separation today is in natural gas processing, where the feed streams often contain light-to-heavy hydrocarbons (Baker, 2008). The presence of light hydrocarbons in the carbon dioxide/methane feed streams has been shown to reduce the permeability and selectivity of both polyimide (Al-Juaied & Koros, 2006) and cellulose acetate membranes (Schell, 1989). Such contaminants are somewhat volatile and can be removed through the use of purge streams and temperature treatments, restoring membrane performance (Al-Juaied & Koros, 2006; Schell, 1989). While the effects of such contaminants are temporary, hydrocarbons with higher

molecular weights are usually non-volatile and can foul the surface of a membrane, reducing the lifespan of the membrane (Baker, 2008). The large-scale compressors used in gas processing can generate mists of aerated, oil-based, lubricants during operation, which may also contribute to this contamination (Majors, 2001).

To minimize contamination, most membrane processes employ various pre-treatment processes to remove particulates and condensable impurities from feed streams (Baker, 2008). A better control of the feed stream quality will improve the reliability of a membrane, although hydrocarbon contaminants in the feed are still believed to be the source of some membrane failures (Al-Juaied & Koros, 2006). To date, as far as we know, there has been no effective method reported in the literature to remove the hydrocarbon foulant from contaminated membranes in order to remediate the membrane performance.

1.1 Objectives

The focus of this thesis was to assess how the presence of heavy hydrocarbons affected the performance of gas separations and to determine if such contamination could be remediated. Cellulose acetate hollow fibre membranes were used as a model membrane because of their current use in natural gas processing and their resistance to benzene, toluene, and xylene (BTX) contamination (Schell, 1989). These hollow fibres were coated with a thin layer of motor oil lubricant to simulate heavy hydrocarbon contamination from large-scale gas compressors and industrial feed streams. Remediation of the membrane was conducted using a solvent exchange process because of the non-volatile nature of the contaminants. The hollow fibres were kept within their housing module during the remediation process to determine if the remediation could be conducted in a straightforward manner.

Gas permeation tests were conducted on the pristine, contaminated and remediated membranes at a variety of pressures and temperatures. The resistance models were used to estimate the gas transport properties of the lubricant. The permeability and selectivity of the membrane were used to evaluate the efficacy of the solvent exchange methods for remediation of contaminated membranes.

1.2 Thesis Outline

The theoretical aspects of membrane technology and gas separation are presented in Chapter 2. Factors affecting gas permeation such as pressure, temperature and contamination are discussed, and the resistance model is introduced in the context of contaminated membranes. Previous work regarding cellulose acetate gas separation membranes is also reviewed. Chapter 3 presents the experimental procedures used in this study, including membrane preparation, membrane contamination, gas permeation tests and contact angle measurements. Remediation methods based on solvent exchange are also presented in this chapter. Chapter 4 presents the results of this study, including the effects of heavy hydrocarbons on membrane performance, the estimated gas transport properties of heavy hydrocarbons and the efficacy of solvent extraction as a remediation method. Chapter 5 presents the general conclusions drawn from this study and offers recommendations for future work.

Chapter 2

Literature Review

The focus of this research was to determine the effects of heavy hydrocarbon contamination on the performance of polymeric gas separation membranes. This literature review covers the fundamentals of membrane transport theory as well as the current literature on contamination in gas separation processes. Using the mass transport models presented here, the separation performance of a membrane system is defined using the gas transport properties of the contaminant and polymer layers. Methods to remediate contaminated membranes using solvent exchange and solvent extraction are also discussed.

2.1 Overview of Membrane Separation Technology

Membranes are thin, semi-permeable barriers between two phases that allow for the selective permeation of certain chemical species while hindering others. Such separations are conducted under such a driving force as an electrical or chemical potential difference across the membrane. Changes in chemical potential ($\Delta\mu$) are often induced by creating gradients in concentration (ΔC), pressure (ΔP) and temperature (ΔT) across the membrane layer, as seen in Figure 2.1 (Mulder, 1991).

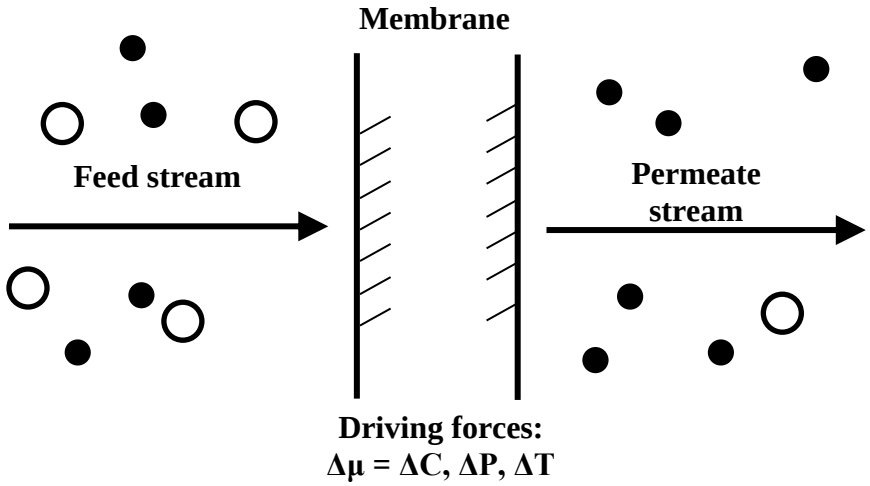

Figure 2.1: Basic schematic of membrane permeation (Mulder, 1991).

Membranes can be constructed out of a variety of materials depending on the requirements of the separation. Generally speaking, synthetic membranes can be composed of both inorganic and organic materials, with most gas separation membranes constructed out of organic polymers. Polymeric membranes are often favored due to their ease of production, reproducibility and low cost (Bernardo, 2009). One classification scheme by Pinnau & Freeman (2000) categorizes synthetic membranes based on their geometries, morphological structures and applications.

Polymeric membranes can take different geometries depending on their application. Flat-sheet membranes are simple to manufacture and can be used in a plate-and-frame or spiral-wound configuration (Baker, 2004c). Hollow fibre membranes must be produced through an extrusion process that requires specialized machinery and rigorous quality control (Baker, 2004c). The cylindrical structure of hollow fibre membranes allows for a much greater area-to-volume ratio than flat-sheet membranes. Most membrane gas separation processes use hollow fibres and spiral-wound membrane configurations (Baker, 2004c). The small volume, easy

installation and low maintenance of such membrane units are ideal for remote locations. The modular aspect of the membrane units also allows for a straightforward scale-up if greater flowrates or multiple separations are required (Bernardo, 2009).

The application and performance of a given polymeric membrane is highly dependent on its macromolecular structure. Depending on the fabrication method, a variety of membrane morphologies can be produced, as shown in Figure 2.2.

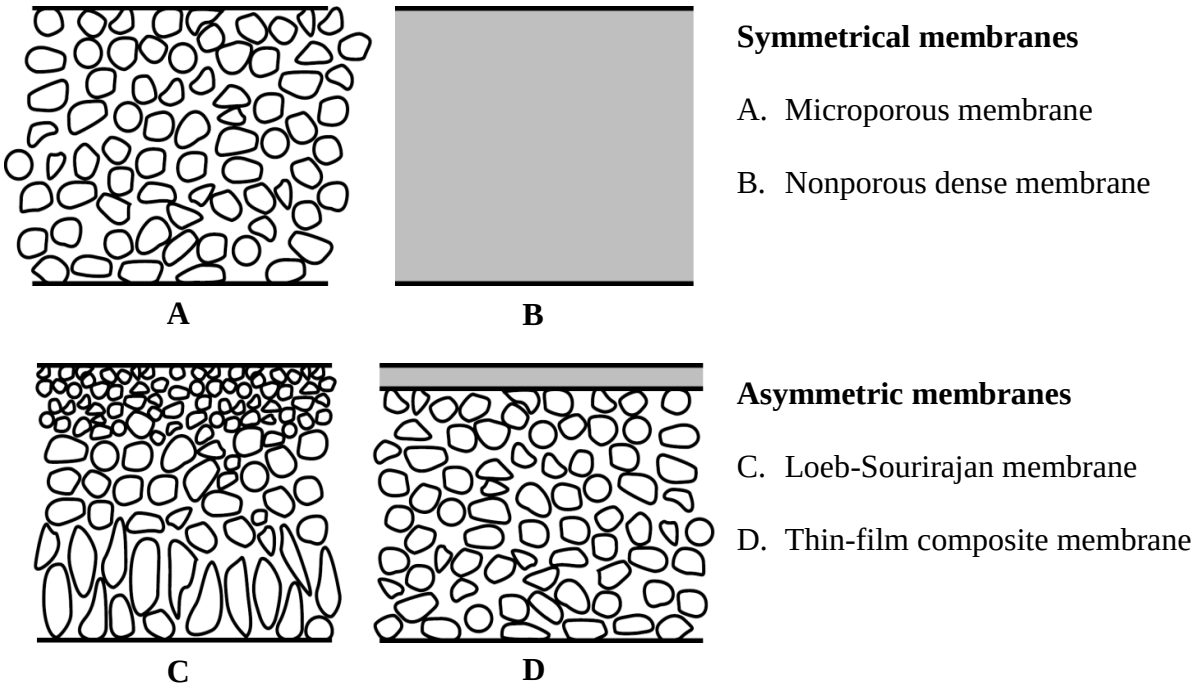

Figure 2.2: Morphologies of polymeric membranes (Baker, 2004d).

Symmetrical membranes have a uniform morphology. Microporous membranes have macro-voids that allow the passage of smaller penetrants, and the porosities of such membranes may be tailored to suit the separation required (Baker, 2004d). Alternatively, dense membranes have no discernible pore structure, and separation occurs by diffusion through the membrane which is governed by the chemical interactions between the polymer and the penetrant (Wijmans

& Baker, 2006). Decreasing the thickness of the membranes can produce a higher permeation flux, although if the membrane is too thin, the driving force of the separation may cause the membrane to break and fail.

Anisotropic membranes may be used to maximize the permeation flux while retaining a suitable selectivity. Such membranes are composed of a thin, selective layer overtop a microporous support layer. The support layer must be porous enough so as not to hinder the transport of penetrants, yet rigid enough to withstand the driving forces of the separation (Baker, 2004c). Loeb-Sourirajan membranes are formed by a controlled precipitation of a polymer out of solution, creating a thin selective layer (500-2000Å thick) and a microporous substructure (50-200μm thick) out of the same material (Al-Juaied & Koros, 2006). The first Loeb-Sourirajan membranes were formed using cellulose acetate; an in-depth discussion regarding their fabrication will be discussed in Section 2.4. Despite having desirable separation properties, certain polymers may not be able to form the asymmetric structures required for practical Loeb-Sourirajan membranes (Baker, 2008). Instead, these polymers can be used to fabricate composite membranes, which employ a greater range of materials by coating a pre-assembled microporous support layer with a polymer of choice (Baker, 2004c).

There are a variety of applications that employ membrane technology for fluid separations. Microfiltration and ultrafiltration membranes have been used by industry for over three decades and are most often used to filter particulates from liquids streams (Baker, 2004d). Reverse osmosis membranes are most commonly used to purify water, with more recent applications involving the separation of liquid organic mixtures (Baker, 2004d). Gas separation and pervaporation membranes are relatively recent developments in the field of membrane technology, involving separations of gaseous and liquid mixtures, respectively (Baker, 2004d).

2.2 Membrane Transport Theory

There are two main models used to describe mass transport through membranes. The first is the pore-flow model, which assumes that penetrants are transported across the membrane through distinct pores in the polymer matrix. Separation of mixtures is based on size exclusion, with smaller particles passing through the membrane more readily than larger particles. (Baker, 2004d). The pore size of the membrane is adjusted to suit the level of filtration required.

When the pore size required for separation falls below 5-10 angstroms, the chemical interactions between the penetrant and membrane begin to govern mass transport (Wijmans & Baker, 2006). In this scenario, mass transport can be described using the solution-diffusion model. This model consists of three basic steps, as shown in Figure 2.3:

1. The penetrant is sorbed onto the surface of the membrane from the feed stream;
2. The penetrant diffuses through the membrane; and
3. The penetrant is desorbed and leaves the membrane surface into the permeate stream (Wijmans & Baker, 2006).

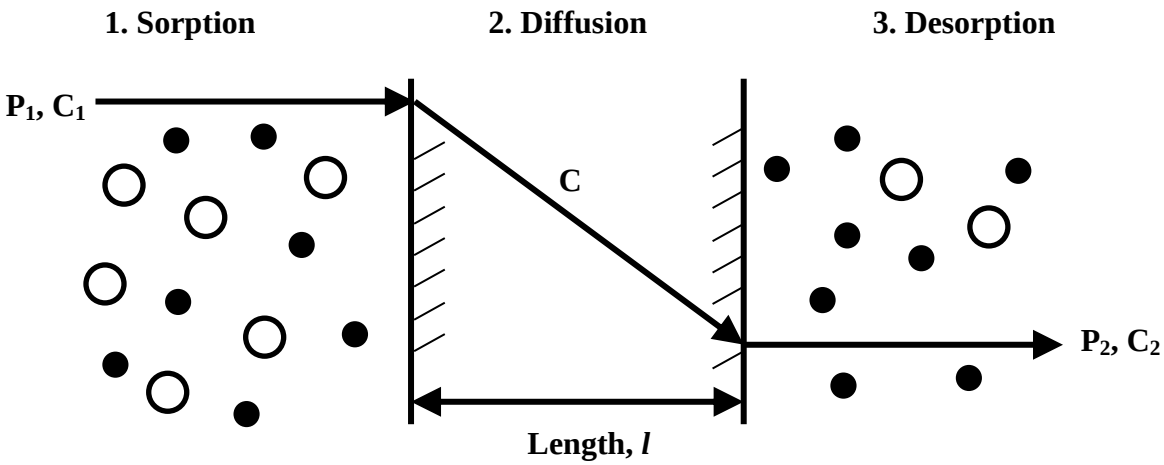

Figure 2.3: Gas transport through a polymeric membrane.

Gas transport through membranes is described using the solution-diffusion model due to the small size of the penetrating molecules (Baker, 2004a). The driving force for gas permeation is caused by a pressure differential between the feed and permeate streams (Mulder, 1991). Once permeation reaches a steady state, the polymer-gas boundaries can be assumed to be at thermodynamic equilibrium (steps 1 and 3). Thus, the rate of gas transport is determined by diffusion through the membrane (step 2), which can be described by the Fick's first law:

$$J = -D\frac{dC}{dx} \tag{2.1}$$

where D is the diffusion coefficient of the penetrant in the membrane, C is the concentration of the gas in the membrane, and *x* is the distance across the membrane. If the solubility of the gas in the polymer is low, the concentration of the gas in the polymer can be considered to the proportional to pressure, similar to the Henry's law (Matteucci *et al.*, 2006):

$$C = \frac{1}{H} \cdot p = S \cdot p \tag{2.2}$$

where H is the Henry's Law constant and S is the solubility constant. Substituting Equation 2.1 into Equation 2.2:

$$J = -D \cdot S\frac{dp}{dx} \tag{2.3}$$

Integrating p from p_1 to p_2 and *x* from 0 to thickness *l*:

$$J = \frac{-D \cdot S \cdot \Delta p}{l} = \frac{-D \cdot S \cdot (p_2 - p_1)}{l} \tag{2.4}$$

Equation 2.4 can be simplified further by introducing the permeability coefficient (P), an inherent property of a membrane material, defined as:

$$P = D \cdot S \tag{2.5}$$

Defining gas transport properties using Equation 2.5 works well for rubbery polymers and allows for approximate descriptions of gas transport in glassy polymers at high pressures (Baker, 2004b). By substituting Equation 2.5 into Equation 2.4, the permeability coefficient can be defined as the gas flux normalized by the membrane thickness and the pressure differential:

$$P = \frac{J}{\Delta p / l} \tag{2.6}$$

Equation 2.6 can be used to determine intrinsic gas transport properties of a membrane using measurable properties. When the thickness of the membrane's selective layer cannot be accurately determined, as is often the case with asymmetric membranes, the permeance (Q) can be used instead, as defined in Equation 2.7:

$$Q = \frac{J}{\Delta p} \tag{2.7}$$

By convention, the units for permeability and permeance are the Barrer and GPU (gas permeance unit), respectively:

$$1\ Barrer = 1 \times 10^{-10} \frac{cm \cdot cm^3(STP)}{cm^2 \cdot s \cdot cmHg}, \qquad 1\ GPU = 1 \times 10^{-6} \frac{cm^3(STP)}{cm^2 \cdot s \cdot cmHg}$$

The extent to which the membrane material is selective to one chemical species over another is referred to as the ideal selectivity (α). Depending of the type of polymer, a membrane may be more selective based on the relative differences in a penetrant's solubility (solubility-selectivity) or diffusivity (diffusivity-selectivity), as seen in Equation 2.8.

$$\alpha_{i/j} = \frac{Q_i}{Q_j} = \frac{(P_i/l)}{(P_j/l)} = \frac{P_i}{P_j} = \left(\frac{D_i}{D_j}\right) \cdot \left(\frac{S_i}{S_j}\right) \tag{2.8}$$

An ideal membrane would have both a high permeability and high selectivity. There is generally a trade-off between these two properties in polymeric membranes, with the least

permeable membranes also often being the most selective (Robeson, 1991). To help address this problem, gas separation membranes are manufactured to be as thin as possible in order to increase the overall gas flux. Any defects in the membranes (such as a pinhole) can be detected by comparing the selectivity of the membrane to the intrinsic values found in literature, such as the selectivity between oxygen (O_2) and nitrogen (N_2).

2.3 Factors Affecting Gas Transport

2.3.1 Polymer-Penetrant Interactions

The operating temperature affects the gas permeation in polymers. Polymers that exist above their glass transition temperature (T_g) are considered to be in a rubbery state; polymers below this temperature are considered to be in a glassy state. The polymer chains of glassy polymers are generally constrained in their movement, with individual segments unable to rotate freely around their bonds or overcome intermolecular forces (Mulder, 1991). Gas permeation through these polymers is mainly governed by the diffusivity of the penetrants through the rigid polymer structure, a kinetic property (Matteucci *et al.*, 2006). Conversely, the chain segments of rubbery polymers are allowed to move more freely and rotate around their bonds, allowing for a greater free volume within the membrane structure (Mulder, 1991). Gas transport through rubbery polymers is mostly related to the solubility of the penetrants, a thermodynamic property (Matteucci *et al.*, 2006). Due to their rigid structure, glassy polymers are generally more stable than rubbery polymers at higher temperatures and pressures (Bernardo, 2009). Rubbery polymers generally have higher permeabilities than glass polymers due to their greater free volume (Matteucci *et al.*, 2006). The polymer used in this study, cellulose acetate, is considered to be a glassy polymer for the temperature range studied.

The solubility of a penetrant into a membrane is mainly affected by its condensability. Penetrants with higher boiling points (T_b) and critical temperatures (T_c) have been found to be more soluble in polymeric materials (Matteucci *et al.*, 2006). Therefore, non-condensable gases such as helium (He) and hydrogen (H_2) have relatively lower permeabilities in rubbery polymers than such condensable gases as methane (CH_4) and carbon dioxide (CO_2). This can be seen from the values in Table 2.1. When a strongly sorbing penetrant dissolves into a polymer, such as CO_2, the polymer may swell, resulting in plasticization of the membrane (Donohue *et al.*, 1989; Sanders, 1988; Visser *et al.*, 2005). Membrane swelling increases the diffusivity of all penetrants, thereby increasing the overall permeability of the membrane while reducing its selectivity.

Table 2.1: Physical properties of the gases used in this study.

Gas	**T_c [a] [K]**	**T_b [a] [K]**	**V_c [a] [cm^3/mol]**	**d_k [b] [Å]**
N_2	126.2	77.35	90.1	3.64
CH_4	190.56	111.66	98.6	3.8
O_2	154.58	90.17	73.37	3.46
CO_2	304.12	–	94.07	3.3
H_2	32.98	20.27	64.2	2.89
He	5.19	4.3	57.3	2.6

[a] (Poling *et al.*, 2001), [b] (Breck, 1974).

The diffusivity of a penetrant through a polymer is mainly related to its size and shape, with larger molecules diffusing more slowly (Matteucci *et al.*, 2006). Diffusivity is often correlated to the kinetic diameter (d_K) of the penetrant, although its critical volume (V_C) can also be used if d_K is not available (Matteucci *et al.*, 2006). In the absence of plasticization, diffusivity

is independent of gas concentration and pressure (Matteucci *et al.*, 2006). The diffusivity-selectivity is much lower in rubbery polymers than in glassy polymers due to their greater free volume, as illustrated in Figure 2.4.

Current models predicting gas transport properties within a polymer are usually restricted to a specific group of polymers. Most gas separation experiments determine the permeability (P) of a polymer and then measure either the diffusivity (D) or the solubility (S) of the penetrant gas, using Equation 2.5 to back-calculate the remaining transport term (Matteucci *et al.*, 2006). The above concept of diffusion and solubility through a polymer may also relate to gas transport through liquid membranes in the absence of complex transport mechanisms, such as facilitated transport (Noble & Koval, 2006).

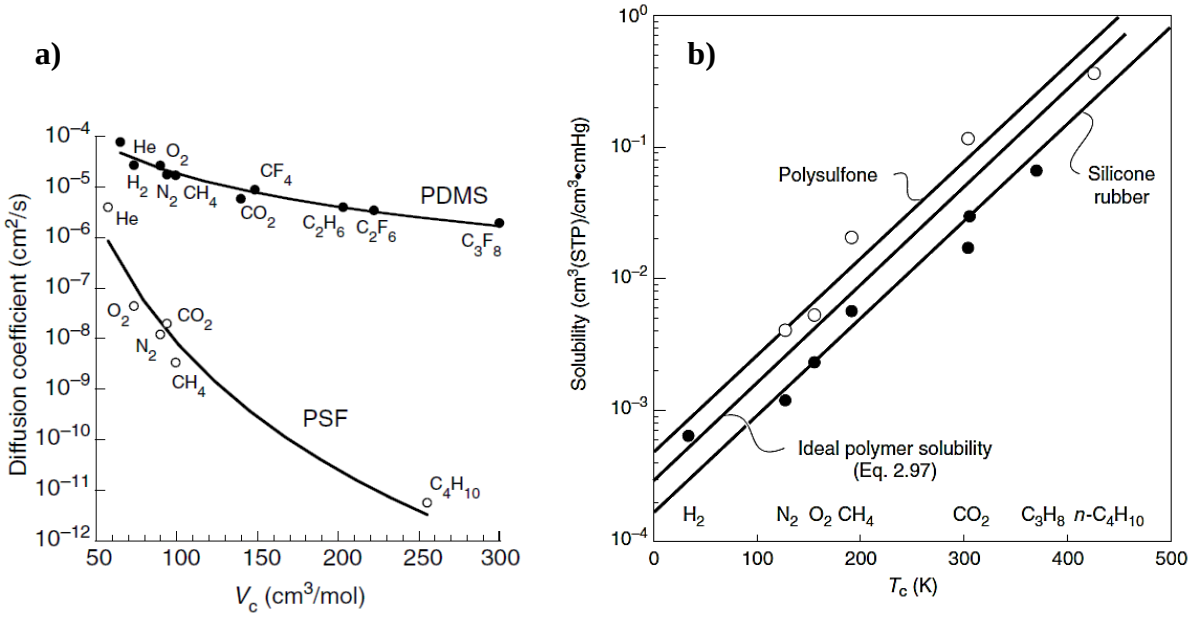

Figure 2.4: Dependence of a) diffusivity and b) solubility coefficients based on gas transport properties in polydimethylsiloxane (PDMS) and polysulfone (PSF). PDMS data was taken from (Merkel *et al.*, 2000) and PSF data was taken from (Ghosal *et al.*, 1996).
The graphs were arranged by Matteucci *et al.* (2006).

Gas transport through glassy polymers may decrease over time due to aging and compaction. Since the structure of a glassy polymeric membrane is relatively rigid, any free volume in the polymer network created during its fabrication is frozen into the membrane morphology (Pfromm, 2006; Struik, 1978). Over time, these voids are filled in by the segmental motion of polymer chains, compacting the polymer structure and reducing its permeability to gases (Huang & Paul, 2004; Rowe *et al.*, 2010). Although the aging of glassy polymers may take years to reach equilibrium, as shown by Rowe *et al.* (2010), the most significant effects of aging take place within months of the membrane's manufacture, after which membrane compaction is no longer a significant effect. This study uses cellulose acetate hollow fibres that have been aged for over 2 years to avoid significant aging effects which can cause scatter in gas permeation measurements.

2.3.2 Feed Pressure

The effect of pressure on the permeability of gases is dependent on the diffusivity and solubility of the penetrants. As stated above, the diffusivity of gases in glassy polymers is relatively independent of pressure (Matteucci *et al.*, 2006). The concentration of gases in polymers increases proportionally to pressure, implying that the solubility coefficient is constant. This proves to work quite well for rubbery polymers and glassy polymers at high pressures (Baker, 2004b). Constant values for both the diffusivity and solubility coefficients in glassy polymers means that the permeability of gases are relatively independent of pressure, as shown by Sidhoum (1988) and Puleo *et al.* (1989) for cellulose acetate membranes above 300kPa for CH_4, H_2, He, N_2 and O_2.

There are a few exceptions to this behaviour. At very low pressures, the concentration of gases in glassy polymers, including cellulose acetate, tends to follow a Langmuir-type isotherm with increasing pressure (Matteucci *et al.*, 2006; Puleo *et al.*, 1989). The operating pressures used in this study were kept high enough to ignore this effect. Also, plasticization from highly sorbing gases, such as CO_2, will cause an increase in the diffusivity with increasing pressure, as shown in literature (Donohue *et al.*, 1989; Sanders, 1988; Visser *et al.*, 2005).

2.3.3 Operating Temperature

When the temperature increases, the polymer segments gain additional kinetic energy to move and rotate within the polymer structure. While these movements are still relatively restrained in glassy polymers, the larger segmental motion of the polymer chains can strongly affect gas diffusion through the polymer. This change in permeation through a polymeric membrane in relation to temperature can be described using the Arrhenius relationship (Ghosal, 1994):

$$P = P_0 e^{\frac{-\mathrm{E_P}}{R_G T}} \tag{2.9}$$

where P_0 is the pre-exponential factor, E_p is the activation energy of permeation and R_G is the gas constant. The above relationship assumes that no substantial morphological changes occur in the polymer during a temperature change, such as the polymer passing through its T_g. Using the solution-diffusion model, Equation 2.9 can be further described in terms of diffusivity and solubility (Ghosal, 1994; Petropoulos, 1994):

$$P = D_0 S_0 e^{\frac{-(E_D + \Delta H_S)}{R_G T}} = D_0 e^{\frac{-\mathrm{E_D}}{R_G T}} \times S_0 e^{\frac{-\Delta H_S}{R_G T}},\ E_P = E_D + \Delta H_S \tag{2.10}$$

where D_0 and S_0 are the pre-exponential factors for diffusion and sorption, respectively, E_D is the activation energy for diffusion and ΔH_S is the enthalpy of dissolution. The value of E_D is usually positive since diffusivity increases with temperature (Ghosal, 1994). Any increase in diffusivity typically results in greater transport gains for larger penetrants, which implies that the selectivity of glassy membranes will tend to decrease at higher operating temperatures (Ghosal, 1994). The value of ΔH_S is dependent on the polymer-penetrant interactions and is usually negative for strongly sorbing penetrants, meaning that an increase in temperature will generally lead to a decrease in solubility (Matteucci *et al.*, 2006).

2.3.4 Contamination

Despite the superior transport properties of newer membrane materials, gas separation membranes often perform poorly outside of laboratory conditions. This is commonly attributed to undesired interactions with contaminants found in industrial gas streams, which can often result in a reduction in flux and selectivity (Bernardo, 2009). Of particular concern are the heavy hydrocarbon contaminants found in natural gas streams and lubricant mists from the gas compressors (Al-Juaied & Koros, 2006).

As most gas separation processes operate at elevated pressures, the use of gas compressors may present a concern if the mechanical lubricant is carried over by the gas into downstream membrane processes. The lubricant oil serves to disperse heat, reduce friction and prevent corrosion of the mechanical parts within the compressor (Majors, 2001). During regular operation, lubricant may be aerated into the pressurized gas to the extent that filtration systems are often required to collect and recirculate any aerated oil (Brown, 1997). Anti-foaming agents can be added to the lubricant to prevent aeration, while molecular sieves, knockout traps and

aftercoolers can be used to filter the exiting gas stream (Majors, 2001). The additional cost of these filtration systems may be necessary in membrane processes since even minute amounts of heavy hydrocarbons can adversely affect membrane performance (Baker, 2008). The issue of lubricant contamination can be circumvented with the use of non-lubricated compressors, although such compressors are usually unsuitable for large, steady flowrates (Danielson, 2001).

One of the largest industrial gas separation processes today is the sweetening of natural gas. As of 2008, membrane technology had only a 5% share of this industry, although this value is expected to rise with the advance of membrane technologies (Baker, 2008). The exact composition of a natural gas depends on its source, and processing the raw feed streams requires the removal of the 2-10% carbon dioxide along with small amounts of moisture, hydrogen sulfide and inert gases (Hugman *et al.*, 1990). Most of these natural gas feeds also carry varying amounts of light-to-heavy hydrocarbons which can adversely affect gas separation membranes (Baker, 2008). Schell (1989) has shown that cellulose acetate membranes preform quite well in the presence of BTX compounds (benzene, toluene, xylene), and are currently the most commonly used membrane in natural gas processing aside from polyimides, as shown in Table 2.2. Coalescing filters, molecular sieves and refrigeration units can be employed to pre-treat inlet streams to ensure membrane stability over a 2-5 year service life (Baker, 2008).

Table 2.2: Membranes used in natural gas processing (Baker, 2008).

Company	Gas Separation	Module Type	Polymer
Medal (Air Liquide)	CO_2	Hollow-fibre	Polyimide
W.R. Grace	CO_2	Spiral-wound	Cellulose acetate
Separex (UOP)	CO_2	Spiral-wound	Cellulose acetate
Cynara (Natco)	CO_2	Hollow-fibre	Cellulose acetate
ABB/MTR	CO_2, N_2, C_{3+} hydrocarbons	Spiral-wound	Perfluoro polymers, silicone rubber
Permea (Air Products)	Water	Hollow-fibre	Polysulfone

Despite the various pre-treatment methods, hydrocarbon contamination is still suspected to be the cause of lowered membrane performance and failure (Al-Juaied & Koros, 2006). Light hydrocarbons ($<C_7$) can be soluble in glassy polymers, causing plasticization of the membrane. Al-Juaied & Koros (2006) showed that a 200psi, 10/90 CO_2/CH_4 feed stream travelling through a polyimide membrane experienced a 20% reduction in permeability when the feed was saturated with toluene or n-heptane. This drop in performance was attributed to the competition between the penetrants for sorption sites on the membrane surface. A similar study by White (1995) showed that at higher pressures (>1000psi), both toluene and n-hexane could plasticize a polyimide membrane, increasing the permeation flux while also reducing selectivity. In both studies, the original membrane performance was restored some time after the contaminants were removed. CA membranes have been shown to be somewhat resistant to hydrocarbon contamination, as was demonstrated in a study by Schell (1989) in which a 6/94 CO_2/CH_4 feed stream saturated with BTX vapours produced only minor drop (<10%) in overall gas flux and CO_2/CH_4 selectivity. The original permeation values were restored once the contaminants were removed from the feed stream.

In certain scenarios, the removal of a contaminant from the feed stream does not restore the original permeance and selectivity of the membrane. This effect is referred to as 'conditioning,' and is caused by an increase in the free volume left by the sorbing component in a glassy polymer (Al-Juaied & Koros, 2006; Rowe *et al.*, 2010). This additional free volume results in an increase in diffusivity and a reduction in the selectivity of a membrane. Since glassy polymers are usually in a state of non-equilibrium, over time, the conditioning will reverse itself as the polymer ages (Rowe *et al.*, 2010). Conditioning can be caused by exposure of highly plasticizing gases such as CO_2 and toluene (Al-Juaied & Koros, 2006). Similar effects have also been found when exposing glassy polymers to hexane vapour (Enscore *et al.*, 1977) and water vapour (Rowe *et al.*, 2007).

In the case of heavy hydrocarbons, allowing the condensation or fouling of materials on the membrane surface can results in severe performance losses. White (1995) demonstrated that in the presence of naphthalene, polyimide membranes will eventually shut down over time. The complete coverage of the membrane by naphthalene limits available sorption sites for permeating gases, steadily reducing gas transport. Jones and Koros (1994) found similar effect for carbon molecular sieve membranes in the presence of C_{6+} compounds. Where possible, the temperature of the separation process can be raised to ensure that feed contaminants are above their dew point to prevent any condensation, although this generally lowers the selectivity of the membranes and would not be effective against non-volatile contaminants (Baker, 2008).

2.4 Membrane Remediation

While purge streams, heat treatment and other industrial regeneration methods may not be suitable for a membrane contaminated with heavy hydrocarbons, solvent extraction may

prove to be a useful alternative. In this study, it was proposed that solvent extraction could be used to remove heavy hydrocarbon contamination without hindering membrane performance. Furthermore, it was proposed that any performance decline caused to the membrane structure by heavy hydrocarbons could be reversed by using a regeneration method that could restore the structure of an asymmetric membrane to its pristine state by mimicking the drying methods used to create gas separation membranes.

The Loeb-Sourirajan method, also known as the 'phase inversion process', was first developed in the 1960's to fabricate asymmetric membranes for desalination (Loeb & Sourirajan, 1963). A solution containing the dissolved polymer is cast into a film and then immersed into a non-solvent, usually water, causing the precipitation of the polymer solution. This immersion causes the outer surface of the film to precipitate more rapidly than the portion underneath, creating a membrane with a thin, dense outer layer supported on a porous substructure, as illustrated in Figure 2.2 (Baker, 2004c). By controlling drying conditions and rates of precipitation, a variety of membrane morphologies can be produced.

Asymmetric membranes used for gas separation must be dried using a solvent exchange method. If a membrane is allowed to dry completely after being immersed in water, the vaporizing water molecules may cause a compaction of the membrane structure, reducing the membrane's performance. The high surface tension of the water paired with the small pore size of the membrane substructure creates large capillary forces that can result in the collapse of the membrane substructure as it dries (Baker, 2004a; Park *et al.*, 1999). To circumvent this problem, the water-soaked membrane is placed into additional solvent baths to remove the water. Solvents with a lower surface tension than water, such as alcohols or alkanes, are used to replace water and allow the membrane to dry without severely collapsing the membrane structure. The solvent

exchange method was first invented in the late 1960s and early 1970s (MacDonald & Pan, 1974; Manos, 1978; Merten *et al.*, 1968).

Minhas *et al.* (1987) developed a solvent exchange protocol to dry cellulose acetate membranes by sequentially immersing the membranes into solutions of decreasing water content. Wet membranes were first placed into an aqueous solution containing 25v% water-miscible solvent (i.e., an alcohol). The membranes were subsequently rinsed in 50%, 75% and 100% solutions of the water-miscible solvent. The membranes were then rinsed with a secondary, non-polar solvent and then allowed to dry. This study concluded that using isopropyl alcohol and hexane as the primary and secondary solvents and then drying the membrane at 80°C produced cellulose acetate membranes with the best selectivity (Minhas *et al.*, 1987). Similar methods have been used to produce many industrial gas separation membranes that are currently in use (Baker, 2004c). This study attempts to use a similar solvent exchange process to remediate contaminated membranes.

An ideal gas separation membrane has a thin asymmetric layer that allows for a high gas flux, supported by a microporous layer that does not substantially affect gas transport. The choice of solvents used for precipitating and drying these membranes largely determines the membrane structure. These effects were shown by Hao & Wang (1998) who controlled the rate of precipitation of CA membranes out of water using various alcohols. They found that using solvents with higher molecular weights resulted in membranes precipitating out of solution more slowly, causing thicker selective layers and denser substructures. This, in turn, reduced the permeability and selectivity of the membrane. Similar effects regarding substructure resistance have been found in the development of CA hollow fibres (Shieh & Chung, 1998), polysulfone membranes (Pinnau, 1992) and polyetherimide membranes (Huang & Feng, 1993). Ensuring that

the solvent extraction process does not negatively impact the microporous support layer in the same manner is imperative to developing a practical remediation method.

2.5 Resistance Model

According the resistance model, gas transport through a membrane can be modelled after the flow of electricity through a circuit, as first suggested by Henis and Tripodi (1981). Using an analog of Ohm's law, the total flowrate though a membrane can be defined as the driving force of permeation (Δp in this case) over the resistance towards gas transport:

$$J \cdot A = \frac{\Delta p}{R} \quad \rightarrow \quad Q \cdot A = \frac{1}{R} \tag{2.11}$$

where R is the resistance, and A is the effective membrane area. The larger the resistance is for a particular penetrant, the greater the barrier to gas transport through the membrane. As with resistors in series, the total resistance across a membrane can be described as the combined resistance of its constituent layers, as shown in Equation 2.12:

$$R_{Total} = R_1 + R_2 + R_3 = \frac{1}{Q_1 \cdot A_1} + \frac{1}{Q_2 \cdot A_2} + \frac{1}{Q_3 \cdot A_3} \tag{2.12}$$

In this study, the penetrants can be described as travelling through the lubricant layer (R_1), the selective layer of the membrane (R_2) and the microporous support layer of the membrane (R_3), as shown in Figure 2.5.

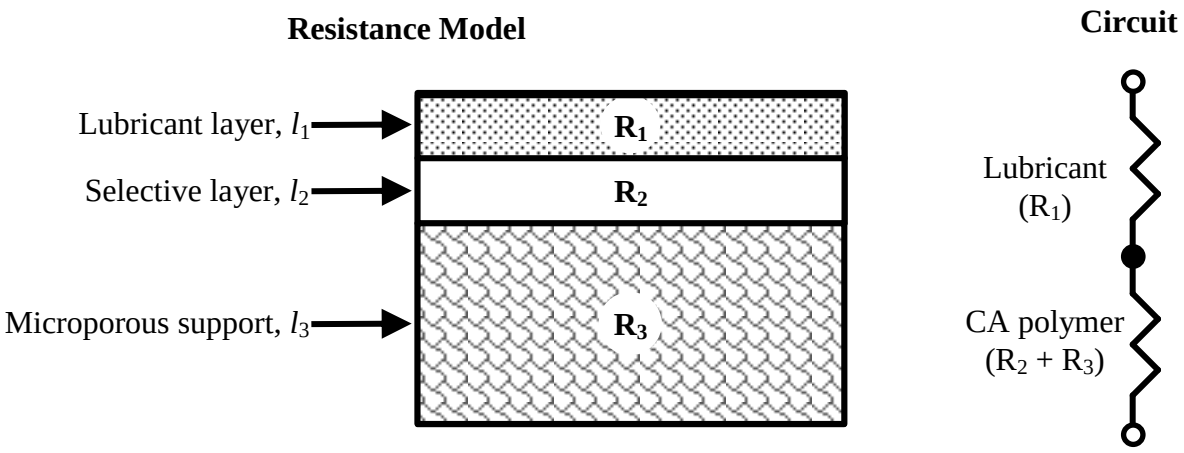

Figure 2.5: Resistance model through a contaminated asymmetric membrane.

By determining the resistance of the membrane to each component, the overall permeation properties of each layer can be evaluated separately. It should be noted that the values of resistance are not normalized against membrane thickness, and are therefore sensitive to the thickness of each layer. The selectivity of the membrane can now be expressed as:

$$\alpha_{i/j} = \frac{R_j}{R_i} = \frac{(R_1+R_2+R_3)_j}{(R_1+R_2+R_3)_i} = \frac{\left(\frac{l_1}{P_1}+\frac{l_2}{P_2}+\frac{l_3}{P_3}\right)_j}{\left(\frac{l_1}{P_1}+\frac{l_2}{P_2}+\frac{l_3}{P_3}\right)_i} \tag{2.13}$$

By increasing the thickness or decreasing the permeance of any given layer, the resistance of that layer will increase. It may be estimated that if the resistance of the selective layer is greater than the resistance of the microporous support by a factor of 10 ($R_2/R_3 > 10$), a pristine membrane should perform at 90% of its intrinsic selectivity (Pinnau, 1991). Therefore, any change to the membrane morphology (R_2, R_3) or the addition of a resistive lubricant layer (R_1) could significantly impact membrane performance.

Gas transport through the microporous support layer (R_3) has been shown to follow a pore-flow behaviour similar to Knudsen diffusion, which separates the penetrants based on their molecular weight, as seen in Equation 2.14 (Pinnau, 1991; Pinnau, 1992; Shieh & Chung, 1998).

$$\alpha_{i/j} = \sqrt{\frac{M_j}{M_i}} \tag{2.14}$$

For the gases used in this study, the Knudsen selectivity against N_2 varies from 0.9 to 3, much lower than the intrinsic selectivity of cellulose acetate found in Table 2.4. Should the microporous support layer govern gas transport, the overall selectivity of the membrane would be greatly reduced.

2.6 Cellulose Acetate

When it was first discovered in 1845 by Shützenburger, cellulose acetate (CA) was an expensive material with little commercial use compared to other cellulosics (Rustemeyer, 2004b). Over the last century, however, the use of CA has grown to involve a range of applications in protective coatings, textiles and electronics. Even though the yearly production of CA continues to fall because of advances in other polymeric materials (Law, 2004), burgeoning applications in desalination and gas separation continue to hold CA as a material of interest (Shibata, 2004). Since their introduction in 1982, CA membranes have become the conventional choice for CO_2 removal and have also been adapted well to other separation applications, such as pervaporation (Bernardo, 2009; Schell, 1989). A comprehensive review on the history, properties and applications of CA has been compiled by Rustemeyer (2004a).

CA is derived from the acetylation of the hydroxyl groups on a cellulose chain, as shown in Figure 2.6.

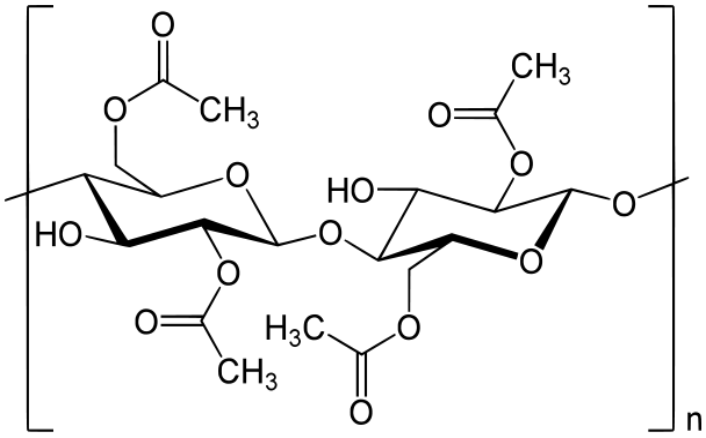

Figure 2.6: The chemical structure of cellulose acetate with a degree of substitution of 2 (Public Domain).

The extent to which the hydroxyl groups are acetylated is referred to as the degree of substitution (DS). The DS depicts the average number of hydroxyl groups that are converted into acetyl groups on each glucose unit, ranging from 0 (pure cellulose) to 3 (cellulose triacetate) (Fischer *et al.*, 2008). For example, the CA depicted in Figure 2 has a DS of 2. The DS significantly affects the gas permeation through CA as well as its physical properties of CA, as seen in Table 2.3.

Table 2.3: Physical properties of CA with varying degrees of substitution (Puleo *et al.*, 1989).

Degree of Substitution	**1.75**	**2.45**	**2.84**
Density (g/cm^3)	1.358	1.327	1.305
T_g (°C)	207	198	193
T_m (°C)	245	233	293
Crystallinty (%)	27	37	52
Elastic Modulus (10^5 MPa)	4.2	4.4	4.9
Tensile Strength (10^3 MPa)	6.6	12.7	14

Increasing the DS uniformly reduces the glass transition temperature (T_g) due to the reduced number of interactions between hydroxyl groups, allowing the polymer segments to move more freely (Kamide & Saito, 1985; Puleo *et al.*, 1989). Conversely, no clear trend regarding the DS and the melting temperature (T_m) has been developed. The hydrophilic nature of the polymer is also affected by the DS, with the hydrophilicity of the polymer decreasing from DS 0.8 to 3 due to a lack of available hydroxyl groups to which water can bond (Gibbons, 1953). Because of this feature, CA is usually referred to as being moderately hydrophilic. An increase in the DS from 1.75 to 3 is also accompanied by an in increase in crystallinity and polymer strength (Puleo *et al.*, 1989; Zugenmaier, 2004).

Despite the first use of CA for gas separation in the late 1960s, the literature on the gas transport properties was found to be incomplete or irregular owing to differences in membrane materials and their preparation (Puleo *et al.*, 1989; Nguyen *et al.*, 1994). Puelo *et al.* (1989) conducted a detailed literature review of CA gas permeation properties and conducted extensive gas permeation test on dense CA films to determine the intrinsic selectivity of CA membranes, seen in Table 2.4.

Table 2.4: Gas transport through dense CA films; 1atm, 35°C (Puleo *et al.*, 1989).

DS	Permeability [Barrer]						Selectivity					
	N_2	CH_4	O_2	CO_2	H_2	He	CO_2/CH_4	CH_4/N_2	O_2/N_2	CO_2/N_2	H_2/N_2	He/N_2
1.75	0.057	0.052	0.32	1.84	6.05	9.3	35.4	0.9	5.6	32.3	106	164
2.45	0.15	0.15	0.82	4.75	12	16.0	31.7	1.0	5.5	31.7	80.0	106
2.85	0.23	0.2	1.46	6.56	15.5	19.6	32.8	0.9	6.3	28.5	67.4	85.2
Knudsen Diffusion							0.60	1.32	0.94	0.80	3.72	2.65

Of the side groups on CA, the interactions between hydroxyl groups are considered to be stronger than hydroxyl-acetyl and acetyl-acetyl interactions (Puleo *et al.*, 1989). As the DS is increased, the reduction of hydroxyl-hydroxyl bonds and the addition of bulky acetyl groups to the polymer reduces the interaction between polymer chains in the increases the intermolecular space in the polymer (Puleo *et al.*, 1989). This results in an overall increase in diffusivity through the polymer, while also reducing the selectivity. This trend is quite significant in the transport of H_2 and He through CA when the DS is increased from 1.75 to 2.85. The permeability of both gases more than doubles, yet their selectivity over nitrogen is reduced by roughly 35%. Greater plasticization effects from CO_2 exposure are also associated with increases in the DS of cellulose acetate (Puleo *et al.*, 1989).

This study used polymeric CA membranes to model the effects of heavy hydrocarbon contamination on gas separation performance. Remediation methods involving solvent extraction and solvent exchange were also evaluated. Using the gas transport models presented here, any change in membrane performance was described in terms of resistance factors though the polymer and oil layers.

Chapter 3

Experimental

In this study, pre-fabricated CA membranes were used to model a gas separation process contaminated with heavy hydrocarbons and remediated with liquid solvents. Membrane fibres were assembled into individual modules and exposed to various chemical treatments such as lubricant contamination and solvent extraction. In order to properly assess the effects of contamination, gas permeation tests were conducted on the membranes modules before and after any chemical treatment. Using the data collected from these measurements, the efficacy of the remediation treatments was also evaluated.

3.1 Materials

Bulk CA hollow fibres were manufactured by Toyobo Co., Japan for use in the desalination of water. These membranes were treated by the solvent exchange method for use in gas separation. The fibres were 200μm in diameter and stored at ambient conditions for over 2 years. CA flat films were also prepared in the lab from powdered CA (CA-398-3, Eastman Chemical Co.), which had an acetyl content of 39.8% (DS ~2.5).

ACS grade acetone (99.5%), ethanol (absolute, ≥99.85%) and isopropanol (99.5%) were obtained from Sigma Aldrich Co. ACS grade cyclohexane (99%) was obtained from BDH

Chemicals Ltd. Pure carbon dioxide (CO_2), helium (He), hydrogen (H_2), methane (CH_4), nitrogen (N_2) and oxygen (O_2) were provided by Praxair Ltd. and all of the gases were of research grade purity. SAE 10W-30 motor oil lubricant was obtained from Pennzoil Co.

3.2 Contact Angle Measurements

Flat sheet membranes were prepared by casting a polymer solution and allowing it to dry into a film. A CA solution was formulated by dissolving powdered CA into an acetone/water mixture; the polymer solution contained 15wt% CA, 80wt% acetone and 5wt% distilled water. The solution was left to mix overnight to completely dissolve the polymer.

To form a flat sheet membrane, the polymer solution was spread across a glass plate using a hand-held casting method. The solution was poured onto the edge of a flat glass plate and a glass rod was used to evenly spread the solution across the rest of the plate. Wires were attached to the end of the glass rod in order to raise the rod to a fixed height and cast a film of uniform thickness. The polymer solution was allowed to dry overnight, forming a thin polymer film. The film was removed from the glass plate manually and cut into 1”x0.5” pieces for sampling. A Tantec contact angle meter fitted with a Teflon needle was used to analyze the contact angle of solvents on the CA film. The sessile drop technique was used to determine the contact angle, with a droplet of solvent placed onto the surface of the film and the angle of the droplet measured immediately afterward.

3.3 Gas permeation Measurements

Each membrane sample was prepared by assembling multiple hollow fibres into copper tubing and anchoring them together with epoxy, as shown in Figure 3.1. A small piece of ¼”

copper tubing (3cm long) was cut using a pipe cutter and had its edges de-burred to prevent any damage to the membrane fibre. The inner surface of the tubing was roughened using circular filing tools to aid with the adhesion of the epoxy. Finally, two Swagelok® nuts were placed onto the tubing and secured with the appropriate ferrules. 6-8 hollow fibres were cut into 15cm strands using a scalpel and placed within the copper tubing. Gloves were worn to prevent contamination of the hollow fibres. Devcon 2 Ton Epoxy ® resin was then used to seal the gaps between the fibres and the tubing. Once the epoxy layer was allowed to set for an hour, another coat of epoxy was used to cap the ends of the hollow fibres. The epoxy resin was then allowed to cure overnight. The free ends of the hollow fibres were then shortened using a scalpel to prevent the fibres from folding upon assembly to form a membrane module. The length of hollow fibre strands were measured after the epoxy had cured, with most measurements varying from 5-7cm.

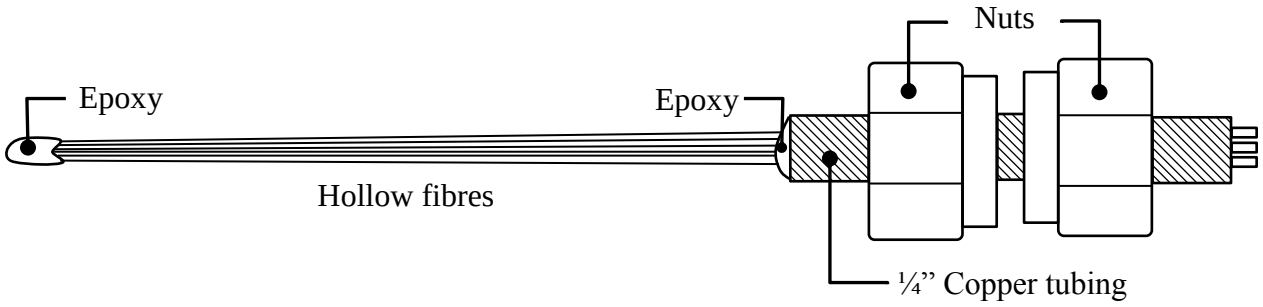

Figure 3.1: Schematic of a membrane sample.

The complete membrane module was assembled as shown in Figure 3.2. Fibres from each membrane sample were fed through a ¼" union tee attached to 15cm of ¼" copper tubing. A feed line was then attached to the union tee to allow for a shell-side feed. A permeate line was attached to the lumen end of the hollow fibres to allow for gas to flow out of the module. All tubing connections were obtained from Swagelok Co.

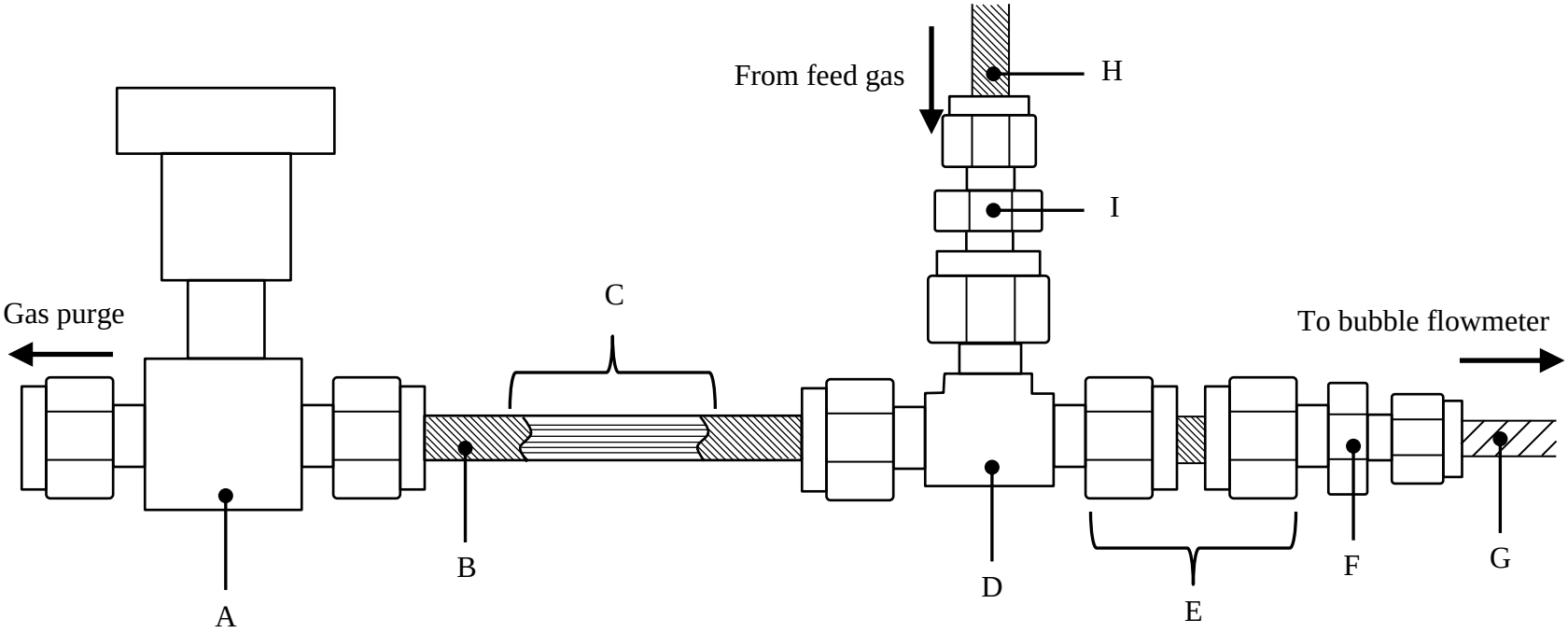

A. ¼” – ¼” Needle valve [B-4HK]

B. ¼” Copper Tubing

C. Hollow Fibres

D. ¼” x 3 Union Tee [B-400-3]

E. Membrane sample as seen in Figure 3.1

F. ¼” – ⅛" Reducing Union [B-400-6-2]

G. ⅛" Polyethylene tubing

H. ⅛" Copper Tubing

I. ¼” – ⅛" Reducer – Fractional [B-200-R-4]

Figure 3.2: Complete module housing, side view. Adapted from Swagelok® CAD drawings. Swagelok product codes in brackets.

The membrane module was placed in a thermal bath and then feed gas (i.e., pure CO_2, He, H_2, CH_4, N_2 or O_2) was supplied, as seen in Figure 3.3. Gas permeation tests were conducted using a shell-side feed through the CA membranes. The feed gas was allowed to permeate through the hollow fibre walls, flow down the fibre bore and then exit into the permeate stream. The permeate flowrate was measured using a bubble flowmeter. Flowrate measurements were taken at 10min-15min intervals until steady state permeation was obtained. Barometric pressure readings were taken from the University of Waterloo Weather Station.

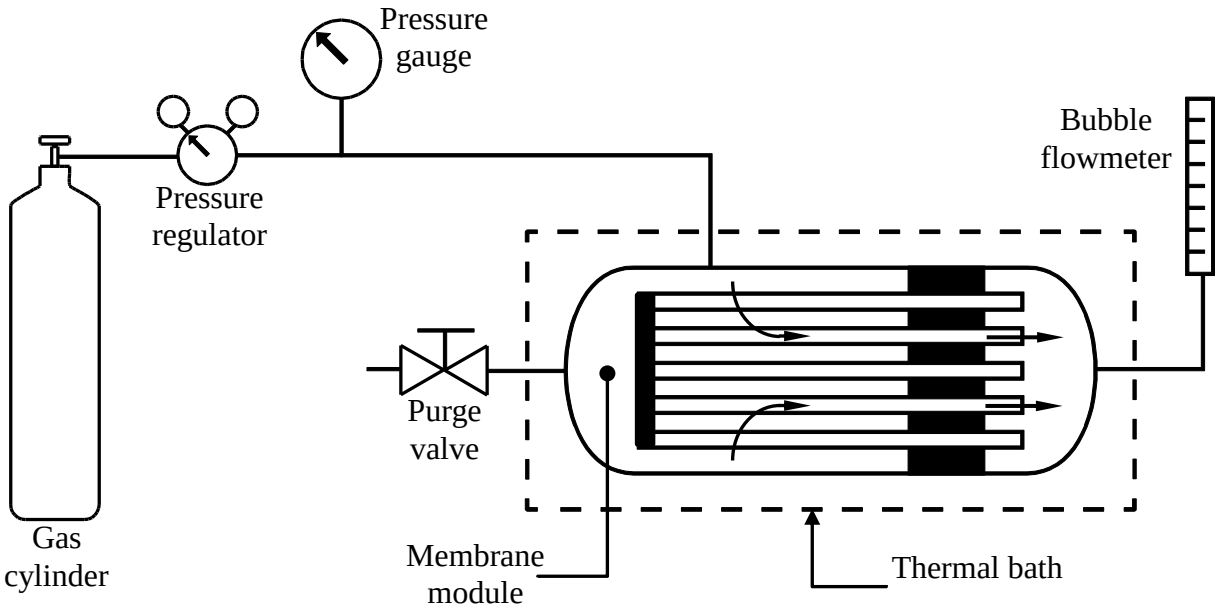

Figure 3.3: Experimental setup.

To assess the effects of pressure on the membrane performance, the operating temperature was held at 300K while the feed pressure was increased from 300kPa to 1500kPa gauge in intervals of 400kPa. To assess the effects of temperature on membrane performance, the pressure was held at 500kPa gauge while the operating temperature was increased from 303K to

323K in intervals of 5K. These tests were repeated after a pristine membrane was contaminated or remediated.

3.4 Membrane Treatments

3.4.1 Contamination

The hollow fibres were subjugated to contamination with lubricant. To contaminate the hollow fibres, the feed and permeate lines (parts I and F in Figure 3.3) were removed from the membrane module and the motor oil lubricant was injected into vessel. At no point was the membrane sample removed from the module. The lubricant was allowed to fill the module for a ½ hour and then drained. Afterwards, an air stream at 200kPa was blown through the module for 30 seconds to remove excess lubricant. The feed and permeate lines were then reattached. The gas permeation measurements described in Section 3.2 were repeated after membrane contamination.

3.4.2 Remediation

To remediate the contaminated membrane, solvent treatment was attempted. As with the contamination, both the feed and permeate lines were removed from the membrane module. Remediation with solvent exchange was carried out by soaking the hollow fibres in the following solvents sequentially:

1. Cyclohexane
2. Isopropanol
3. Ethanol
4. 80% aq. ethanol
5. 50% aq. ethanol
6. 25% aq. ethanol
7. 10% aq. ethanol
8. Water

Each solvent was allowed to soak the membrane fibres for a ½ hour and was then replaced by the next solvent in the sequence. Water was allowed to soak the membranes for a full hour and then the process was continued in reverse sequence (i.e., from 8 to 1). The solvents were exchanged rapidly to prevent the membrane fibres from drying out. Once the solvent exchange process was completed, the hollow fibres were allowed to dry overnight at ambient conditions.

Alternatively, the membrane remediation was also conducted with a simple cyclohexane treatment. Cyclohexane was allowed to soak the hollow fibres for a ½ hour and was then drained from the module. Once the cyclohexane remediation was completed, the hollow fibres were allowed to dry overnight. After either remediation method was conducted, the gas permeation measurements described in Section 3.2 were repeated.

The contact angle measurements allowed for a qualitative assessment of the polymer-solvent interactions during remediation. Using the data collected from the gas permeation tests, the separation properties of the CA membranes were assessed in their pristine, contaminated and remediated states. With this data, the effects of contamination and remediation on the separation performance of the CA membranes were then evaluated.

Chapter 4

Results and Discussion

The separation performance of the CA membranes was determined before and after contamination using gas permeation tests. By assessing the physical properties of the lubricant layer, the gas transport properties of the lubricant were estimated. An attempt to remediate the contaminated CA membranes using solvent exchange and cyclohexane extraction was also conducted and the separation performance of the remediated membranes was also assessed.

4.1 Properties of Pristine Cellulose Acetate Hollow Fibres

Figure 4.1 shows that the permeance of most gases was relatively independent of feed pressure and the permeation flux was proportional to an increase in feed pressure. This is attributed to low solubility of the penetrants in membrane. CO_2 is more soluble in CA and demonstrated moderate plasticization effects, although the pressure range was not large enough to produce dramatic changes in gas transport behaviour. This is consistent with the research findings of Puleo *et al.* (1989). As CA is a glassy polymer, gas transport through the membrane was mostly governed by diffusion. The gas permeability through the pristine membrane was found to follow the order of $N_2 < CH_4 < O_2 < CO_2 < H_2 < He$, in reverse order to the kinetic diameters of the penetrant gases.

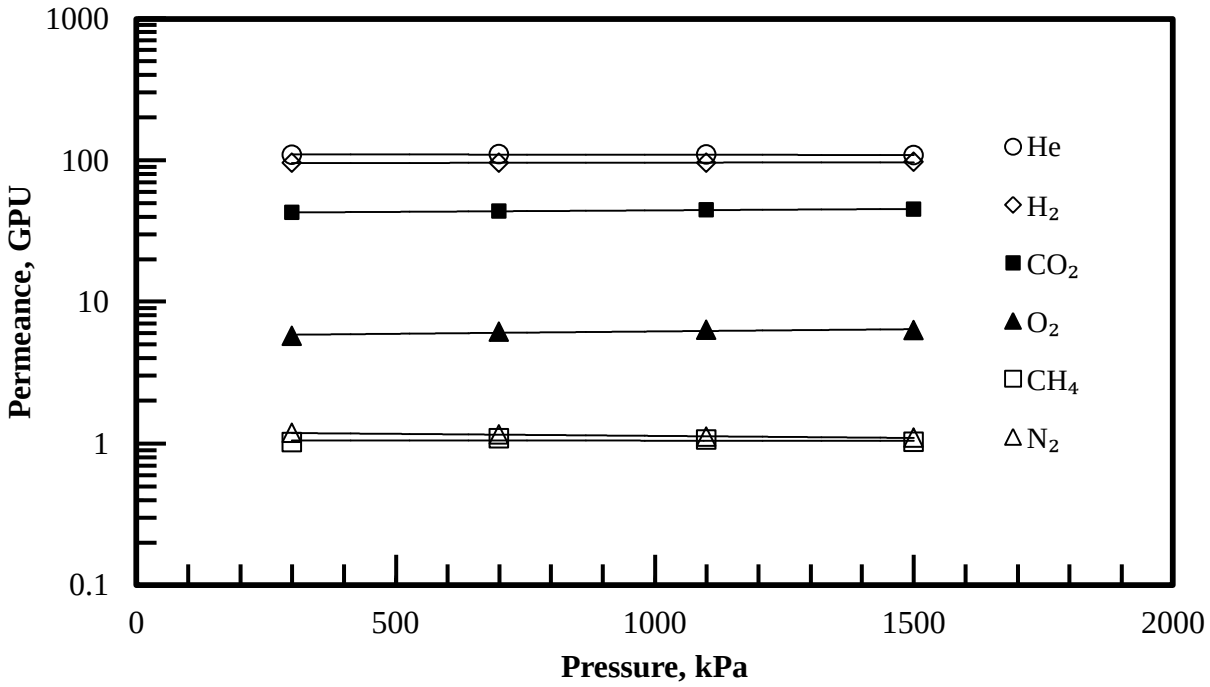

Figure 4.1: Effect of feed pressure on the permeance of a pristine membrane sample; Module #1, 300K.

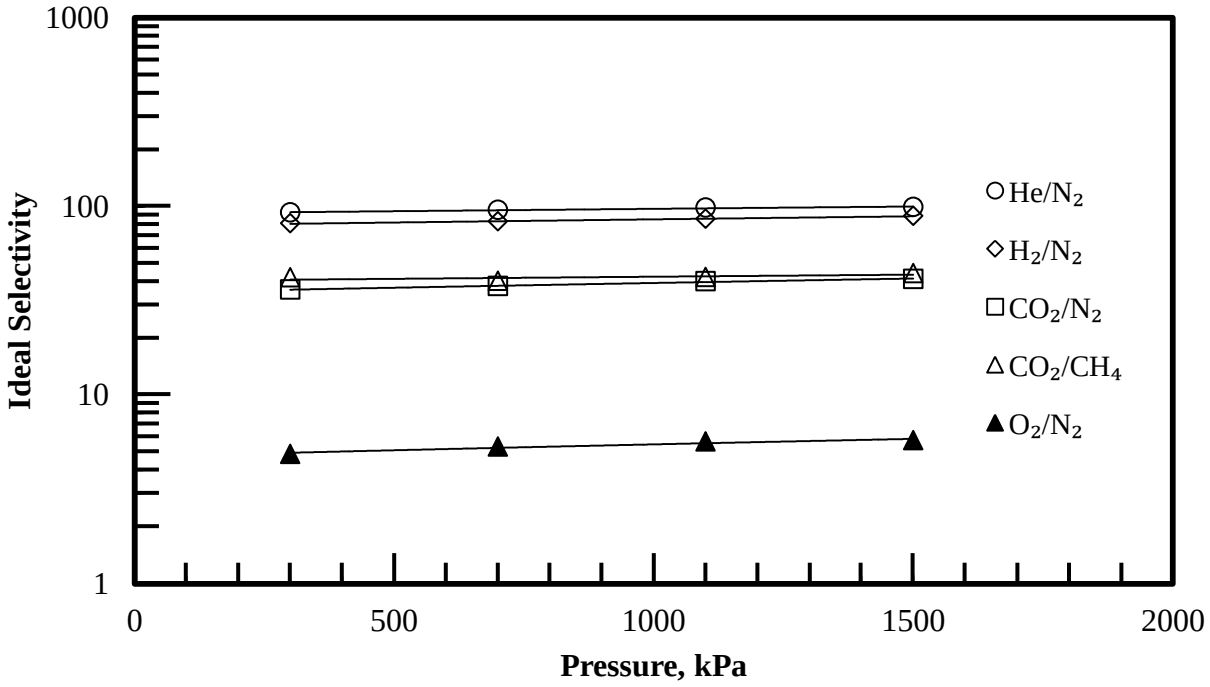

Figure 4.2: Effect of feed pressure on the selectivity of a pristine membrane sample; Module #1, 300K.

Most studies on gas transport through CA membranes report values of permeability coefficient, a thickness-normalized property. Since the thickness of the selective layer on the asymmetric hollow fibres could not accurately be determined, the selectivities of each membrane sample were used for comparison instead. The selectivities of gases against N_2 (such as O_2/N_2, CO_2/N_2, H_2/N_2 and He/N_2) were plotted over a range of pressures, as shown in Figure 4.2. The CO_2/CH_4 selectivity was also plotted since this ratio is industrially relevant to natural gas separations. The CH_4/N_2 selectivity was omitted due to the similar permeabilities of N_2 and CH_4. The H_2/N_2 and He/N_2 selectivities were found to have the largest variance between membrane samples and were very sensitive to the permeance of N_2.

Comparing the selectivities determined to the values reported in literature show good agreement for the slow permeating gases. The H_2/N_2 and He/N_2 selectivities show the largest spread in the literature due to the varying degrees of acetylation in the polymer and the variety of membrane preparation procedures. Based on the gas transport properties of the membranes in the study, the DS for the membrane is estimated to be in the range of 2.5-2.85.

Table 4.1: Gas transport though CA hollow fibres at 27 and 35°C.

Temp. [°C]	**Permeance [GPU]**						**Selectivity**					
	N_2	**CH_4**	**O_2**	**CO_2**	**H_2**	**He**	**CO_2/CH_4**	**CH_4/N_2**	**O_2/N_2**	**CO_2/N_2**	**H_2/N_2**	**He/N_2**
27	1.36	1.36	7.48	48.3	101	114	35.6	1.00	5.52	35.6	74.2	84.4
35	1.58	1.64	8.83	42.8	104	120	26.6	1.05	5.64	27.6	66.8	77.3

In order to determine whether the membrane modules were defect-free, the permeation of select gases were measured and compared to the intrinsic selectivity of the polymer. The ideal O_2/N_2 selectivity of CA polymers falls in the range of 5-6, as shown in Table 4.1.

As shown in Figure 4.3, the permeance of all gases increased with an increase in temperature and the temperature dependence followed the Arrhenius relationship. As the temperature increased, the selectivity of the membrane decreased as shown in Figure 4.4, indicating a reduction in the diffusivity-selectivity.

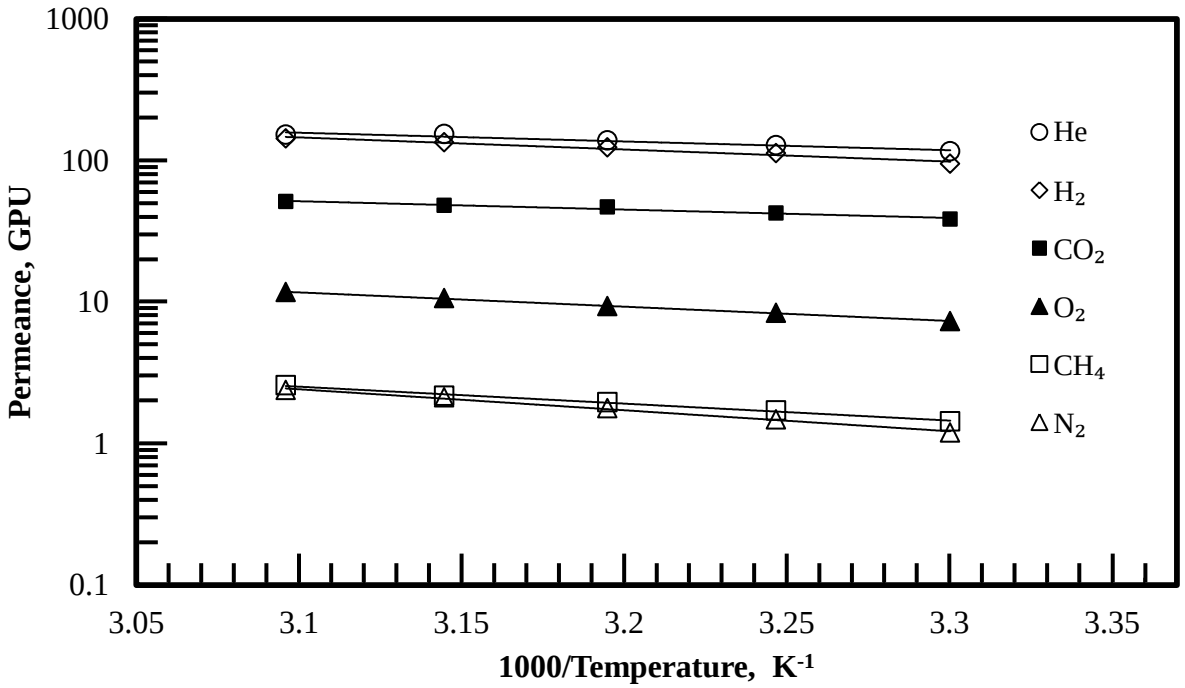

Figure 4.3: Effect of operating temperature on the permeance of a pristine membrane; Module #1, 500kPa.

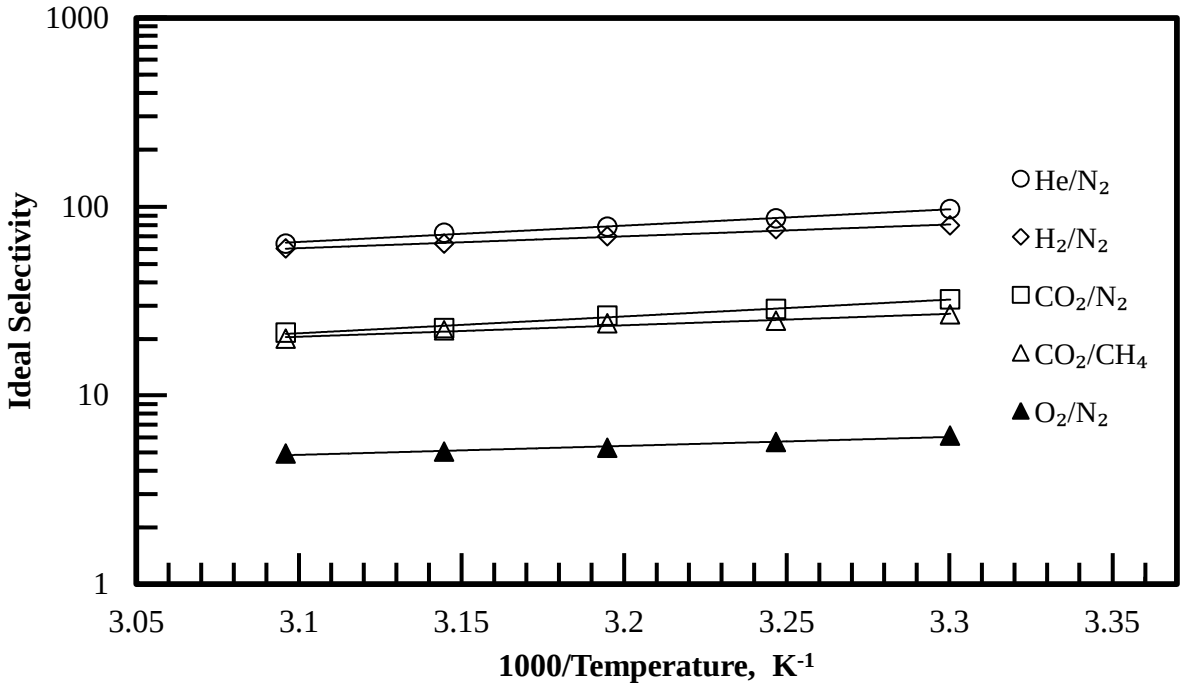

Figure 4.4: Effect of operating temperature on the selectivity of a pristine membrane sample; Module #1, 500kPa.

4.2 Analysis of Contamination

4.2.1 Effect of Lubricant Coating

The permeance of gases though the contaminated membranes were found to be relatively independent of pressure, as shown in Figure 4.5. Gas permeability through the contaminated membranes was found to follow the order of $N_2 < CH_4 < O_2 < CO_2 < H_2 < He$, which is the same as that for the pristine membrane samples. This suggests that diffusivity still dominated gas transport. The overall permeation flux through the membrane decreased in the presence of the lubricant; H_2 and He experienced the highest reductions in permeance. The permeance of He was found to decrease by roughly 50-65% across all contaminated samples in contrast to permeance of N_2 which was found to decrease by 10-30%. The different extent of change in the gas transport properties is reflected in the selectivity of the contaminated samples, with the H_2/N_2 and He/N_2 selectivities falling in the range of 40-50, as shown in Figure 4.6, where the ideal selectivities of the contaminated membrane are illustrated.

Similar trends were observed at different temperatures. The overall permeance and selectivity of H_2 and He decreased more significantly than the other penetrant gases studied here, as shown in Figures 4.7 and 4.8. Using the Arrhenius relationship, the activation energies of permeation through the pristine and contaminated membranes were determined for each penetrant, as they are shown in Table 4.2. The activation energies of permeation in the pristine membrane were compared with literature values, and they were found to be in good agreement, except for CH_4. The activation energy increased for all gases once the membrane became contaminated, confirming the result that the lubricant layer presents a barrier to gas transport.

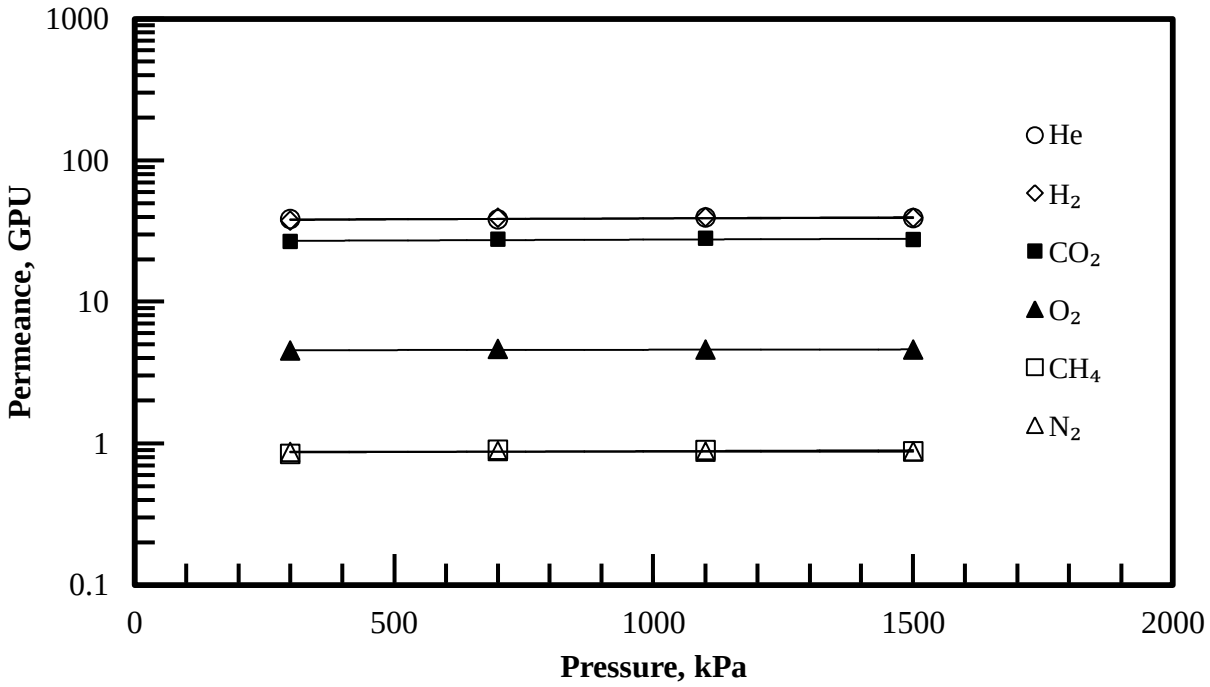

Figure 4.5: Effect of feed pressure on the permeance of a contaminated membrane sample; Module #1, 300K.

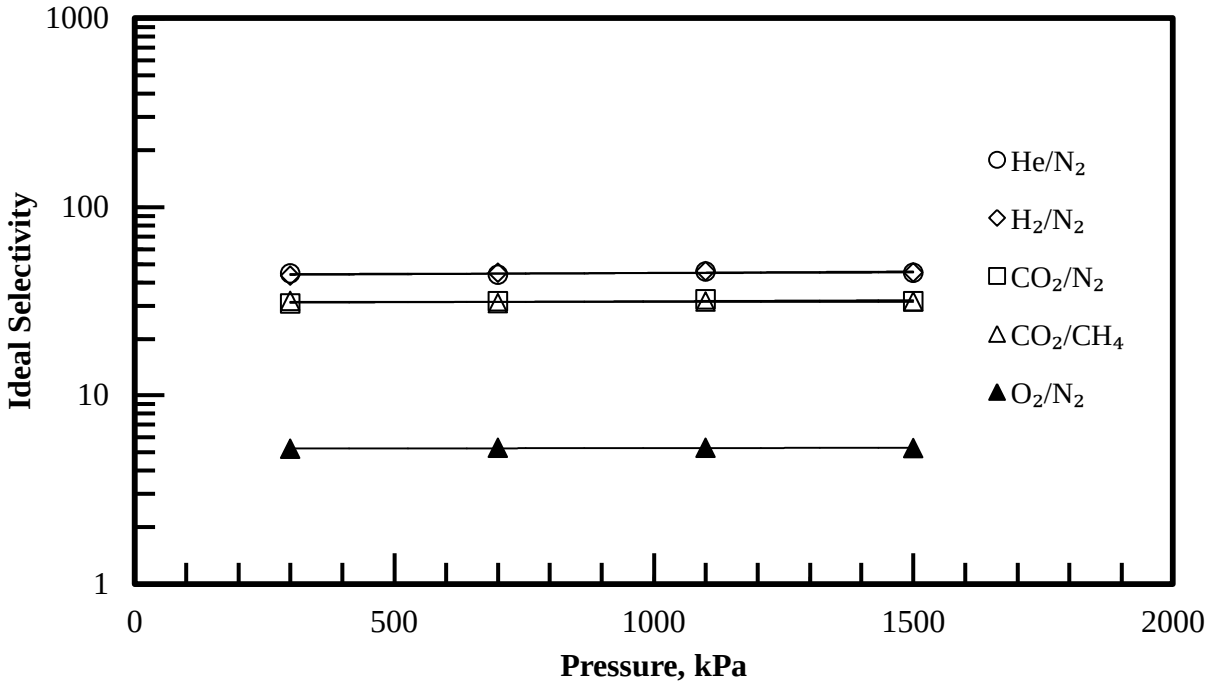

Figure 4.6: Effect of feed pressure on the selectivity of a contaminated membrane sample; Module #1, 300K.

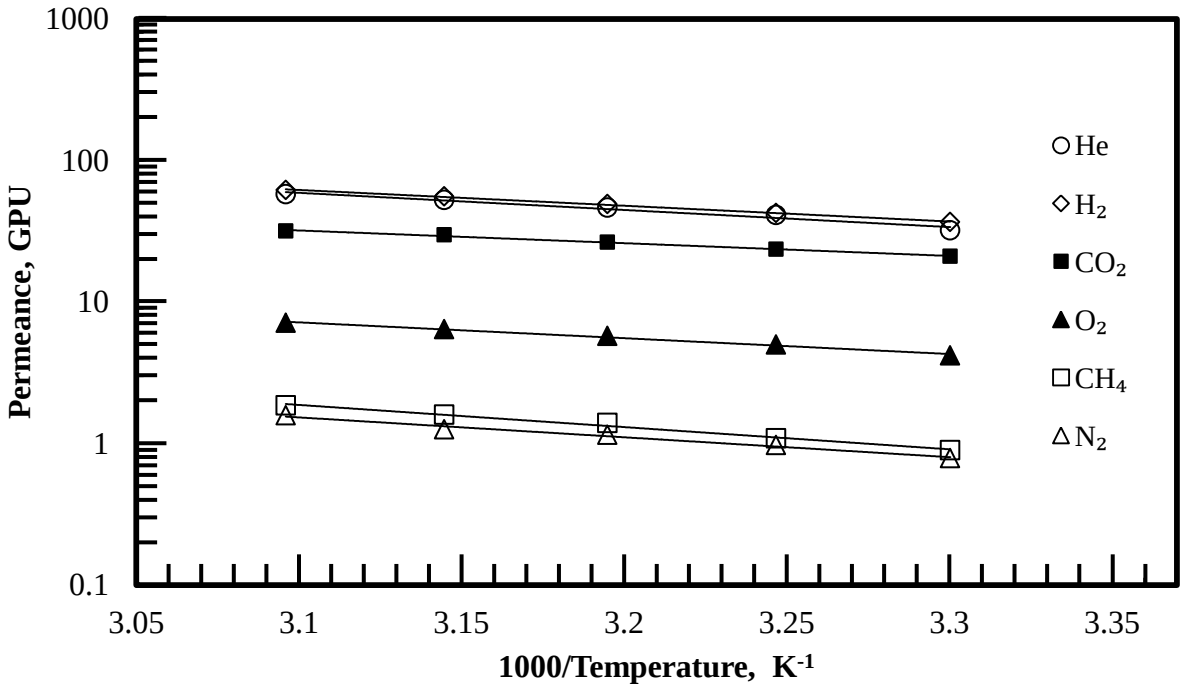

Figure 4.7: Effect of operating temperature on the permeance of a contaminated membrane sample; Module #1, 500kPa.

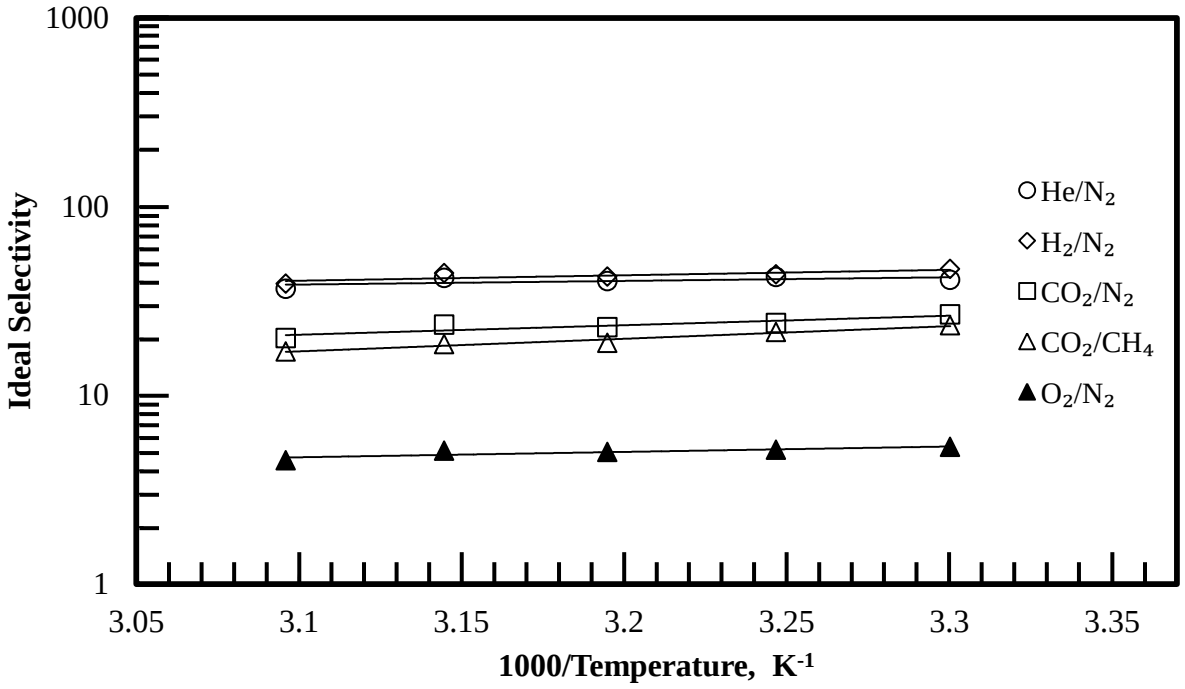

Figure 4.8: Effect of operating temperature on the selectivity of a contaminated membrane sample; Module #1, 500kPa.

This effect appears to be more significant for the faster permeating gases, suggesting that a penetrant with a lower solubility suffers a greater loss in permeability. The gas transport properties of the lubricant must be properly defined to verify if this is true.

Table 4.2: Average activation energies for pristine and contaminated membranes at 500kPa [kJ/mol].

Gas	Previous Studies		This Study		
	DS 2.4[a]	DS 2.4[b]	Pristine	Contam.	% Change
N_2	23	21.5	25.8	28.9	+12.2
CH_4	–	20.7	26.8	30.3	+13.3
O_2	19	16.2	18.4	26.0	+41.8
CO_2	11	8.95	12.4	16.7	+35.0
H_2	–	14.8	16.3	19.4	+19.3
He	14	14.4	13.1	19.5	+49.1

[a] (Haraya *et al.*, 1986; Nakai *et al.*, 2005).

The change in the gas transport can be seen more clearly by plotting the decrease in permeance against the permeance of the penetrants in pristine membranes, as shown in Figure 4.9. The overall trend appears to show that the greatest losses in performance occur to the gases with the greatest permeance. This also suggests that the lubricant layer is solubility-selective. The extent of the performance loss varied between membrane samples because of the varying amounts of lubricant that covered each sample. The variability in the performance loss between the membrane samples appeared to decrease with increasing temperature as well.

As the temperature was increased, the loss in membrane performance was reduced for most gases, as shown in Figure 4.10. This behaviour may correspond to an increase in diffusivity through the lubricant layer when the temperature increased since the solubility of gases in liquids generally decreases with increasing temperature.

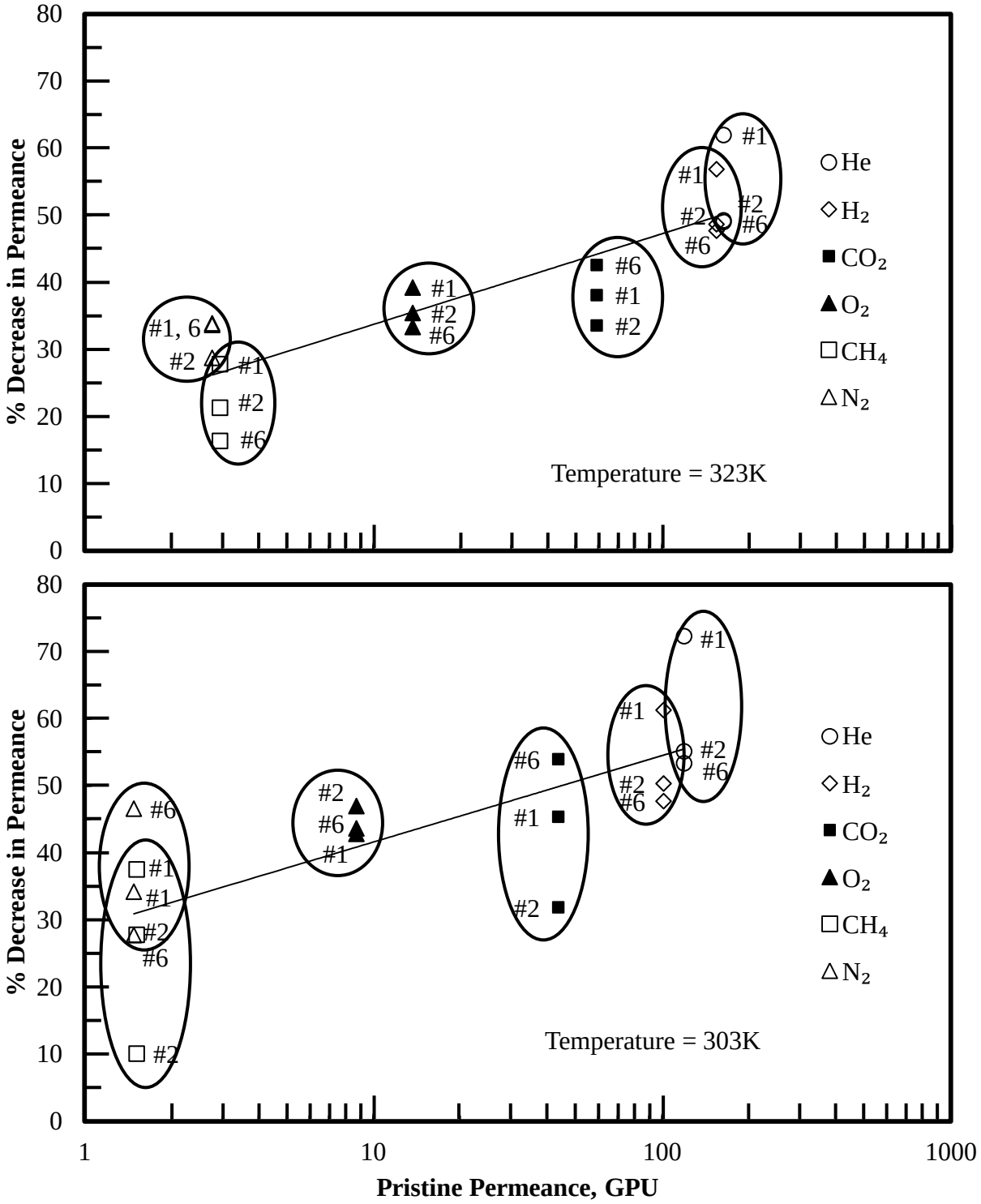

Figure 4.9: Performance loss of membrane permeance due to contamination; 500kPa. The membrane samples (#1, 2 and 6) were contaminated by the lubricant to different degrees.

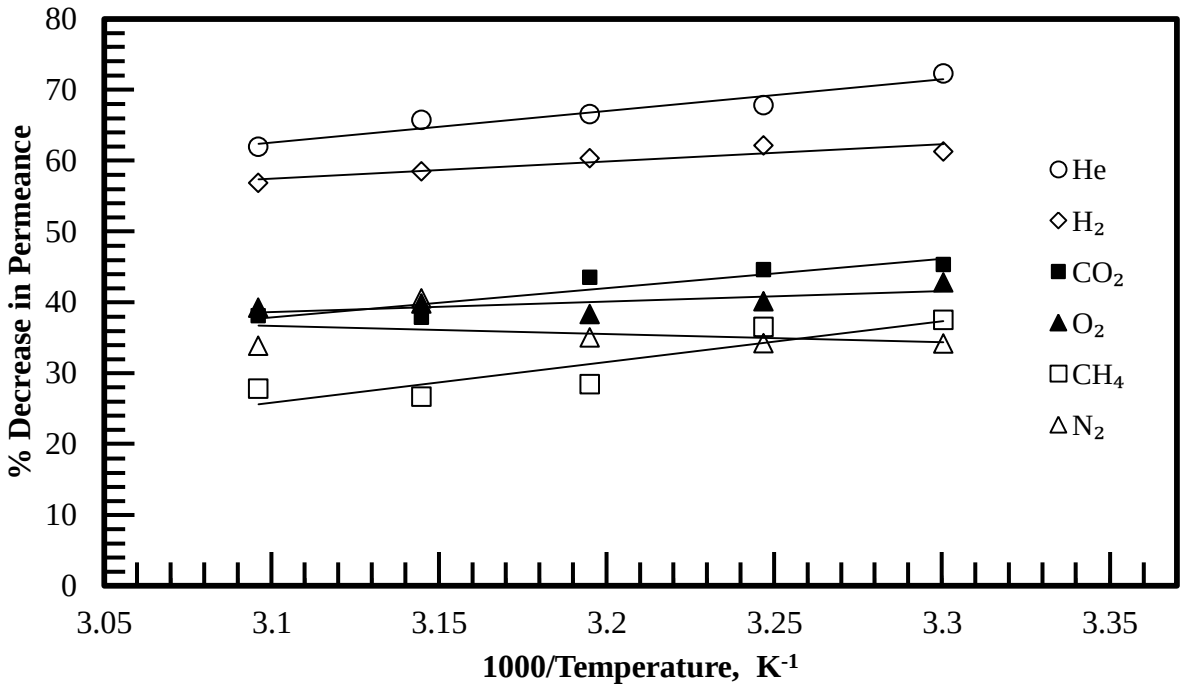

Figure 4.10: Permeance reduction at different operating temperatures; Module #1, 500kPa.

Prior work regarding the contamination of gas separation membranes usually involves a contaminant in the feed stream that accumulates over time and gradually reduces gas permeability (Schell, 1989; Al-Juaied & Koros, 2006). This study is instead concerned with a more static form of contamination. Since the hollow fibres have been submerged in the lubricant, it is assumed that gas transport is taking place through an additional liquid layer on top of the CA membrane, as shown in Figure 2.5. To simplify the calculations, it was assumed that the presence of the lubricant has not significantly altered the morphology of the CA membrane and that any change in separation performance can be attributed to the lubricant layer itself. This assumption will be addressed in Section 4.3.

4.2.2 Gas Transport through Heavy Hydrocarbons

In order to determine the gas transport properties of the lubricant layer, the permeation resistance of the membrane was evaluated before and after contamination, as described in Section 2.5. Figure 4.11 shows that the permeation resistance of CO_2, H_2, and He in the oil layer are nearly equal, denoting a similar transport through the lubricant.

Converting the permeation resistance of the lubricant into permeance values presented a clearer picture of the gas transport through the lubricant, as shown in Figure 4.12. The gas permeance through the lubricant appears to be somewhat pressure-dependant, and the permeance follows the order of $N_2 < CH_4 < O_2 < He \sim H_2 \sim CO_2$. The order of He, H_2 and CO_2 appears to vary between samples, and may be attributed to experimental error.

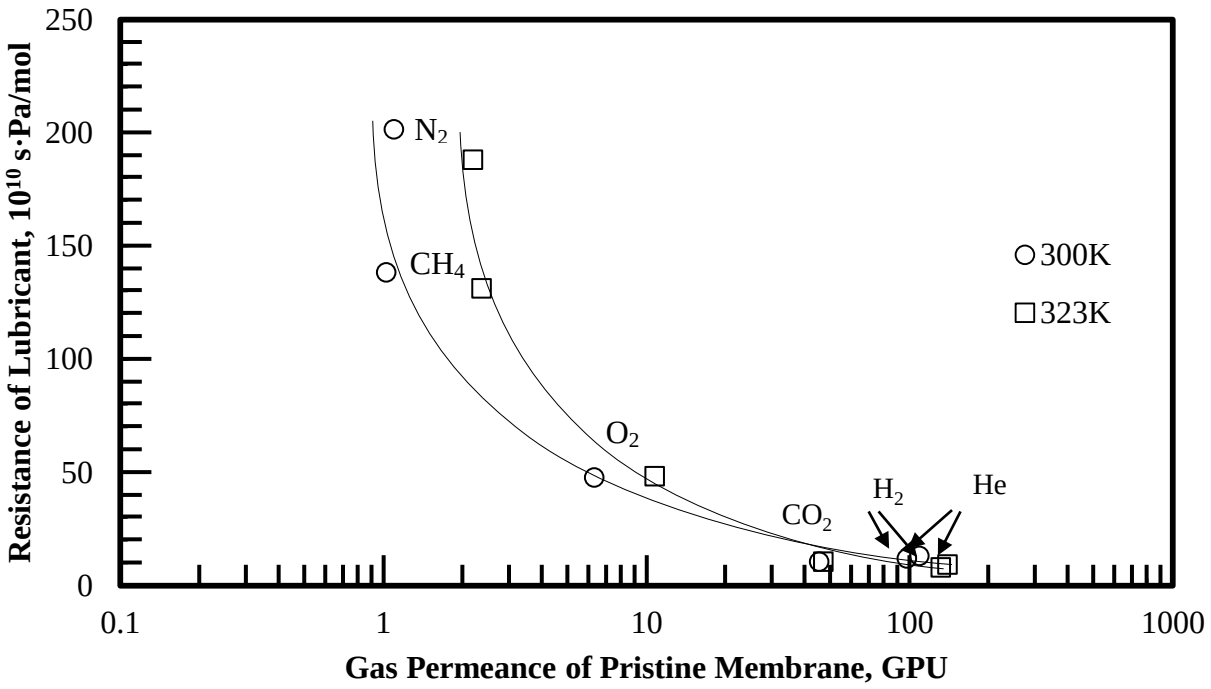

Figure 4.11: Permeation resistance of the lubricant layer versus gas permeance of pristine membrane; Module #1, 500kPa.

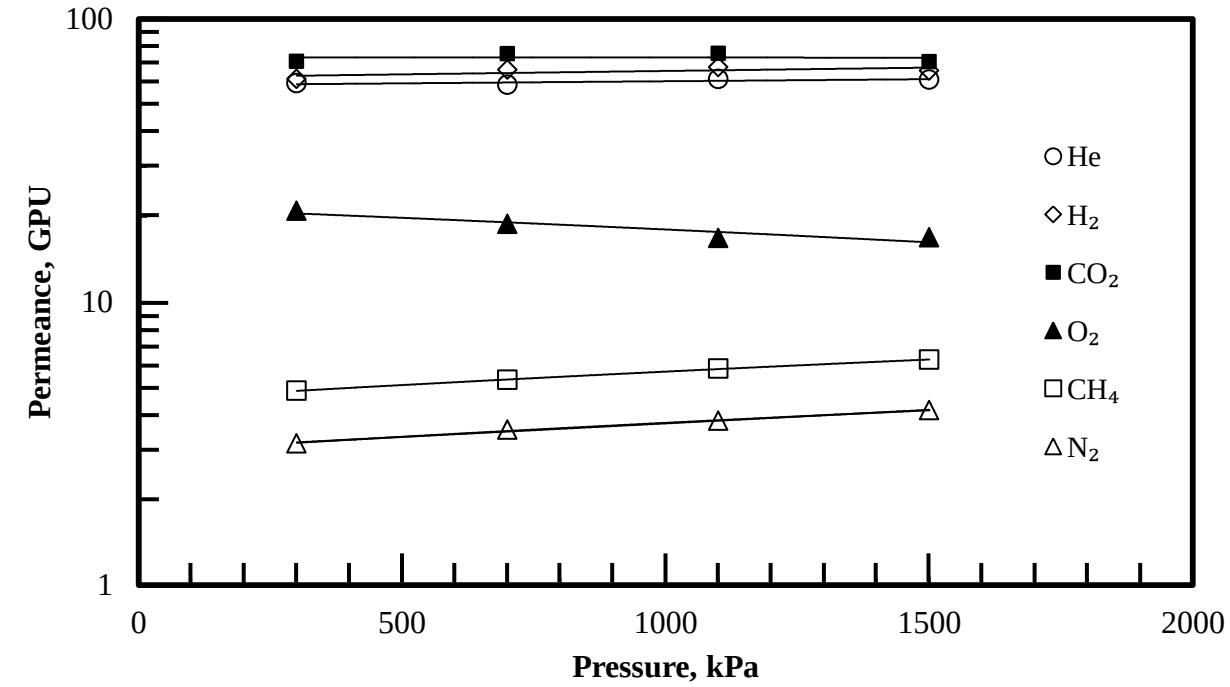

Figure 4.12: Effect of feed pressure on the permeance of the lubricant layer; Module #1, 300K.

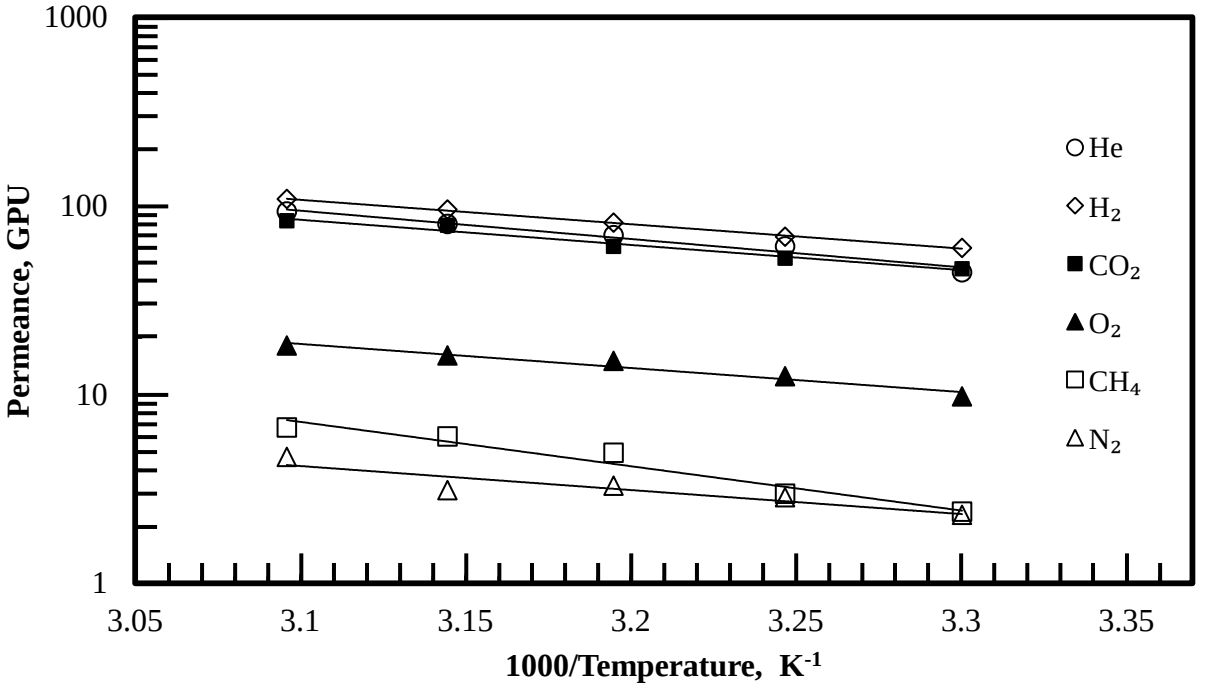

Figure 4.13: Effect of operating temperature on the permeance of the lubricant layer; Module #1, 500kPa.

Figure 4.13 shows the effects of temperature on the gas permeance of the lubricant layer. The order of permeation appears to be sensitive to changes with temperature and was found to follow the order of $N_2 < CH_4 < O_2 < CO_2 < He < H_2$ in all contaminated samples at temperatures above 303K.

The data in Figures 4.12 and 4.13 shows that the permeance of most gases appears to be greater in the lubricant layer than through the pristine CA membrane. It may be noted that greater amounts of lubricant deposited on the membrane surface would result in lower permeance values. This also explains the variability in the overall permeance of the contaminated membranes with different degrees of contamination (Figure 4.9).

The thickness of the lubricant layer can be estimated using the solution-diffusion model based on the gas permeation data. The solution-diffusion model may apply to liquid layers in the absence of any complex gas-liquid interactions (e.g., facilitated-transport) (Noble & Koval, 2006). If the diffusivity and solubility of the penetrants in the lubricant are known, the thickness of the lubricant layer can be derived from the permeance data using Equations 2.5 and 2.6. Since attaining accurate values of the diffusivity and solubility of gases in heavy hydrocarbons is difficult, these properties were estimated based on literature data.

The American Society for Testing and Materials (ASTM) has developed standards for determining the physical properties of industrially-relevant materials. Of these, ASTM Method 3827 is specifically used to estimate the solubility of gases in lubricants. Using the product specifications of the lubricant provided from Pennzoil ("*Pennzoil®*", 2010) and the corresponding ASTM methods, the solubility of the gases in the lubricant were estimated for the experimental conditions used in this study, as shown in Figure 4.14. Complete calculations of the gas solubility can be found in Appendix A.

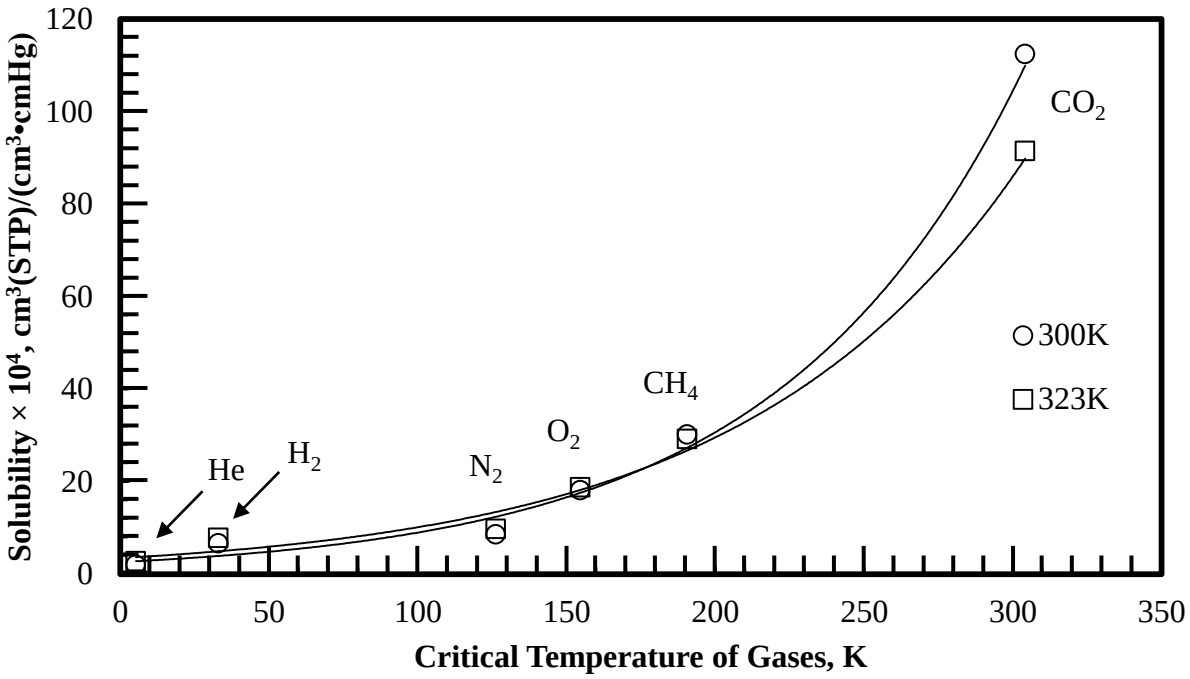

Figure 4.14: Solubility coefficients of select penetrants in the lubricant layer.

The estimated order of solubility in the lubricant follows the order of He < H_2 < N_2 < O_2 < CH_4 < CO_2. This trend further suggests that the lubricant layer is solubility-selective, given that the largest decreases in gas permeance of contaminated membranes occurred to both He and H_2, the least soluble gases. However, this trend does not explain the large drop in CO_2 permeance after membrane contamination as it was the most soluble gas in the lubricant yet suffered a greater permeance loss than both N_2 and O_2, primarily due to its relatively large molecular size.

Currently, there is no uniform testing procedure or conclusive model to determine the diffusivity of gases in heavy hydrocarbons (Etminan *et al.*, 2009; Zainal *et al.*, 2009). The variety of testing procedures that are available are not only time-consuming but the measured values often vary by more than an order of magnitude for the same gas-liquid system.

Table 4.3: Viscosities of a few heavy hydrocarbons.

Gas Solute	Temp. [°C]	Viscosity [mPa.s]	Reference
n-Dodecane (n-C_{12})	50	0.930	(Haynes, 2012)
n-Hexadecane (n-C_{16})	50	1.879	(Haynes, 2012)
n-Octacosane (n-C_{28})	40	~13.1	(Korsten, 2001)
Pennzoil SAE 10W-30	40	60.8	(*Pennzoil® motor oil - technical data sheet*, 2010)
Heavy Oil	48	5000	(Zhang, Hyndman, & Maini, 2000)
Athabasca Bitumen	50	~100,000	(Etminan, 2010)

Table 4.4: Diffusivity coefficients for gases in various hydrocarbons, D x 10^9 m^2/s.

Solvent	Temp. [°C]	Test Gas			Study
		H_2	CO_2	CH_4	
n-C_{12}	45			4.32	(Etminan, 2010)
	65			4.86	
	31	10.9	3.9		(Matthews, 1987)
	99	27.1	8.68		
n-C_{16}	50	10.5	3.48		(Matthews, 1987)
	98	20.8	6.57		
n-C_{28}	98	13.4	3.8		(Rodden, 1988)
	141	20.5	6.21		
	21		4.1	16.1	(Tharanivasan, 2004)
Heavy Oil	21		4.9	8.6	(Zhang *et al.*, 2000)
Bitumen	50		0.36		(Etminan, 2010)
	75		0.5		

Systematic studies on the gas diffusivities in heavy hydrocarbons are uncommon, although there have been a few studies on the diffusion of CO_2 and CH_4 in heavy oil and bitumen (Jamialahmadi *et al.*, 2006; Zainal *et al.*, 2009).

A cursory look at measured diffusivity coefficients in the literature show a general decrease in diffusivity with increasing viscosity of the liquid and kinetic diameter of the penetrant gas, with values in the range of 10^{-8} to 10^{-9} m^2/s for most n-alkanes, as shown in Table 4.3 and 4.4. Out of the diffusion data available, octacosane (n-C_{28}) was chosen to model the lubricant in this study because its viscosity is closest to that of the lubricant.

Appendix B summarizes the procedure of estimation of diffusivities of H_2 and CO_2 in the oil. The diffusivity-selectivity from these values is greater than that of the membrane ($H_2/CO_2 \approx 4$ for the lubricant, ≈ 2.5 for the membrane).

Using the derived solubility and diffusivity values for CO_2 and H_2, the thickness of the lubricant layer was estimated for a range of temperatures, as shown in Table 4.5. The estimated thicknesses were found to be between 3-33μm, well within the range for viscous coatings on hollow-fibres of low porosity (Tsai *et al.*, 1995). Estimating the lubricant thickness using H_2 transport was found to produce consistent results over the entire temperature range. In contrast, the lubricant thickness estimated from CO_2 transport was found to decrease with increasing temperature. This difference may be attributed to the large difference in solubility between the two gases. Unlike CO_2, H_2 is considered to be a non-condensable gas. This would imply that the solubility of CO_2 in this specific lubricant estimated by ASTM Method 3827 is underestimated at higher temperatures. It should also be noted that the permeance loss of the contaminated membrane does not scale uniformly to the estimated thickness due to the nature of the resistance calculations, as shown in Table 4.5.

Table 4.5: Estimated thicknesses of the lubricant layer.

Gas	Sample #	Thickness [μm]					
		303 K	308 K	313 K	318 K	323 K	Average
H_2	1	5.81	5.53	5.24	4.99	4.90	5.29
	2	3.25	3.04	3.05	2.90	2.89	3.03
	6	3.12	2.91	3.02	3.08	3.26	3.08
CO_2	1	29.2	26.0	23.7	19.2	19.0	23.4
	2	14.4	14.0	13.7	13.6	12.3	13.6
	6	32.9	22.0	21.2	18.1	18.6	22.5

As previously mentioned, the above estimations of the lubricant thickness are merely speculative. Accurate measurements would require high-resolution imaging of the membrane cross-section or the precise gas transport properties of the lubricant. Regardless, it appears that even a 3μm coating of heavy hydrocarbons can drastically reduce membrane performance. Typical industrial gas separation membranes have very large surface areas, ranging from 20-300m^2 per module depending on the membrane geometry (Baker, 2004c). It is unlikely that a lubricant deposit would be allowed to form a complete monolayer on such membranes during operation before the membrane is shut down, although reductions in performance according to the trends found here could help identify the presence of a foulant.

4.3 Remediation of Contaminated Membranes

4.3.1 Remediation with Solvent Exchange

The substructure of a gas separation membrane is sensitive to the capillary pressure caused by any liquid within its pores, a property that is strongly dependent on the liquid's surface tension (Park *et al.*, 1999). By slowly changing the surface tension of the solvents during the solvent exchange process, it was hypothesized that the membrane structure would be preserved during the remediation process. Solvents that display lower contact angles on a polymer surface denote a reduced surface tension (Bialopiotrowicz & Jańczuk, 2002).

The solvent exchange method described in Section 3.4 was used to remediate the contaminated CA membranes. The surface tensions of the solvents used in this experiment are shown in Table 4.6. The membrane samples were soaked in a series of solvents that gradually increased, then decreased, in surface tension. The contact angle of the ethanol-water solutions decreased with decreasing water content, as shown in Figure 4.15, denoting a gradual change in surface tension during the solvent exchange process. Complete spreading of the liquid on the surface of the CA film was observed for cyclohexane, isopropanol, ethanol and 80% aq. ethanol. Excess lubricant was visibly removed from the membrane module during the first cyclohexane rinse.

Table 4.6: Surface tensions of solvents at 25°C and 1atm (Haynes, 2012).

Solvent	**γ [mN/m]**
Cyclohexane	24.16
Isopropanol	20.93
Ethanol	21.97
Water	71.99

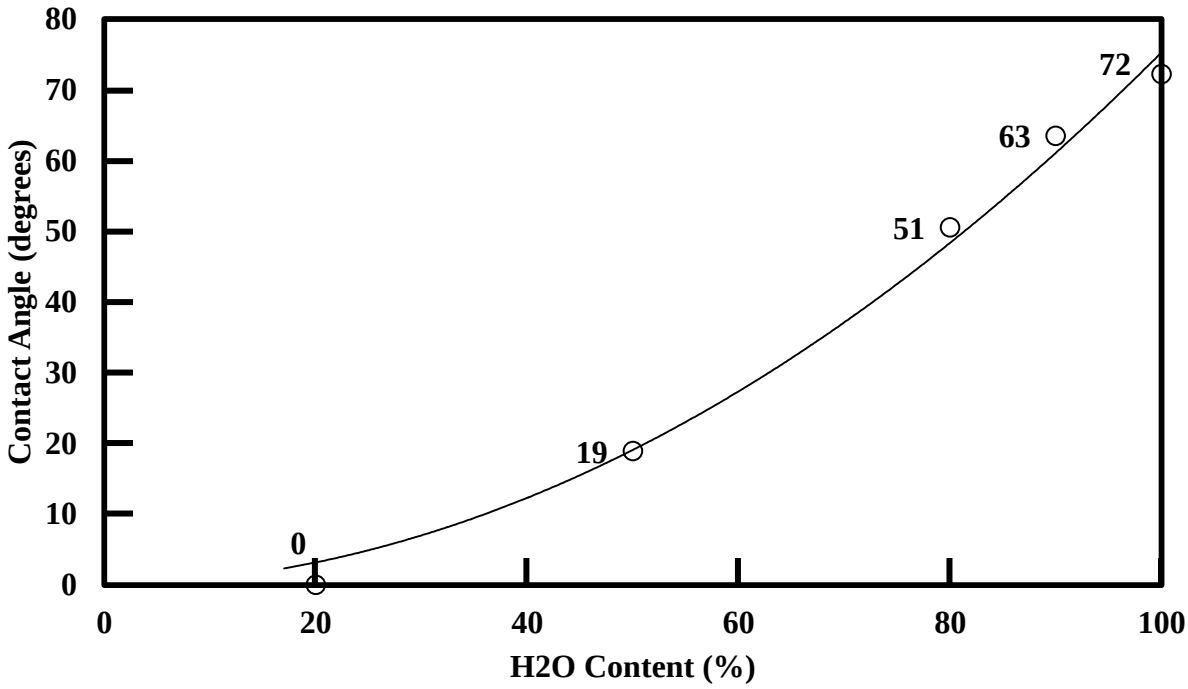

Figure 4.15: Contact angles of for ethanol-water solutions on flat-sheet CA at 298K.

Contaminated membrane samples that were remediated using the solvent exchange method did not appear to fully recover to their original permeance values, as shown in Figure 4.16. When compared to the contaminated membrane samples, the remediated membranes were actually found to perform worse, despite the visual removal of some of the lubricant. Repeating the solvent exchange process on a pristine membrane sample produced similar results, as seen in Figure 4.17. The performance loss of the remediated membranes follows the same trend as the contaminated membranes, with the highest permeating gases displaying the greatest decreases in transport, as seen in Figures 4.16 and 4.17.

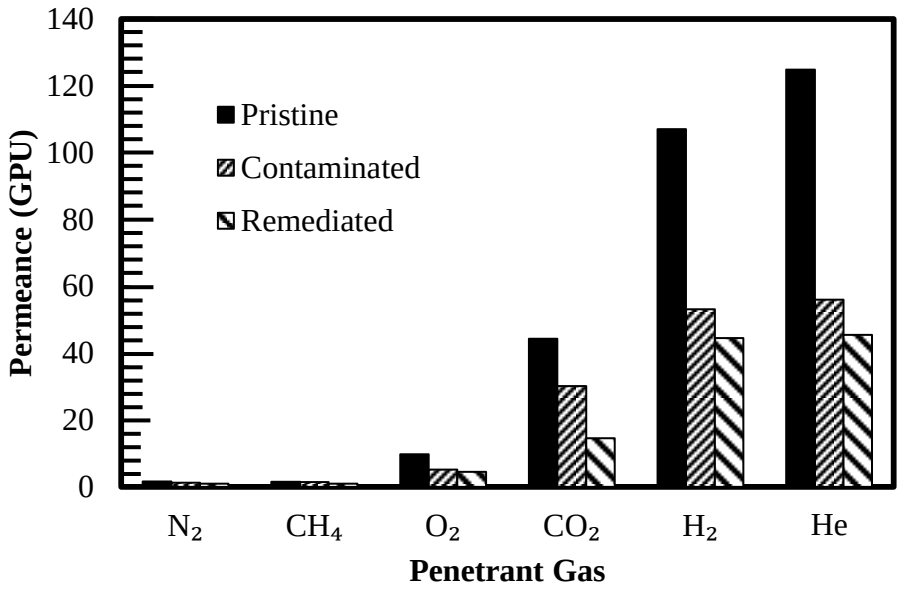

Figure 4.16: Membrane performance before/after contamination and after solvent exchange remediation; Module #2, 500kPa, 303K.

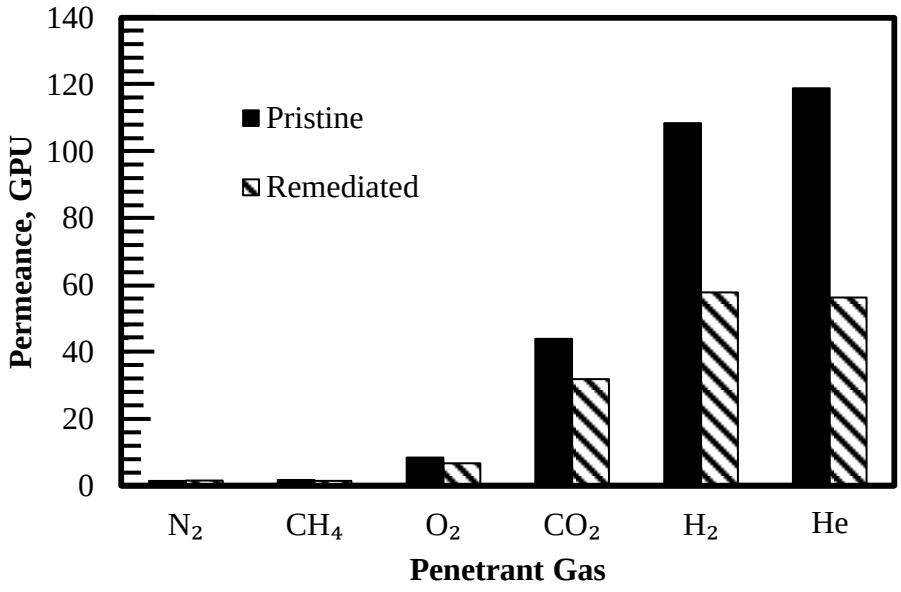

Figure 4.17: Membrane performance before/after solvent exchange remediation; Module #4, 500kPa, 303K.

Permeation through the remediated membranes was independent of pressure and found to follow the order of $N_2 < CH_4 < O_2 < CO_2 < H_2 < He$, as shown in Figure 4.18. Figure 4.19 shows the selectivity of the remediated membranes. The reduced transport of higher permeating gases resulted in lower selectivities than the pristine membranes. Similar decreases in permeation and selectivity were observed at different temperatures, as shown in Figure 4.20 and Figure 4.21. The loss in selectivity may be attributed to a structural change in the membrane. It has become well known that water-wet CA membranes may undergo structural changes or even collapse if the membrane drying conditions are not properly controlled (Baker, 2004a).

In the absence of contamination or membrane defects, the reduction in permeance and selectivity suggests the presence of significant substructure resistance, as described in Section 2.5. The immersion of the hollow fibres into polar solvents may have disrupted the membrane morphology due to the hydroxyl-hydroxyl interactions between the polymer and solvents. This disruption may have caused the microporous support layer to become more compact, thereby increasing the membrane resistance to gas transport (Pinnau, 1991). Since gas transport through microporous supports has been shown to be governed by Knudsen diffusion, this change in the membrane morphology may be the cause of the decrease in both the permeance and selectivity.

A simple estimation of this effect can be determined by comparing the relative resistance of selective layer (R_2) to that of the microporous support (R_3). The resistance to mass transport in the pristine membrane is mostly attributed to the selective layer, and it was assumed that this value did not change after the remediation process. The value for R_3 was then obtained from the increase in resistance following the remediation process, as shown in Table 4.7.

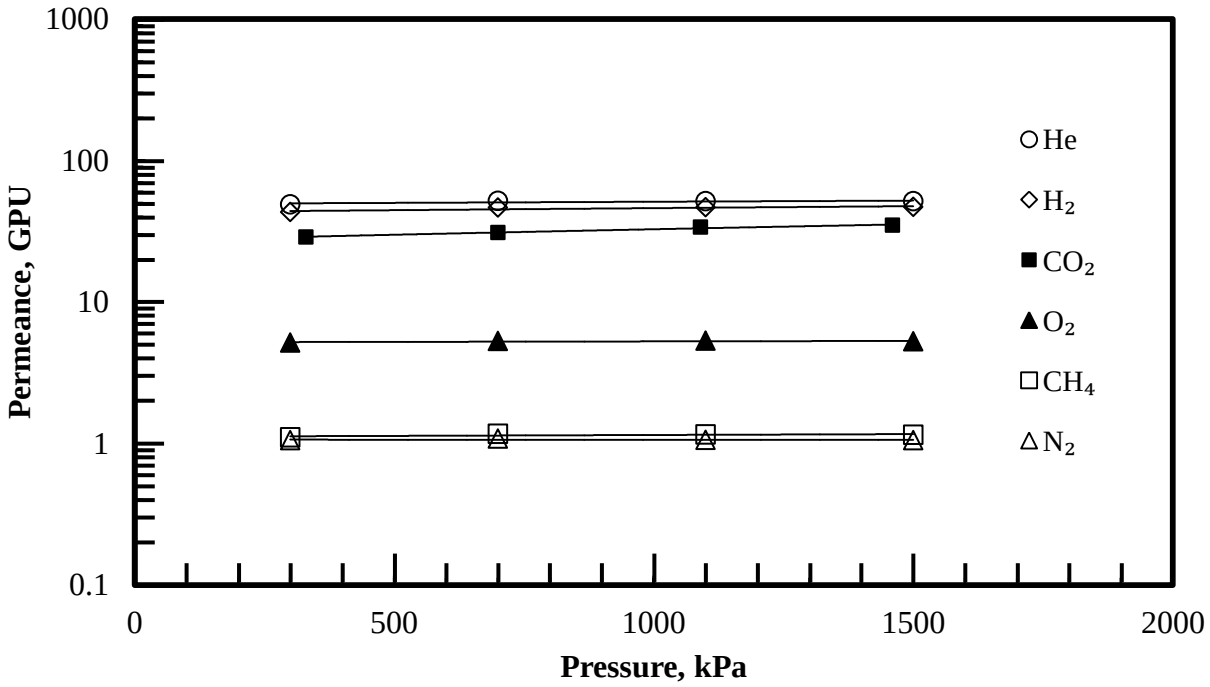

Figure 4.18: Effect of feed pressure on the permeance of a solvent exchange remediated membrane; Module #4, 300K.

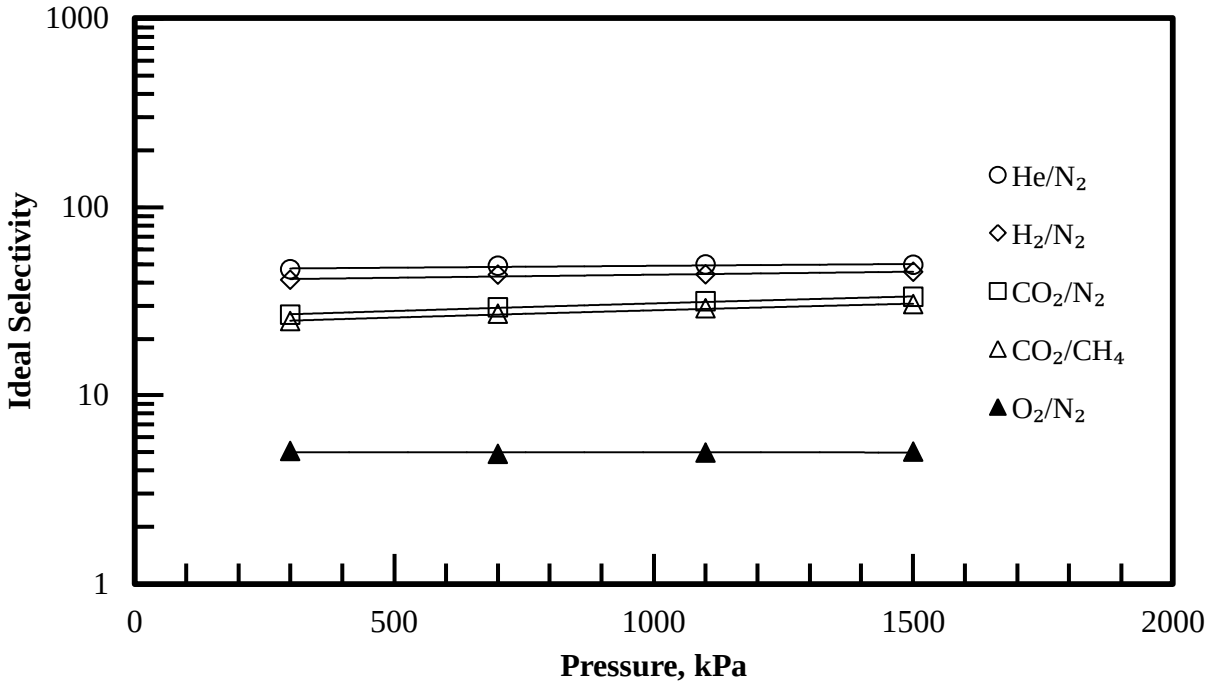

Figure 4.19: Effect of feed pressure on the selectivity of a solvent exchange remediated membrane; Module #4, 300K.

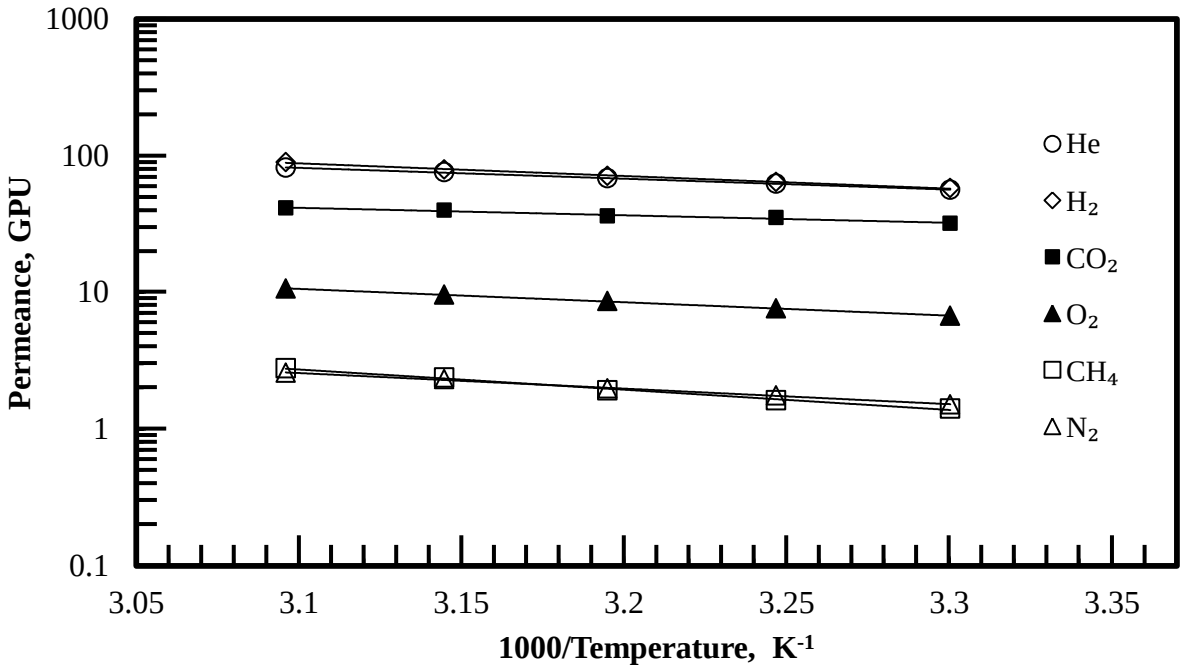

Figure 4.20: Effect of operating temperature on the permeance of a solvent exchange remediated membrane; Module #4, 500kPa.

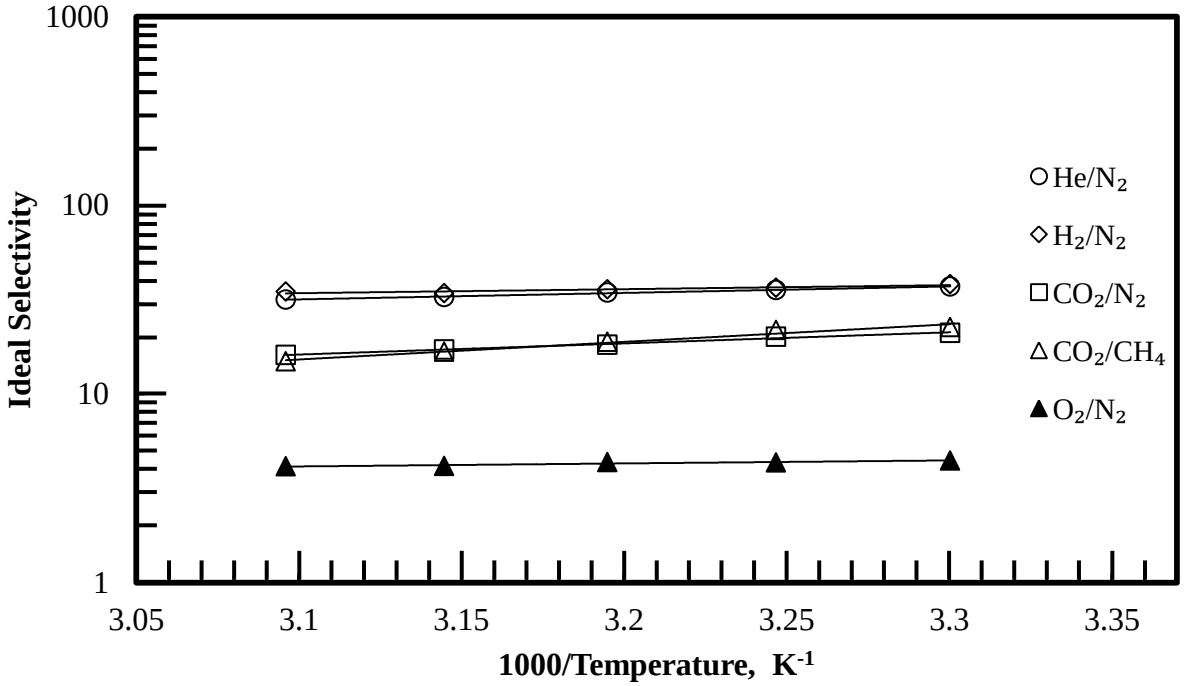

Figure 4.21: Effect of operating temperature on the selectivity of a solvent exchange remediated membrane; Module #4, 500kPa.

If the ratio between R_2 and R_3 is less than 10, the membranes can be said to be operating with less than 90% of the intrinsic selectivity of the polymer (Pinnau, 1991).

Table 4.7: Relative resistance between the selective layer and microporous support; Module #4, 1500kPa, 300K.

Gas	**R_2 [10^{-10} s.Pa/mol]**	**R_{Total} [10^{-10} s.Pa/mol]**	**$R_3 = R_{Total} - R_2$ [10^{-10} s.Pa/mol]**	**R_2/R_3**
N_2	861	1174	313	2.75
CH_4	790	1074	284	2.78
O_2	148	235	87.6	1.68
CO_2	28.2	35.5	7.33	3.84
H_2	11.8	26.4	14.6	0.81
He	10.4	24.0	13.6	0.77

The above result is merely an approximation; clearly, after solvent exchange remediation, the membrane substructure has undergone a significant change, resulting in a drastic increase in the resistance of the sublayer.

Nevertheless, the solvent exchange method used in this study is shown not to be an effective technique for remediating contaminated CA membranes. Despite the gradual change in surface tension during the remediation process, a significant amount of substructure resistance is created as a result of remediation process, resulting in a performance loss that is similar to contamination.

4.3.2 Remediation with Cyclohexane

The cyclohexane remediation method described in Section 3.4 was used to remediate contaminated CA membranes as an alternative to the solvent exchange remediation method. Excess lubricant was visibly removed from the membrane module during the cyclohexane rinse.

The gas transport properties of the contaminated membranes markedly improved after cyclohexane remediation, as shown in Figure 4.22. Note that to test whether cyclohexane affected the CA membrane, cyclohexane treatment was also performed on pristine CA membranes, and no considerable change in the permeance or selectivity of the membranes was observed, as shown in Figure 4.23. This implies that the membrane morphology was not significantly affected by the presence of cyclohexane, presumably due to the lack of hydrogen bonding interactions between the polymer and the solvent. Gas permeability through the remediated membranes remained independent of pressure, and closely mirrored the permeance and selectivity of pristine membranes, as shown in Figures 4.24 and 4.25. The effect of temperature on the permeance and selectivity of remediated membranes was also similar to that of pristine membranes, as shown in Figures 4.26 and 4.27.

All membrane samples were shown to have regained their original permselectivity after remediation with cyclohexane, regardless of any previous contamination. This implies that the lubricant itself did not adversely affect the membrane structure. This also suggests that the lubricant was not able to penetrate through the membrane, even in the presence of cyclohexane. This could be attributed to the large sizes of the heavy hydrocarbon molecules in the lubricant that were unable to penetrant the non-porous selective layer of the membrane, even at elevated temperatures and pressures. From these results, it can be presumed that the lubricant formed a distinct layer over top of the membranes and did not dissolve into the membrane structure, which has been the basis used in the analysis of membrane permselectivity after contamination and remediation with the solvent exchange method.

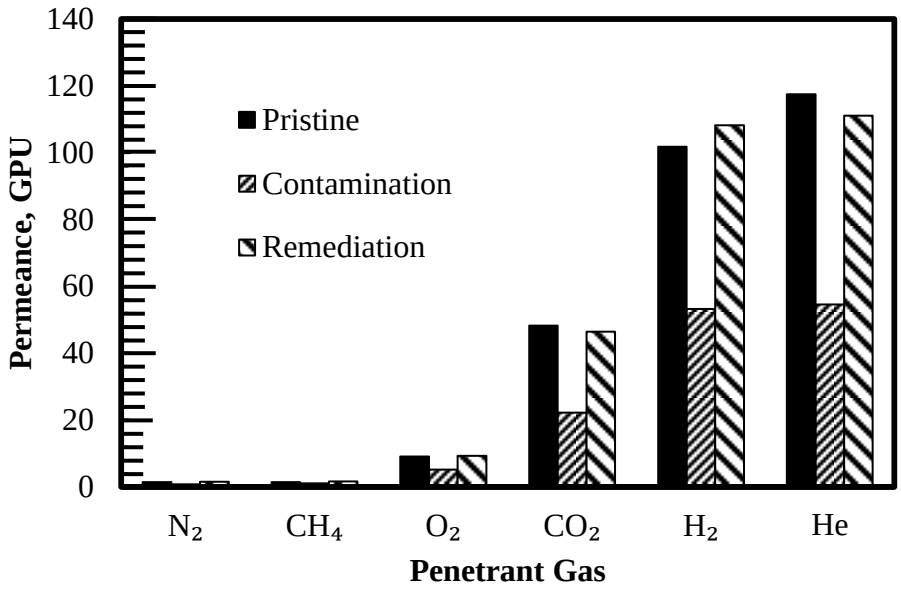

Figure 4.22: Membrane performance before/after contamination and cyclohexane treatment; Module #6, 500kPa, 303K.

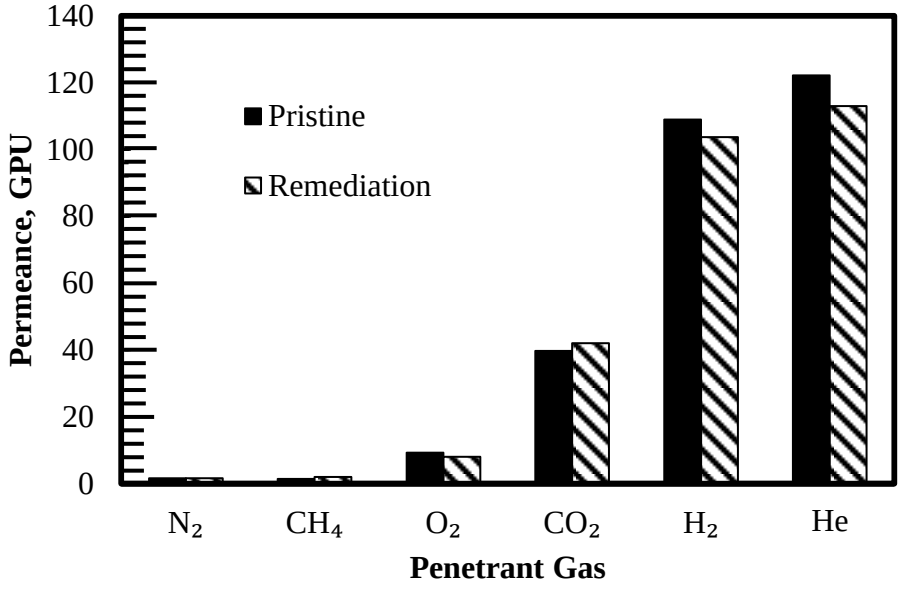

Figure 4.23: Membrane performance before/after cyclohexane treatment; Module #8, 500kPa, 303K.

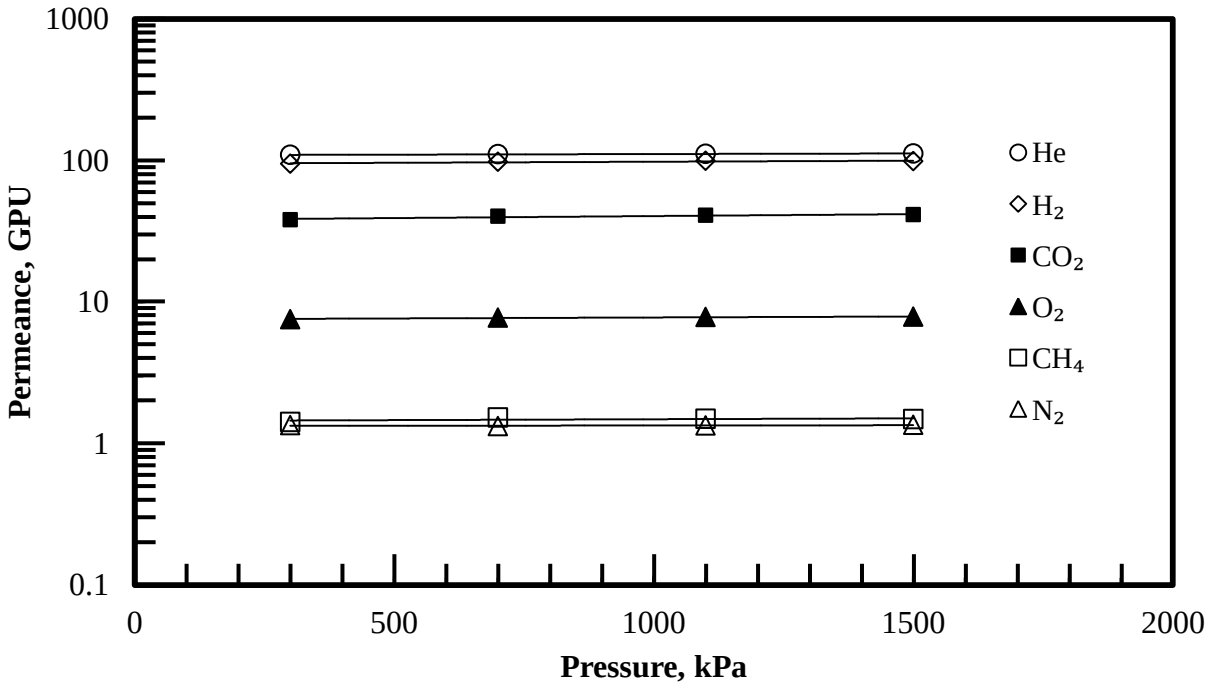

Figure 4.24: Effect of feed pressure on the permeance of a cyclohexane remediated membrane; Module #8, 300K.

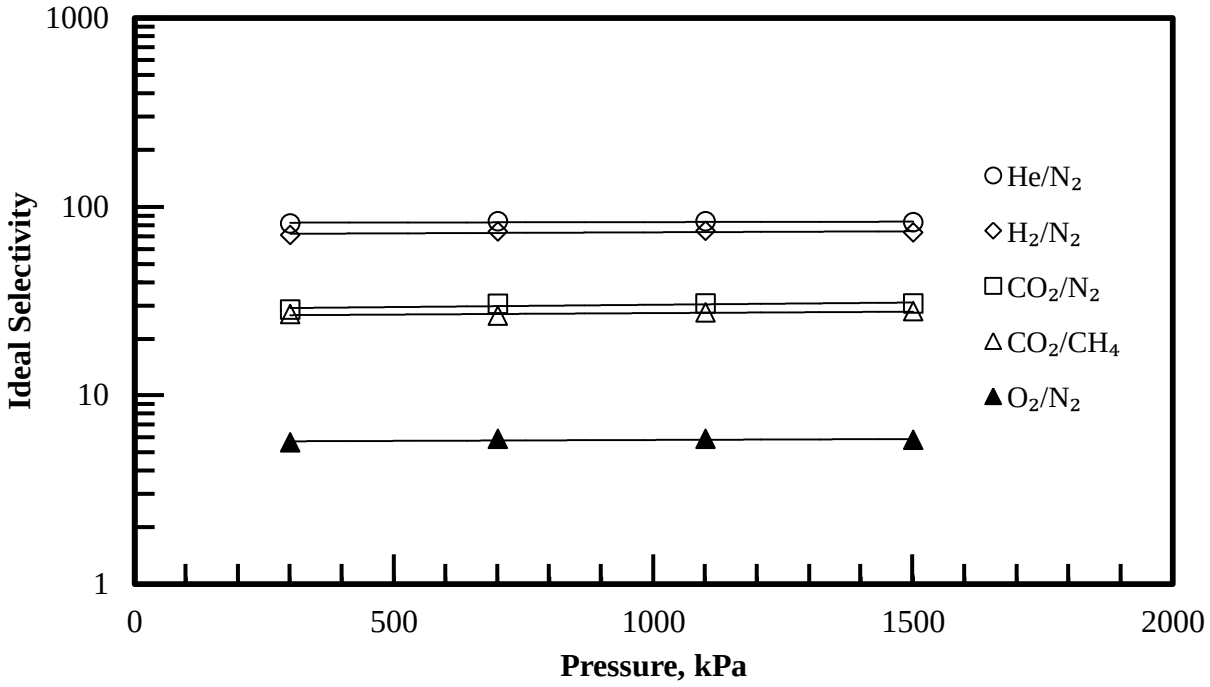

Figure 4.25: Effect of feed pressure on the selectivity of a cyclohexane remediated membrane; Module #8, 300K.

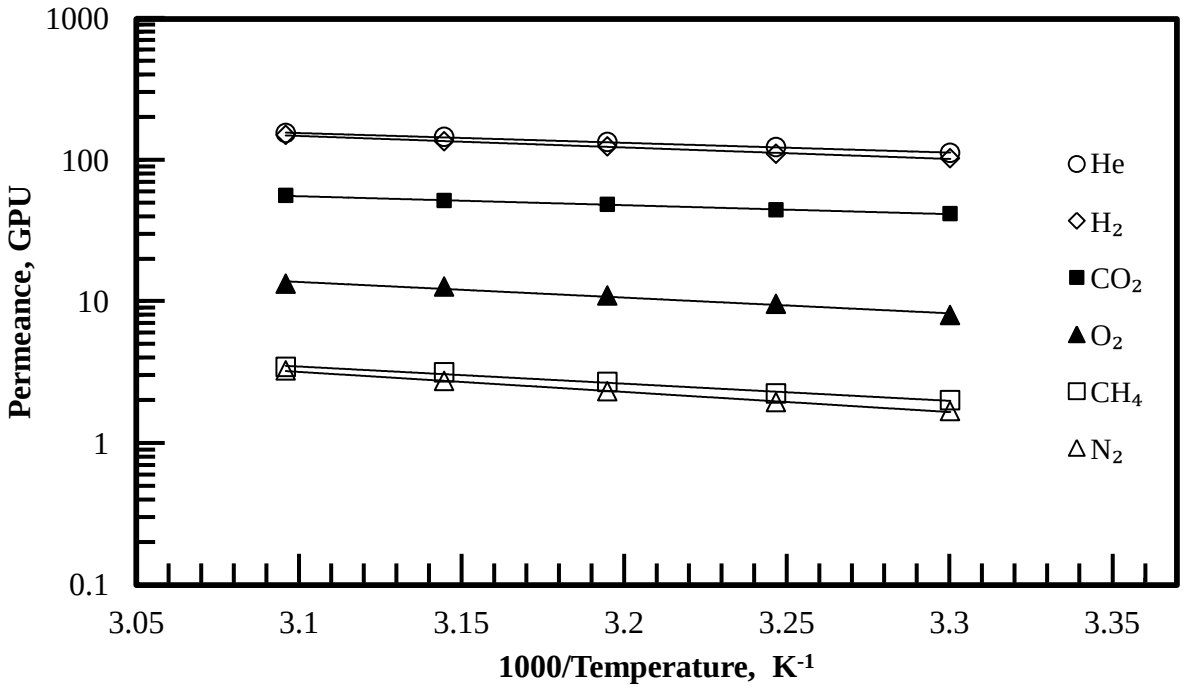

Figure 4.26: Effect of operating temperature on the permeance of a cyclohexane remediated membrane; Module #8, 500kPa.

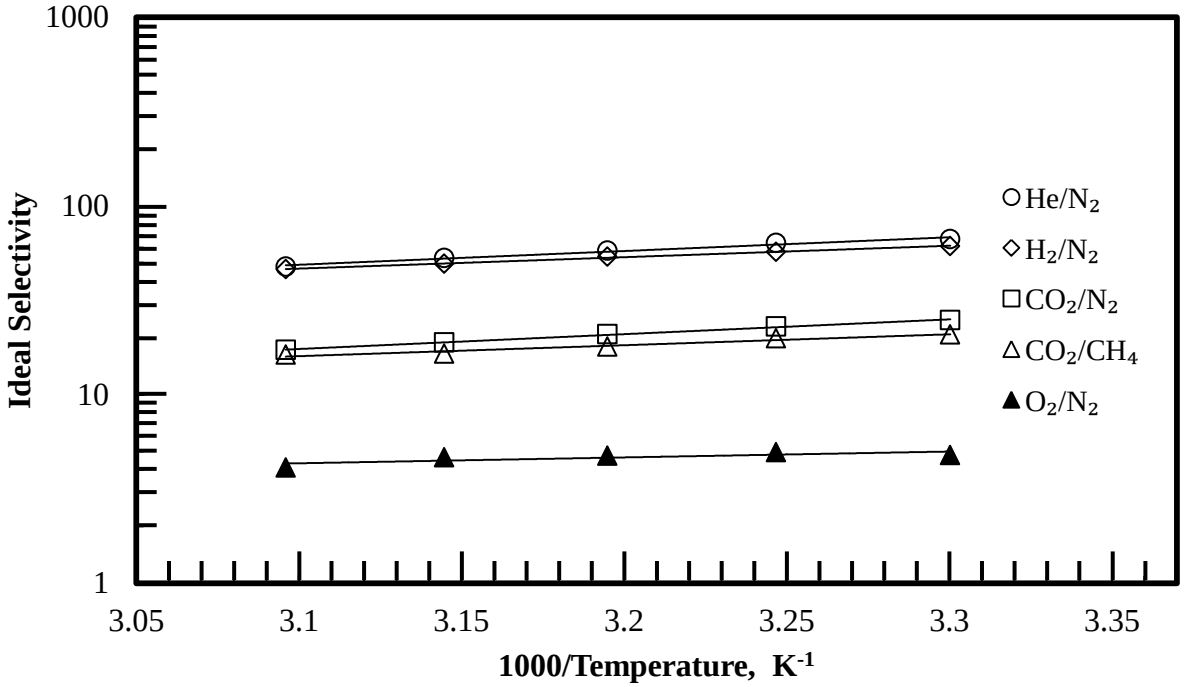

Figure 4.27: Effect of operating temperature on the selectivity of a cyclohexane remediated membrane; Module #8, 500kPa.

It is interesting to note that most gases even displayed a slight increase in permeance after cyclohexane treatment, as shown in Table 4.8. The consistently higher rates of permeation may be attributed to the conditioning of the membrane by cyclohexane. The sorption of cyclohexane into the membrane could have increased the free volume of the polymer, which favours diffusive transport through the membrane. This would have resulted in enhanced diffusion for all penetrants through the membrane. Any increase in diffusive transport typically results in greater permeance gains for larger molecules, as shown in Table 4.8, where some of the largest gains are shown to occur for N_2 and CH_4. Since the hollow fibres used in this study have been aged for over 2 years, it is expected that conditioning of the membrane may have a more pronounced effect due to the compact structure of the polymer. Since the hollow fibres were allowed to dry overnight after the cyclohexane treatment was conducted, significant relaxation of the polymer structure may have reduced the conditioning effects before any subsequent testing, returning the membrane to its original permselectivity.

Of the two remediation methods used in this study, cyclohexane extraction appears to be the most effective in restoring the separation performance after heavy hydrocarbon contamination. This appears to be attributed to the lack of polymer-solvent interactions between cyclohexane and CA, as opposed to the hydroxyl-hydroxyl interactions present in the solvent exchange process. The cyclohexane extraction method can be performed without removing the hollow fibres from their containment and can be easily scaled to suit the full size of hollow fibre modules used in industry (Baker, 2004c).

Table 4.8: Change in permeance after cyclohexane treatment; 1500kPa, 300K.

Gas	Change in Permeance [%]			
	Contam. Samples		Pristine Samples	
	#6	#7	#8	#9
N_2	+17.2	–18.3	+2.38	–9.10
CH_4	+14.1	+4.78	+18.7	+5.42
O_2	+15.9	+5.24	+3.95	+13.6
CO_2	+10.4	+4.77	–6.74	+17.0
H_2	+1.96	–1.71	–1.34	+3.38
He	+4.80	–7.09	–2.00	+11.7

Chapter 5

Conclusions and Recommendations

5.1 General Conclusions

In this study, cellulose acetate hollow fibres were coated with a thin layer of motor oil lubricant to simulate the contamination found in industrial gas streams. Gas permeation tests were conducted on both pristine and contaminated membranes using N_2, CH_4, O_2, CO_2, H_2 and He at pressures ranging from 300 to 1500kPa and at temperatures ranging from 300 to 323K. After contamination, it was observed that greatest reductions in permeance occurred to the highest permeating gases, with a 50-65% reduction in permeance for H_2 and He compared to a 10-30% reduction in permeance for CH_4 and N_2 at 323K. The disproportionate reduction in gas permeance also led to a reduction in the membrane selectivity.

The changes in membrane permeance were analyzed in terms of gas transport through the lubricant layer based on the resistance model. It was shown that the lubricant layer was permselective based on solubility. The thickness of the lubricant layer on the membrane surface was estimated to be in the range of 3-33μm.

In this study, solvent extraction was used to remove heavy hydrocarbon contamination from CA membranes without hindering membrane performance. Remediation of the CA fibres was conducted using two different solvent treatment methods:

(1) Solvent exchange. The hollow fibres were submerged in a series of solutions of varying organic content. By imitating the solvent exchange method used to fabricate asymmetric membranes, it was anticipated that any change in the membrane properties due to contamination could be reversed. Unfortunately, the solvent exchange protocol did not appear to be particularly suitable for remediating contaminated CA membranes as the remediated membrane did not perform much better than the contaminated membrane. It is speculated that hydrogen bonding interactions between the solutions and the polymer disrupted the membrane morphology enough to create a significant amount of substructure resistance that lowered both the permeance and selectivity of the membrane.

(2) Solvent extraction. This involved a direct extraction of the contaminant using cyclohexane. This method was able to restore membrane performance after contamination, and was found to have essentially no or little effect on the membrane structure. Slight increases in permeance were found in certain samples after remediation, possibly due to conditioning of the membrane by cyclohexane.

The solvent extraction is only one step used in the solvent exchange method. It was the polar solvents used in the solvent exchange that were believed to have caused the collapse or compaction of the membrane substructure, which resulted in a reduction in membrane permselectivity.

Heavy hydrocarbon contamination is a concern for industrial membrane separation. The use of solvent extraction developed in this study provides a cost-effective solution to remediation of contaminated membranes, allowing for effective repair of membranes instead of the expensive replacement with new membranes.

5.2 Recommendations

This study used single-component feed streams to evaluate the performance of gas separation membranes. Industrial separations involve gas mixtures, which may have different transport behaviors because of penetrant-penetrant interactions. When two or more penetrants are highly soluble in a polymer, they may compete for the sorption sites in the polymer before diffusing through the membrane. Due to the competitive sorption effects, the selectivity may be lower than what is estimated from pure gas measurements (Matteucci *et al.*, 2006). Furthermore, the presence of plasticising components in a multicomponent feed stream can increase the permeability of all penetrants, which often causes a reduction in selectivity. In order to properly account for these effects, membranes should be tested using gas mixtures of interest. For example, studies with applications in natural gas processing often use 10/90 CO_2/CH_4 mixtures to simulate industrial feed streams (White, 1995; Al-Juaied & Koros, 2006). In order to properly evaluate the effects of heavy hydrocarbons on industrial gas separations, further testing must include a relevant multicomponent feed stream.

Accurate determination of gas transport properties in heavy hydrocarbons may prove effective in identifying their presence, especially in the case of varying feed streams. This will allow for the detection of membrane contamination by heavy hydrocarbons amongst other effects such as plasticization and conditioning. The lubricant used in this study was considered to be a model of a heavy hydrocarbon contaminant, which was composed of an undisclosed composition of organic components and additives ("*MSDS - Pennzoil® SAE 10W-30 Motor Oil"*, 2010). By defining the specific contaminants involved in a given separation process, the gas transport through contaminated membranes may become easier to predict and analyze.

The applicability of solvent extraction as a remediation method lies in the compatibility of the solvent with the membrane material and its contaminants. As shown in this study, the selection of an incompatible solvent can negatively affect the membrane performance, possibly causing irreparable damage. The variety of polymers used for industrial gas separation membranes have different susceptibilities, and the application of the remediation methods described here would require the rigorous testing to properly select solvents that can remove contaminants of interest while maintaining the membrane undamaged.

Bibliography

Al-Juaied, M., & Koros, W. J. (2006). Performance of natural gas membranes in the presence of heavy hydrocarbons. *Journal of Membrane Science, 274*(1-2), 227-243.

Baker, R. W. (2004a). Gas separation. In *Membrane Technology and Applications* (2nd ed., pp. 354). Wiley.

Baker, R. W. (2004b). Membrane transport theory. In *Membrane Technology and Applications* (2nd ed., pp. 15-88). Wiley.

Baker, R. W. (2004c). Membranes and modules. In *Membrane Technology and Applications* (2nd ed., pp. 89-160). Wiley.

Baker, R. W. (2004d). Overview of membrane science and technology. In *Membrane Technology and Applications* (2nd ed., pp. 1-14). Wiley.

Baker, R. W. (2008). Natural gas processing with membranes: an overview. *Industrial & Engineering Chemistry Research, 47*(7), 2109-2121.

Bernardo, P. (2009). Membrane gas separation: A review/state of the art. *Industrial & Engineering Chemistry Research, 48*(10), 4638-4663.

Bialopiotrowicz, T., & Jańczuk, B. (2002). The wettability of a cellulose acetate membrane in the presence of bovine serum albumin. *Applied Surface Science, 201*(1-4), 146-153.

Breck, D. W. (1974). *Zeolite Molecular Sieves : Structure, Chemistry, and Use*. R.E. Krieger, 1984.

Brown, R. N. (1997). *Compressors : Selection and Sizing* (2nd ed.). Gulf Publishing Company.

Danielson, P. (2001). Making the oil-sealed vs oil-free decision.(vacuum pumps, environmental considerations). *R & D Magazine, 43*(7), 66.

Donohue, M. D., Minhas, B. S., & Lee, S. Y. (1989). Permeation behavior of carbon-dioxide methane mixtures in cellulose-acetate membranes. *Journal of Membrane Science, 42*(3), 197-214.

Enscore, D. J., Hopfenberg, H. B., Stannett, V. T., & Berens, A. R. (1977). Effect of prior sample history on n-hexane sorption in glassy polystyrene microspheres. *Polymer, 18*(11), 1105-1110.

Etminan, S. R., Maini, B. B., Hassanzadeh, H., & Chen, Z. (2009). Determination of concentration dependant diffusivity coefficient in solvent gas heavy oil system. *SPE Annual Technical Conference and Exhibition,* New Orleans, Louisiana, USA (SPE 124832).

Etminan, S. R. (2010). Constant- pressure technique for gas diffusivity and solubility measurements in heavy oil and bitumen. *Energy & Fuels, 24*(1), 533-549.

Fischer, S., Thummler, K., Volkert, B., Hettrich, K., Schmidt, I., & Fischer, K. (2008). Properties and applications of cellulose acetate. *Macromolecular Symposia, 262*(1), 89-96.

Ghosal, K., Chern, R. T., & Freeman, B. D. (1996). Effect of basic substituents on gas sorption and permeation in polysulfone. *Macromolecules, 29*(12), 4360-4369.

Ghosal, K. (1994). Gas separation using polymer membranes: An overview. *Polymers for Advanced Technologies, 5*(11), 673-697.

Gibbons, G. C. (1953). The moisture regain of methylcellulose and cellulose acetate. *Journal of the Textile Institute Transactions, 44*(5), 201.

Haynes, W.M. (Ed.) (2012). *CRC Handbook of Chemistry and Physics* (92nd ed.). CRC Press.

Hao, J. H., & Wang, S. (1998). Influence of quench medium on the structure and gas permeation properties of cellulose acetate membranes. *Journal of Applied Polymer Science, 68*(8), 1269-1276.

Haraya, K., Obata, K., Hakuta, T., & Yoshitome, H. (1986). Permeation of gases through a symmetric cellulose acetate membrane. *Journal of Chemical Engineering of Japan, 19*(5), 464.

Henis, J. M. S. (1981). Composite hollow fiber membranes for gas separation: The resistance model approach. *Journal of Membrane Science, 8*(3), 233-246.

Huang, R. Y. M., & Feng, X. (1993). Resistance model approach to asymmetric polyetherimide membranes for pervaporation of isopropanol/water mixtures. *Journal of Membrane Science, 84*(1-2), 15-27.

Huang, Y., & Paul, D. R. (2004). Physical aging of thin glassy polymer films monitored by gas permeability. *Polymer, 45*(25), 8377-8393.

Hugman, R. H., Springer, P. S., & Vidas, E. H. (1990). *Chemical composition in discovered and undiscovered natural gas in the lower-48 united states.* Arlington, VA: Energy and Environmental Analysis, Inc. (No. GRI-90/0248).

Jamialahmadi, M., Emadi, M., & Müller-Steinhagen, H. (2006). Diffusion coefficients of methane in liquid hydrocarbons at high pressure and temperature. *Journal of Petroleum Science and Engineering, 53*(1-2), 47-60.

Jones, C. W., & Koros, W. J. (1994). Carbon molecular - sieve gas separation membranes .2. Regeneration following organic exposure. *Carbon, 32*(8), 1427-1432.

Kamide, K., & Saito, M. (1985). Thermal analysis of cellulase acetate solids with total degrees of substitution of 0.49, 1.75, 2.46, and 2.92. *Polymer, 17*(8), 919.

Kerry, F. G. (2007). *Industrial Gas Handbook : Gas Separation and Purification*. CRC Press.

Korsten, H. (2001). Viscosity of liquid hydrocarbons and their mixtures. *AIChE Journal, 47*(2), 453-462.

Law, R. (2004). Cellulose acetate in textile application. *Macromolecular Symposia, 208*, 255-265.

Loeb, S., & Sourirajan, S. (1963). Sea water demineralization by means of an osmotic membrane. In *Saline Water Conversion-II* (Advances in Chemistry Series Number 28, pp. 117-132). Washington, DC: ACS.

MacDonald, W., & Pan, C. (1974). In Alberta Helium Limited (Ed.), *Method for drying water-wet membranes*, US Patent No. 3,842,515.

Majors, G. (2001). Compressor lubrication. In P. C. Hanlon (Ed.), *Compressor Handbook* (pp. 18.1). McGraw Hill.

Manos, P. (1978). *Solvent drying of cellulose ester membranes*, US Patent No. 4,068,387.

Matteucci, S., Yampolskii, Y., Freeman, B. D., & Pinnau, I. (2006). Transport of gases and vapors in glassy and rubbery polymers. In Y. P. Yampolskii, I. Pinnau & B. D. Freeman (Eds.), *Materials Science of Membranes for Gas and Vapour Separation* (pp. 159-48). Wiley.

Matthews, M. A. (1987). High- temperature diffusion of hydrogen, carbon monoxide, and carbon dioxide in liquid n-heptane, n-dodecane, and n-hexadecane. *Journal of Chemical & Engineering Data, 32*(3), 319-322.

Merkel, T. C., Bondar, V. I., Nagai, K., Freeman, B. D., & Pinnau, I. (2000). Gas sorption, diffusion, and permeation in poly(dimethylsiloxane). *Journal of Polymer Science Part B - Polymer Physics, 38*(3), 415-434.

Merten, U., Beach, S., & Gantzel, P. K. (1968). *Method and apparatus for gas separation by diffusion*, US Patent No. 3,415,038.

Minhas, B. S., Matsuura, T., & Sourirajan, S. (1987). Formation of asymmetric cellulose acetate membranes for the separation of carbon dioxide-methane gas mixtures. *Industrial & Engineering Chemistry Research, 26*(11), 2344-2348.

MSDS - Pennzoil® SAE 10W-30 motor oil. (2010). Retrieved September/11, 2010, from http://www.epc.shell.com.

Mulder, M. (1991). *Basic Principles of Membrane Technology* (1st ed.). Springer.

Nakai, Y., Yoshimizu, H., & Tsujita, Y. (2005). Enhanced gas permeability of cellulose acetate membranes under microwave irradiation. *Journal of Membrane Science, 256*(1-2), 72-77.

Nguyen, X. Q., Sipek, M., Hynek, V., & Nguyen, Q. T. (1994). Flow method for study of gas - transport in polymers - application to the study of oxygen, nitrogen, and carbon-dioxide permeation through cellulose-acetate membranes. *Journal of Applied Polymer Science, 54*(12), 1817-1825.

Noble, R. D., & Koval, C. A. (2006). Review of facilitated-transport membranes. In Y. P. Yampolskii, I. Pinnau & B. D. Freeman (Eds.), *Materials science of membranes for gas and vapour separation* (pp. 411-436). Wiley.

Park, H. C., Moon, Y. S., Rhee, H. W., Won, J., Kang, Y. S., & Kim, U. Y. (1999). Effect of solvent exchange on the morphology of asymmetric membranes. In I. Pinnau, & B. D. Freeman (Eds.), *Membrane Formation and Modification* (pp. 110-124) ACS.

Pennzoil® motor oil - technical data sheet. (2010). Retrieved September 11, 2010, from http://www.epc.shell.com

Petropoulos, J. H. (1994). Mechanisms and theories for sorption and diffusion of gases in polymers. In D. R. Paul, & Y. P. Yampolskii (Eds.), *Polymeric Gas Separation Membranes* (pp. 17082-82). CRC Press.

Pfromm, P. H. (2006). The impact of physical aging of amorphous glassy polymers on gas separation membranes. In Y. P. Yampolskii, I. Pinnau & B. D. Freeman (Eds.), *Materials Science of Membranes for Gas and Vapour Separation* (pp. 293-306). Wiley.

Pinnau, I., & Freeman, B. D. (2000). Formation and modification of polymeric membranes: Overview. In I. Pinnau, & B. D. Freeman (Eds.), *Membrane Formation and Modification* (pp. 1-22). ACS Symp. Ser. 744: ACS.

Pinnau, I. (1991). Relationship between substructure resistance and gas separation properties of defect-free integrally skinned asymmetric membranes. *Industrial & Engineering Chemistry Research, 30*(8), 1837-1840.

Pinnau, I. (1992). Influence of quench medium on the structures and gas permeation properties of polysulfone membranes made by wet and dry/ wet phase inversion. *Journal of Membrane Science, 71*(1-2), 81-96.

Poling, B. E., Prausnitz, J. M., & O'Connell, J. P. (2001). *The Properties of Gases and Liquids* (5th ed.). McGraw-Hill.

Puleo, A. C., Paul, D. R., & Kelley, S. S. (1989). The effect of degree of acetylation on gas sorption and transport behavior in cellulose acetate. *Journal of Membrane Science, 47*(3), 301.

Robeson, L. M. (1991). Correlation of separation factor versus permeability for polymeric membranes. *Journal of Membrane Science, 62*(2), 165-185.

Rodden, J. B. (1988). Mutual diffusion coefficients for several dilute solutes in n-octacosane and the solvent density at 371-534 K. *Journal of Chemical & Engineering Data, 33*(4), 450-453.

Rowe, B. W., Freeman, B. D., & Paul, D. R. (2007). Effect of sorbed water and temperature on the optical properties and density of thin glassy polymer films on a silicon substrate. *Macromolecules, 40*(8), 2806-2813.

Rowe, B. W., Freeman, B. D., & Paul, D. R. (2010). Influence of previous history on physical aging in thin glassy polymer films as gas separation membranes. *Polymer, 51*(16), 3784-3792.

Rustemeyer, P. (2004a). In Rustemeyer P. (Ed.), *Cellulose Acetates: Properties and Applications* (Macromolecular Symposia 208). Wiley.

Rustemeyer, P. (2004b). History of CA and evolution of the markets. *Macromolecular Symposia, 208*, 1-6.

Sanders, E. S. (1988). Penetrant- induced plasticization and gas permeation in glassy polymers. *Journal of Membrane Science, 37*(1), 63-80.

Schell, W. (1989). Recent advances in cellulosic membranes for gas separation and pervaporation. *Gas Separation & Purification, 3*(4), 162-169.

Shibata, T. (2004). Cellulose acetate in separation technology. *Macromolecular Symposia, 208*, 353-369.

Shieh, J., & Chung, T. S. (1998). Effect of liquid-liquid demixing on the membrane morphology, gas permeation, thermal and mechanical properties of cellulose acetate hollow fibers. *Journal of Membrane Science, 140*(1), 67-79.

Sidhoum, M. (1988). Asymmetric cellulose acetate hollow fibers: Studies in gas permeation. *AIChE Journal, 34*(3), 417-425.

Struik, L. C. E. (1978). *Physical Aging in Amorphous Polymers and Other Materials*. Elsevier.

Tharanivasan, A. (2004). Comparison of three different interface mass transfer models used in the experimental measurement of solvent diffusivity in heavy oil. *Journal of Petroleum Science and Engineering, 44*(3-4), 269-282.

Tsai, F. J., Kang, D., & Anand, M. (1995). Thin-film-composite gas separation membranes: On the dynamics of thin film formation mechanism on porous substrates. *Separation Science and Technology, 30*(7-9), 1639-1652.

Visser, T., Koops, G. H., & Wessling, M. (2005). On the subtle balance between competitive sorption and plasticization effects in asymmetric hollow fiber gas separation membranes. *Journal of Membrane Science, 252*(1-2), 265-277.

White, L. S. (1995). Properties of a polyimide gas separation membrane in natural gas streams. *Journal of Membrane Science, 103*(1-2), 73-82.

Wijmans, J. G., & Baker, R. W. (2006). The solution- to diffusion model: A unified approach to membrane permeation. In Y. P. Yampolskii, I. Pinnau & B. D. Freeman (Eds.), *Materials Science of Membranes for Gas and Vapour Separation* (pp. 159-189). Wiley.

Zainal, S., Vai Yee, H., Saaid, I. M., & Jelani, J. (2009). An evaluation of gas diffusivity measurement in reservoir fluid from low to high pressure systems for oil recovery applications. *International Petroleum Technology Conference,* Doha, Qatar. (IPTC 13638)

Zhang, Y. P., Hyndman, C. L., & Maini, B. B. (2000). Measurement of gas diffusivity in heavy oils. *Journal of Petroleum Science and Engineering, 25*(1-2), 37-47.

Zugenmaier, P. (2004). Characterization and physical properties of cellulose acetates. *Macromolecular Symposia, 208*, 81-166.

Appendix A

Estimates of Gas Solubility in Hydrocarbons using ASTM Guidelines

The American Society for Testing and Materials (ASTM) has developed internationally-recognized standards for determining the physical properties of industrially-relevant materials. These standards have been used within this thesis to estimate the solubility of gases within Pennzoil® Motor Oil 10W-30. The physical data of Pennzoil® Motor Oil 10W-30 provided by the manufacturer can be seen in Table A.1.

Table A.1: Physical and chemical data for Pennzoil 10W-30 ("*Pennzoil® "*, 2010)**.**

Test	Method	Temperature	Result
Specific Gravity	ASTM D-287	15.6°C	0.872
Viscosity	ASTM D-445	40°C	69.7cSt
Viscosity	ASTM D-445	100°C	10.53cSt

ASTM D-2502 is designated as the "Standard Test Method for Estimation of Mean Relative Molecular Mass of Petroleum Oils from Viscosity Measurements". It uses a correlation referred to as the *H* function to estimate the relative molecular mass of petroleum oils. Using the applicable procedures provided in the ASTM guideline, the mean molecular mass of the motor oil lubricant was determined as follows:

1. Using the tabulations of the *H* function provided in ASTM D-2502, the viscosity of the motor oil at 40°C was found to correspond to an *H* value of approximately 385.

2. Using the viscosity-mean relative molecular mass chart provided in ASTM D-2502, the molecular mass of the motor oil was determined from the value of the *H* function and the viscosity of the motor oil at 100°F, as shown in Figure A.1.

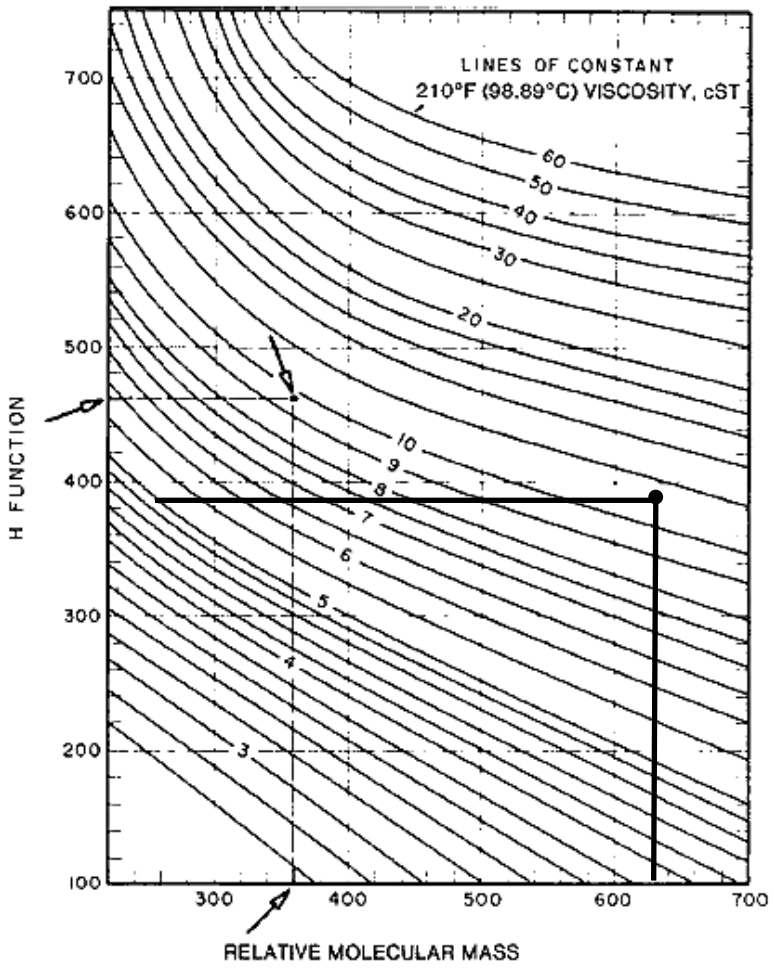

Figure A.1: Viscosity-mean relative molecular mass chart (ASTM 2502).

From the above correlations, the relative molecular mass of the motor oil was estimated to be 595 g/mol.

ASTM D-3827 is designated as the "Standard Test Method for Estimation of Solubility of Gases in Petroleum and Other Organic Liquids." This ASTM method uses the physical properties of the lubricant along with the operating conditions of the experiment to determine the solubility of specific gases within the lubricant.

Sample calculations were based on a system with a feed pressure (p) of 0.5MPa and an operating temperature (T) of 300K. Equations A-1 to A-6 were provided in ASTM D-3827. Using the applicable procedures provided in ASTM D-3827, the solubility of hydrogen in Pennzoil® Motor Oil 10W-30 was estimated as follows:

1. The solubility parameter of the motor oil, δ_1, was determined using Equation A-1 using a density (ρ) of 0.872g/mL.

$$\delta_1(MPa^{1/2}) = 12.03\rho + 7.36 \qquad \text{(A-1)}$$

$$\delta_1 = 12.03\left(\frac{0.872g}{mL}\right) + 7.36 = \mathbf{17.85\ MPa^{1/2}}$$

2. The solubility parameter of the gas (δ_2) was determined from Table A.2.

Table A.2: Solubility Parameters of Gaseous Solutes (ASTM D-3827).

Gas	M_2 [g/mol]	δ_2 at 298K [$MPa^{½}$]
N_2	28	6.04
CH_4	16	9.1
O_2	32	7.75
CO_2	44	14.81
H_2	2	5.52
He	4	3.35

In order to obtain a value for the overall solubility of hydrogen in the appropriate format, several conversions between solubility parameters were conducted.

3. The Ostwald coefficient (L), which is a measure of the solubility of a gas in a liquid at equilibrium, was determined using Equation A-2.

$$L_O = \exp\left[(0.0395(\delta_1 - \delta_2)^2 - 2.66)\left(1 - \frac{273}{T}\right) - 0.303\delta_1 - 0.0241(17.60 - \delta_2)^2 + 5.731\right] \quad \text{(A-2)}$$

$$L_O = \exp\left[(0.0395[17.85 - 5.52]^2 - 2.66)\left(1 - \frac{273}{300}\right) - 0.303(17.85) - 0.0241(17.60 - 5.52)^2 + 5.731\right] = \mathbf{0.5539}$$

4. The Bunsen coefficient (B), which is a measure of the solubility of a gas in a liquid at 273K and 0.10MPa, was determined using Equation A-3. The vapour pressure of the motor oil (p_v) was assumed to be negligible.

$$B = 2697(p - p_v)L_O/T \quad \text{(A-3)}$$

$$B = 2697(0.5 - 0)(0.5539)/(300) = \mathbf{0.2490}$$

5. The density of the motor oil at the operating temperature was determined using Equation A-4.

$$\rho_t(g/mL) = \rho\left(1 - \frac{0.000595(T-288.2)}{\rho^{1.21}}\right) \quad \text{(A-4)}$$

$$\rho_t = (0.872)\left(1 - \frac{0.000595\big((300) - 288.2\big)}{(0.872)^{1.21}}\right) = \mathbf{0.865\ g/mL}$$

6. The overall solubility (G) was determined using Equation A-5.

$$G(mg/kg) = 44.6\ (BM_2)/p_t \quad \text{(A-5)}$$

$$G = 44.6\frac{(0.2490)(2\ g/mol)}{(0.865 g/mL)} = \mathbf{25.68\ mg\ /kg}$$

7. The overall solubility as a mole fraction (X) was calculated using Equation A-6. The molecular weight of the gas (M_2) was taken from Table A.1. The molecular weight of the oil (M_1) was derived from ASTM D-2502.

$$X\left(\frac{mol\ gas}{mol\ oil}\right) = 10^{-6}GM_1/M_2 \quad \text{(A-6)}$$

$$X = 10^{-6}(25.68)\left(\frac{595\frac{g}{mol}}{2\frac{g}{mol}}\right) = \mathbf{0.00764}\ \boldsymbol{\frac{mol\ gas}{mol\ oil}}$$

8. The Henry's law constant (H) was calculated using Equation A.7.

$$H\left(MPa \cdot \boldsymbol{\frac{mol\ oil}{mol\ gas}}\right) = (p - p_v)/X \tag{A-7}$$

$$H = \frac{0.5\ MPa - 0\ MPa}{0.00764\left(\frac{mol\ gas}{mol\ oil}\right)} = \mathbf{65.44}\ \boldsymbol{MPa} \cdot \boldsymbol{\frac{mol\ oil}{mol\ gas}}$$

The Henry's Law constant is independent of pressure and was determined for the gases of interest, as seen in Table A.3. With the Henry's Law constant calculated, the appropriate solubility parameter for membrane permeation could be quickly deduced, as seen in Appendix B.

Table A.3: Henry's Law constants, H $\times 10^4$ MPa·mol/mol.

Temp. [K]	**N_2**	**CH_4**	**O_2**	**CO_2**	**H_2**	**He**
300	8.61	30.2	18.2	112	6.69	2.08
323	9.77	29.2	18.8	91.5	7.85	2.83

Appendix B

Sample Calculations

B.1 Permeance Calculations

The following calculations were conducted for a pristine membrane module that contained 6 strands of hollow fibres at a length of 5.2cm and a diameter 0.02cm. The test gas was pure hydrogen at a gauge pressure of 1500kPa and at an operating temperature of 300K. It took 41.53 seconds for 10.0mL of gas to leave the membrane module.

Flowrate Calculation

The flowrate, ($\dot{V}$), was determined by measuring the amount of gas passing through a bubble flowmeter.

$$\boldsymbol{\dot{V} = \frac{V}{t}} \tag{B-1}$$

where V is the volume of gas and t is the time of measurement.

$$\dot{V} = \frac{10.0\ mL}{41.53\ s} = 2.41 \times 10^{-1}\frac{mL}{s}\left(\frac{1\ cm^3}{1\ mL}\right) = \boldsymbol{2.41 \times 10^{-1}\frac{cm^3}{s}}$$

Flux Calculation

The flux of a given gas (J) was expressed as volumetric flowrate at standard temperature and pressure (STP) per membrane area.

$$\boldsymbol{J = \frac{\dot{V}_{STP}}{A} = \dot{V}\left(\frac{1}{N\pi dL}\right)\left(\frac{273.15\ K}{T_{amb}}\right)\left(\frac{p_{baro}}{101.325\ kPa}\right)} \tag{B-2}$$

where $\dot{V}_{STP}$ is the volumetric flowrate at STP, N is the number of hollow fibres in the samples, d is the outside diameter of the fibre, L is the length of the fibre, T_{amb} is the ambient temperature and p_{baro} is the barometric pressure.

$$J = \left(2.41 \times 10^{-1} \frac{cm^3}{s}\right)\left(\frac{1}{(6)\pi(5.2\ cm)(0.02\ cm)}\right)\left(\frac{273.15\ K}{296\ K}\right)\left(\frac{99.9\ kPa}{101.325\ kPa}\right)$$

$$J = \mathbf{1.01 \times 10^{-1}} \frac{\boldsymbol{cm^3(STP)}}{\boldsymbol{cm^2 \cdot s}}$$

Permeance Calculation

The permeance (Q) was evaluated using a pressure-normalized flux.

$$Q = \frac{J}{\Delta p} \tag{B-3}$$

$$Q = \frac{\left(1.01 \times 10^{-1} \frac{cm^3(STP)}{cm^2 \cdot s}\right)}{1500\ kPa}\left(\frac{101.325\ kPa}{76\ cmHg}\right) = 9.80 \times 10^{-5} \frac{cm^3(STP)}{cm^2 \cdot s \cdot cmHg}$$

By convention, the standard gas permeance unit (GPU).

$$1\ GPU = 1 \times 10^{-6} \frac{cm^3(STP)}{cm^2 \cdot s \cdot cmHg}$$

Therefore,

$$Q = \mathbf{98.0\ GPU}$$

Ideal Selectivity Calculation

Under the same operating conditions, the permeance of nitrogen was found to be 0.6 GPU. Using the ratio between permeance of hydrogen and nitrogen, the ideal selectivity (α) could be determined.

$$\alpha_{H_2/N_2} = \frac{Q_{H_2}}{Q_{N_2}} = \frac{98.0\ GPU}{1.16\ GPU} = \mathbf{84.0} \quad \text{(B-4)}$$

B.2 Activation Energy Calculations

The following calculations were conducted for a pristine membrane module that contained 6 strands of hollow fibres at a length of 5.2cm and a diameter 0.02cm. The test gas was pure hydrogen. As stated in Chapter 2, the change in permeance as a function of temperature can be described using the Arrhenius equation.

$$Q = Q_0 \exp(-E_p/R_G T) \quad \text{(B-5)}$$

where Q_0 is the pre-exponential factor of permeation, E_P is the activation energy of permeation and R_G is the gas constant. Linearizing the above equation,

$$\ln Q = \left(-\frac{E_P}{R_G}\right)\left(\frac{1}{T}\right) + \ln(Q_0) \quad \text{(B-6)}$$

By plotting lnQ versus 1/T, the slope of the linearized Arrhenius plot can be determined using linear regression.

Table B.1: Permeance data for hydrogen at 500kPa.

Temperature [K]	1000/T [1/K]	Permeance [GPU]	ln[Q]
303	3.30	104	4.65
308	3.25	112	4.72
313	3.19	123	4.82
318	3.14	142	4.96
323	3.10	150	5.01

$$slope\text{:}\ \frac{E_P}{R_G} = 1.88 \times 10^3 K$$

$$\left(\frac{E_P}{R_G}\right)(R_G) = (1.88 \times 10^3 K)\left(8.3145 \frac{J}{mol \cdot K}\right) = \mathbf{15.6}\,\boldsymbol{\frac{kJ}{mol}}$$

B.3 Resistance Model Calculations

The following calculations were conducted for a membrane module contaminated with motor oil. The test gas was pure hydrogen at a gauge pressure of 1500kPa at 300K. The permeance of hydrogen through the contaminated membrane was 45.4 GPU. The effective membrane area was 1.96cm^2.

Percent Decrease in Performance

$$\%\ Decrease = \left(\frac{Initial - Final}{Initial}\right) \times 100\%$$

$$\%\ Decrease = \left(\frac{98.0\ GPU - 45.4\ GPU}{98.0\ GPU}\right) \times 100\% = \mathbf{53.7}\%$$

Resistance (R_1) of Contaminant Layer

In order to estimate the resistance of the lubricant (R_1) layer on the membrane surface, the total resistance of the contaminated membrane was determined.

$$R_{Total} = 1/(Q \cdot A) \tag{B-7}$$

$$R_{Total} = \frac{1}{(45.4GPU)(1.96\ cm^2)} = \frac{\left(\frac{22{,}414\ cm^3(STP)}{mol}\right)\left(\frac{101{,}325\ Pa}{76\ cmHg}\right)}{\left(4.54\ \times 10^{-5}\frac{cm^3(STP)}{cm^2 \cdot s \cdot cmHg}\right)(1.96 cm^2)}$$

$$R_{Total} = \mathbf{33.6 \times 10^{10}\ \frac{s \cdot Pa}{mol}}$$

Calculating the resistance of the same membrane module before contamination (R_2) with a permeance of 98.0 GPU, produces a resistance of 15.6x10^{10} s.Pa/mol. Using the resistance in series model described in Section 2.5, the value of R_1 can be determined from the change in the resistance after contamination.

$$R_{Total} = R_1 + R_2 \tag{B-8}$$

$$R_1 = R_{Total} - R_2$$

$$R_1 = (33.6 - 15.6) \times 10^{10}\ \frac{s \cdot Pa}{mol} = 18.0 \times 10^{10}\ \frac{s \cdot Pa}{mol}$$

Oil Permeance

The permeance through the lubricant can be determined from the estimated resistance of the lubricant, R_1.

$$Q_1 = 1/(R_1 A)$$

$$Q_1 = \frac{1}{(18.6 \times 10^{10}\ \frac{s \cdot Pa}{mol})(1.96\ cm^2)} = \frac{\left(\frac{22{,}414\ cm^3(STP)}{mol}\right)\left(\frac{101{,}325\ Pa}{76\ cmHg}\right)}{\left(18.6 \times 10^{10}\ \frac{s \cdot Pa}{mol}\right)(1.96 cm^2)}$$

$$Q_1 = 8.45 \times 10^{-5} \frac{cm^3(STP)}{cm^2 \cdot s \cdot cmHg}\left(\frac{1\ GPU}{1 \times 10^{-6} \frac{cm^3(STP)}{cm^2 \cdot s \cdot cmHg}}\right) = \mathbf{84.5\ GPU}$$

B.4 Diffusivity Estimation

The following calculations were conducted in order to estimate the diffusivity of hydrogen in Pennzoil® SAE 10W-30 Motor Oil. As mentioned in Section B.2, the change in diffusivity as a function of temperature can be described using the Arrhenius equation.

$$D = D_0 \exp\left(-\frac{E_A}{R_G T}\right) \tag{B-11}$$

where D_0 is the pre-exponential factor of diffusion and E_A is the activation energy of diffusion. Linearizing the above equation.

$$\ln D = \ln D_0 - \frac{E_A}{R_G}\left(\frac{1}{T}\right) \tag{B-12}$$

The values of D_0 and E_A/R_G can be estimated by calculating the slope of a line between two known data points on a plot of ln(D) versus 1/T. According to Rodden *et al.* (1988), the diffusion coefficients for H_2 in octacosane at 371K and 414K are 2.05×10^{-4} and 1.34×10^{-4} cm^2/s, respectively. The value of E_A/R_G was determined from.

$$-\frac{E_A}{R_G} = \frac{\ln\left(\frac{D_1}{D_2}\right)}{\left(\frac{1}{T_2}\right) - \left(\frac{1}{T_1}\right)} \tag{B-13}$$

$$-\frac{E_A}{R_G} = \frac{\ln\left(\frac{1.34 \times 10^{-4}\,\frac{cm^2}{s}}{2.05 \times 10^{-4}\,\frac{cm^2}{s}}\right)}{\left(\frac{1}{414K}\right) - \left(\frac{1}{371K}\right)} = -1.52 \times 10^3 K$$

The value of D_0 was obtained from:

$$D_0 = \frac{D_1}{\exp\left(-\frac{E_A}{R_G T_1}\right)} = \frac{\left(1.34 \times 10^{-4}\,\frac{cm^2}{s}\right)}{\exp\left(\frac{1.52 \times 10^3 K}{317K}\right)} = 8.03 \times 10^{-3}\,\frac{cm^2}{s}$$

Substituting the values of E_A/R_G and D_0 into Equation B-11, the diffusion coefficient at the desired temperatures could be obtained. For 300K, the diffusion coefficient of hydrogen in oil was found to be **5.09×10^{-5} cm^2/s**. The diffusion coefficients of CO_2 and H_2 at 300 and 323K are determined to be:

Table B.2: Diffusion coefficients, D $\times 10^5$ cm^2/s

Temperature [K]	**CO_2**	**H_2**
300	1.24	5.09
323	1.88	7.29

B.5 Solubility Calculations

The Henry's Law constants of gases within the lubricant were estimated using ASTM D-3827 (see Section Appendix A). The solubility coefficient of a gas in the oil layer (S) was determined by using the following unit conversions:

$$S = \frac{1}{H} = 0.01528\left(\frac{1}{MPa}\right)\left(\frac{mol\ gas}{mol\ oil}\right)$$

$$S = 0.01528\left(\frac{1}{MPa}\right)\left(\frac{mol\ gas}{mol\ oil}\right)\left(\frac{MPa}{1000\ kPa}\right)\left(\frac{101.3\ kPa}{76\ cmHg}\right) = 0.01528\left(\frac{1}{cmHg}\right)\left(\frac{mol\ gas}{mol\ oil}\right)$$

$$S = 0.01528\left(\frac{22414\ cm^3(STP)}{mol\ gas}\right)\left(\frac{mol\ oil}{595\ g}\right)\left(\frac{0.872g}{cm^3}\right)$$

$$S = 6.69 \times 10^{-4}\,\frac{cm^3(STP)}{cm^3 \cdot cmHg}$$

The solubility coefficients of select gases were determined in a similar fashion, as shown in Table B-3.

Table B.3: Solubility coefficients, S $\times 10^4$ cm^3(STP)/cm^3·cmHg.

Temp.[K]	**N_2**	**CH_4**	**O_2**	**CO_2**	**H_2**	**He**
300	8.61	30.2	18.2	112	6.69	2.08
323	9.77	29.2	18.8	91.5	7.85	2.83

B.6 Thickness of the Contaminant Layer

The thickness (*l*) of the lubricant layer on the contaminated membrane was determined by using the permeance, diffusion and solubility of gases within the oil layer.

$$P = Q \cdot l = D \cdot S \tag{B-13}$$

$$l = \frac{D \cdot S}{Q} \tag{B-14}$$

$$l = \frac{\left(5.09 \times 10^{-5}\,\frac{cm^3}{s}\right)\left(6.69 \times 10^{-4}\,\frac{cm^3(STP)}{cm^3 \cdot cmHg}\right)}{\left(8.45 \times 10^{-5}\,\frac{cm^3(STP)}{cm^2 \cdot s \cdot cmHg}\right)} = 4.03 \times 10^{-6} cm = \mathbf{4.03\mu m}$$

Appendix C

Experimental Data

C.1 Testing parameters

The gas permeance of cellulose acetate membranes were tested at different temperatures (T) and pressures (P) under various treatment methods as shown in Table C.1. Treatments methods included lubricant contamination (L), solvent exchange remediation (S) and cyclohexane remediation (C). To assess the effects of pressure on the membrane performance, the operating temperature was held at 300K while the feed pressure was increased from 300kPa to 1500kPa gauge in intervals of 400kPa. To assess the effects of temperature on membrane performance, the pressure was held at 500kPa gauge while the operating temperature was increased from 303K to 323K in intervals of 5K.

Table C.1: Testing parameters.

	Module	**Treatments**	**Parameters**
Contamination – only	#1	L	P, T
Solvent exchange remediation	#2	L, S	P, T
	#3	L, S	P
	#4	S	P, T
	#5	S	P
Cyclohexane remediation	#6	L, C	P, T
	#7	L, C	P
	#8	C	P, T
	#9	C	P

C.2 Raw Permeation Data at Different Feed Pressures

Module: #1
Dimensions: 8 strands, 7.3cm long
Treatment: Lubricant contamination

Pristine membrane; operating temperature held at 300K

Gas	Differential Pressure [kPa]	Barometric Pressure [kPa]	Ambient Temp. [K]	Volume [mL]	Time [s]		Average Flux [cm^3(STP)/cm^2·s]	Permeance [GPU]
N_2	300	100.7	296	0.10	91.16	91.22	2.67×10^{-4}	1.19
	700	100.6	296	0.20	80.03	79.91	6.08×10^{-4}	1.16
	1100	100.6	296	0.20	52.71	52.71	9.23×10^{-4}	1.12
	1500	100.6	296	0.20	39.43	39.31	1.23×10^{-3}	1.10
CH_4	300	100.6	296	0.10	106.88	104.75	2.30×10^{-4}	1.02
	700	100.6	296	0.20	84.97	85.60	5.70×10^{-4}	1.09
	1100	100.6	296	0.20	55.62	55.35	8.76×10^{-4}	1.06
	1500	100.7	296	0.20	42.28	42.15	1.15×10^{-3}	1.02
O_2	300	100.9	296	1.00	188.09	187.72	1.30×10^{-3}	5.77
	700	100.9	296	1.00	75.10	75.56	3.24×10^{-3}	6.16
	1100	100.9	296	1.00	46.60	46.62	5.23×10^{-3}	6.34
	1500	100.8	296	1.00	34.21	34.21	7.12×10^{-3}	6.33
CO_2	300	100.7	296	5.00	127.03	125.12	9.65×10^{-3}	42.9
	700	100.6	296	10.0	105.97	105.46	2.30×10^{-2}	43.8
	1100	100.5	296	10.0	65.66	65.54	3.70×10^{-2}	44.9
	1500	100.5	296	10.0	46.80	48.50	5.10×10^{-2}	45.3
H_2	300	100.8	296	10.0	111.50	113.43	2.17×10^{-2}	96.2
	700	100.9	296	10.0	47.81	48.62	5.05×10^{-2}	96.2
	1100	100.9	296	10.0	30.31	30.56	8.01×10^{-2}	97.1
	1500	100.9	296	10.0	21.89	22.51	1.10×10^{-1}	97.5
He	300	100.7	296	10.0	98.16	98.54	2.47×10^{-2}	110
	700	100.7	296	10.0	41.75	41.87	5.82×10^{-2}	111
	1100	100.7	296	10.0	26.75	26.69	9.10×10^{-2}	110
	1500	100.7	296	10.0	19.88	19.81	1.23×10^{-1}	109

Contaminated membrane; operating temperature held at 300K

Gas	Differential Pressure [kPa]	Barometric Pressure [kPa]	Ambient Temp. [K]	Volume [mL]	Time [s]		Average Flux [cm^3(STP)/cm^2·s]	Permeance [GPU]
N_2	300	101.3	296	0.05	63.00	62.00	1.96×10^{-4}	0.87
	700	101.3	296	0.10	53.53	52.29	4.63×10^{-4}	0.88
	1100	101.3	296	0.20	67.63	68.25	7.21×10^{-4}	0.87
	1500	101.3	296	0.20	49.72	49.53	9.87×10^{-4}	0.88
CH_4	300	101.3	296	0.05	64.22	64.66	1.90×10^{-4}	0.84
	700	101.2	296	0.10	51.16	52.16	4.73×10^{-4}	0.90
	1100	101.2	296	0.20	66.75	65.22	7.41×10^{-4}	0.90
	1500	101.2	296	0.20	49.50	49.22	9.90×10^{-4}	0.88
O_2	300	101.4	296	0.30	72.91	71.38	1.02×10^{-3}	4.52
	700	101.4	296	0.50	50.41	49.97	2.44×10^{-3}	4.65
	1100	101.4	296	1.00	64.88	64.06	3.80×10^{-3}	4.60
	1500	101.4	296	1.00	47.38	47.16	5.18×10^{-3}	4.60
CO_2	300	101.5	296	2.00	82.87	80.28	6.01×10^{-3}	26.7
	700	101.5	296	5.00	83.30	85.24	1.46×10^{-2}	27.7
	1100	101.5	296	5.00	51.77	53.81	2.32×10^{-2}	28.2
	1500	101.5	296	5.00	38.86	40.12	3.11×10^{-2}	27.6
H_2	300	101.4	296	2.00	58.28	57.98	8.43×10^{-3}	37.5
	700	101.4	296	5.00	58.71	60.28	2.06×10^{-2}	39.2
	1100	101.4	296	10.0	74.25	75.28	3.28×10^{-2}	39.7
	1500	101.4	296	10.0	54.94	56.03	4.41×10^{-2}	39.2
He	300	101.4	296	2.00	57.00	56.06	8.67×10^{-3}	38.5
	700	101.4	296	5.00	61.28	60.59	2.01×10^{-2}	38.3
	1100	101.4	296	5.00	37.55	37.69	3.26×10^{-2}	39.5
	1500	101.4	296	10.0	55.69	55.65	4.40×10^{-2}	39.1

Selectivity of pristine and contaminated membranes

Pressure [kPa]	Pristine						Contaminated					
	CO_2/CH_4	CH_4/N_2	O_2/N_2	CO_2/N_2	H_2/N_2	He/N_2	CO_2/CH_4	CH_4/N_2	O_2/N_2	CO_2/N_2	H_2/N_2	He/N_2
300	42.4	0.85	4.87	36.2	81.2	92.8	31.7	0.97	5.20	30.7	43.0	44.3
700	40.2	0.94	5.32	37.8	83.1	95.7	30.7	1.02	5.27	31.5	44.5	43.4
1100	42.3	0.95	5.67	40.1	86.0	98.7	31.4	1.03	5.27	32.3	45.5	45.2
1500	44.3	0.93	5.77	41.3	88.9	99.2	31.4	1.00	5.25	31.5	44.7	44.6

% Decrease in permeance due to membrane contamination

Pressure [kPa]	N_2	CH_4	O_2	CO_2	H_2	He
300	26.5	16.5	21.5	37.7	61.1	65.0
700	23.9	17.3	24.6	36.7	59.3	65.4
1100	21.9	15.2	27.3	37.2	58.7	64.2
1500	20.1	13.9	27.2	39.1	59.8	64.1

Resistance values [10^{10} s·Pa/mol] of pristine and contaminated membranes to gas permeation

Pressure [kPa]	Pristine						Contaminated					
	N_2	CH_4	O_2	CO_2	H_2	He	N_2	CH_4	O_2	CO_2	H_2	He
300	669	784	137	18.5	8.24	7.21	911	940	175	29.7	21.2	20.6
700	684	727	129	18.1	8.23	7.15	899	879	171	28.6	20.2	20.7
1100	709	748	125	17.7	8.24	7.19	908	883	172	28.1	20.0	20.1
1500	722	775	125	17.5	8.12	7.28	904	901	172	28.7	20.2	20.3

Gas permeance [GPU] of the lubricant layer

Pressure [kPa]	N_2	CH_4	O_2	CO_2	H_2	He
300	3.32	5.17	21.3	71.8	62.1	60.1
700	3.74	5.29	19.1	76.5	67.1	59.3
1100	4.04	5.97	17.1	76.7	68.6	62.3
1500	4.42	6.40	17.1	71.6	66.5	61.9

Module: #2
Dimensions: 6 strands, 5.2cm long
Treatment: Lubricant contamination, solvent exchange remediation

Pristine membrane permselectivity

Pressure [kPa]	Permeance [GPU]						Selectivity					
	N_2	CH_4	O_2	CO_2	H_2	He	CO_2/CH_4	CH_4/N_2	O_2/N_2	CO_2/N_2	H_2/N_2	He/N_2
300	1.60	1.21	7.17	51.8	92.9	107	43.0	0.75	4.49	32.4	58.1	67.1
700	1.54	1.24	7.53	51.1	99.1	113	41.3	0.80	4.88	33.1	64.2	73.4
1100	1.52	1.23	7.47	51.6	98.9	115	41.9	0.81	4.93	34.1	65.3	75.9
1500	1.48	1.22	7.50	50.8	99.3	116	41.7	0.82	5.06	34.3	67.0	78.3

Contaminated membrane permselectivity

Pressure [kPa]	Permeance [GPU]						Selectivity					
	N_2	CH_4	O_2	CO_2	H_2	He	CO_2/CH_4	CH_4/N_2	O_2/N_2	CO_2/N_2	H_2/N_2	He/N_2
300	0.89	1.02	5.16	33.5	35.6	40.7	32.7	1.15	5.79	37.6	39.9	45.8
700	0.95	1.05	5.28	35.7	42.4	46.3	34.1	1.10	5.54	37.4	44.4	48.6
1100	0.97	1.00	5.35	35.3	44.4	47.2	35.4	1.03	5.54	36.5	45.9	48.9
1500	0.95	1.01	5.31	35.2	45.9	48.4	34.9	1.06	5.60	37.2	48.4	51.1

Remediated membrane permselectivity

Pressure [kPa]	Permeance [GPU]						Selectivity					
	N_2	CH_4	O_2	CO_2	H_2	He	CO_2/CH_4	CH_4/N_2	O_2/N_2	CO_2/N_2	H_2/N_2	He/N_2
300	0.96	1.06	3.67	15.4	42.4	44.9	14.6	1.10	3.81	16.0	44.0	46.7
700	0.96	1.05	3.73	15.0	42.6	46.2	14.3	1.10	3.90	15.7	44.6	48.4
1100	0.98	1.03	3.67	16.0	43.7	45.4	15.4	1.06	3.74	16.3	44.6	46.4
1500	1.01	1.04	3.68	16.1	44.6	46.7	15.5	1.03	3.65	16.0	44.3	46.4

% Decrease in permeance due to membrane contamination

Pressure [kPa]	N_2	CH_4	O_2	CO_2	H_2	He
300	44.3	15.0	28.1	35.3	61.7	62.0
700	38.2	15.4	29.8	30.2	57.3	59.1
1100	36.2	19.2	28.4	31.7	55.1	59.0
1500	36.0	17.4	29.2	30.7	53.8	58.2

% Decrease in permeance of the remediated membrane as compared to the pristine membrane

Pressure [kPa]	N_2	CH_4	O_2	CO_2	H_2	He
300	39.7	12.4	48.8	70.2	54.4	58.1
700	38.1	15.2	50.4	70.6	57.0	59.2
1100	35.3	16.1	50.9	69.0	55.8	60.5
1500	32.1	14.9	51.0	68.3	55.1	59.8

Resistance values [10^{10} s·Pa/mol] of pristine and contaminated membranes to gas permeation

Pressure [kPa]	Pristine						Contaminated					
	N_2	CH_4	O_2	CO_2	H_2	He	N_2	CH_4	O_2	CO_2	H_2	He
300	954	1265	213	29.4	16.4	14.2	1.71×10^3	1.49×10^3	296	45.5	42.9	37.4
700	987	1231	202	29.8	15.4	13.5	1.60×10^3	1.46×10^3	289	42.7	36.0	32.9
1100	1006	1236	204	29.5	15.4	13.2	1.58×10^3	1.53×10^3	285	43.2	34.3	32.3
1500	1029	1249	203	30.0	15.4	13.1	1.61×10^3	1.51×10^3	287	43.3	33.2	31.5

Gas permeance [GPU] in the lubricant layer

Pressure [kPa]	N_2	CH_4	O_2	CO_2	H_2	He
300	2.01	6.82	18.3	94.8	57.6	65.7
700	2.49	6.81	17.7	118	74.0	78.4
1100	2.67	5.18	18.8	111	80.6	80.1
1500	2.63	5.80	18.2	115	85.2	83.2

Module: #3
Dimensions: 8 strands, 6.5cm long
Treatment: Lubricant contamination, solvent exchange remediation

Pristine membrane permselectivity

Pressure [kPa]	Permeance [GPU]						Selectivity					
	N_2	CH_4	O_2	CO_2	H_2	He	CO_2/CH_4	CH_4/N_2	O_2/N_2	CO_2/N_2	H_2/N_2	He/N_2
300	1.31	1.32	7.13	50.3	100	116	38.1	1.01	5.44	38.4	76.4	88.7
700	1.35	1.36	7.54	50.9	99.6	116	37.4	1.01	5.59	37.7	73.8	85.7
1100	1.33	1.33	7.39	50.0	101	116	37.5	1.00	5.55	37.5	75.6	87.2
1500	1.33	1.31	7.38	52.1	101	116	39.8	0.99	5.56	39.3	76.3	87.7

Contaminated membrane permselectivity

Pressure [kPa]	Permeance [GPU]						Selectivity					
	N_2	CH_4	O_2	CO_2	H_2	He	CO_2/CH_4	CH_4/N_2	O_2/N_2	CO_2/N_2	H_2/N_2	He/N_2
300	1.07	1.16	5.51	32.0	52.7	51.0	27.5	1.09	5.16	30.0	49.4	47.8
700	1.05	1.17	5.42	32.4	53.3	50.1	27.7	1.12	5.18	31.0	50.9	47.9
1100	1.05	1.16	5.43	34.5	52.9	51.2	29.8	1.11	5.19	33.0	50.6	48.9
1500	1.04	1.14	5.44	37.3	52.4	50.2	32.7	1.10	5.25	36.0	50.6	48.5

Remediated membrane permselectivity

Pressure [kPa]	Permeance [GPU]						Selectivity					
	N_2	CH_4	O_2	CO_2	H_2	He	CO_2/CH_4	CH_4/N_2	O_2/N_2	CO_2/N_2	H_2/N_2	He/N_2
300	0.72	1.10	4.52	10.3	22.5	19.5	9.38	1.53	6.30	14.4	31.3	27.2
700	0.79	0.97	4.59	10.5	23.5	22.4	10.8	1.23	5.82	13.3	29.8	28.4
1100	0.76	0.98	4.58	11.2	24.7	22.1	11.5	1.30	6.07	14.9	32.7	29.2
1500	0.77	0.96	4.59	12.0	25.5	22.3	12.5	1.24	5.96	15.6	33.1	28.9

% Decrease in permeance due to membrane contamination

Pressure [kPa]	N_2	CH_4	O_2	CO_2	H_2	He
300	18.6	11.8	22.7	36.3	47.4	56.2
700	22.4	13.8	28.1	36.2	46.5	56.6
1100	21.5	13.1	26.6	31.0	47.5	56.0
1500	21.9	13.1	26.3	28.4	48.2	56.8

% Decrease in permeance of the remediated membrane as compared to the pristine membrane

Pressure [kPa]	N_2	CH_4	O_2	CO_2	H_2	He
300	45.2	16.42	36.5	79.4	77.6	83.2
700	41.5	28.4	39.1	79.3	76.4	80.6
1100	43.4	26.5	38.0	77.5	75.5	81.0
1500	41.9	26.9	37.8	77.0	74.7	80.8

Resistance values [10^{10} s·Pa/mol] of pristine and contaminated membranes to gas permeation

Pressure [kPa]	Pristine						Contaminated					
	N_2	CH_4	O_2	CO_2	H_2	He	N_2	CH_4	O_2	CO_2	H_2	He
300	697	693	128	18.2	9.13	7.86	857	786	166	28.5	17.3	17.9
700	678	673	121	18.0	9.19	7.91	874	781	169	28.2	17.2	18.2
1100	686	687	124	18.3	9.08	7.87	874	791	168	26.5	17.3	17.9
1500	689	697	124	17.5	9.04	7.86	883	802	168	24.5	17.4	18.2

Gas permeance [GPU] of the lubricant layer

Pressure [kPa]	N_2	CH_4	O_2	CO_2	H_2	He
300	5.73	9.89	24.3	88.2	111	90.8
700	4.67	8.48	19.3	89.6	115	88.5
1100	4.86	8.83	20.4	111	111	91.4
1500	4.72	8.70	20.7	131	109	88.3

Module: #4
Dimensions: 6 strands, 6.4cm long
Treatment: Solvent exchange remediation

Pristine membrane permselectivity

Pressure [kPa]	Permeance [GPU]						Selectivity					
	N_2	CH_4	O_2	CO_2	H_2	He	CO_2/CH_4	CH_4/N_2	O_2/N_2	CO_2/N_2	H_2/N_2	He/N_2
300	1.43	1.50	8.29	40.7	101	116	27.1	1.05	5.82	28.5	70.7	81.4
700	1.40	1.62	8.35	42.9	104	116	26.5	1.15	5.95	30.5	73.9	83.0
1100	1.42	1.58	8.39	43.5	105	118	27.5	1.12	5.92	30.7	74.3	83.6
1500	1.44	1.57	8.40	44.0	105	119	28.1	1.09	5.84	30.6	72.8	82.6

Remediated membrane permselectivity

Pressure [kPa]	Permeance [GPU]						Selectivity					
	N_2	CH_4	O_2	CO_2	H_2	He	CO_2/CH_4	CH_4/N_2	O_2/N_2	CO_2/N_2	H_2/N_2	He/N_2
300	1.05	1.10	5.17	28.8	43.1	49.0	26.1	1.05	4.91	27.3	40.9	46.5
700	1.08	1.17	5.29	31.0	46.3	51.7	26.5	1.08	4.89	28.7	42.9	47.8
1100	1.06	1.16	5.32	33.8	46.8	51.6	29.2	1.09	5.01	31.8	44.1	48.6
1500	1.06	1.15	5.27	34.9	46.9	51.5	30.3	1.09	4.99	33.1	44.5	48.9

% Decrease in permeance of the remediated membrane as compared to the pristine membrane

Pressure [kPa]	N_2	CH_4	O_2	CO_2	H_2	He
300	26.1	26.58	37.7	29.3	57.3	57.8
700	23.0	27.8	36.7	27.8	55.3	55.6
1100	25.1	27.0	36.6	22.3	55.6	56.5
1500	26.6	26.4	37.2	20.7	55.2	56.6

Module: #5
Dimensions: 6 strands, 4.6cm long
Treatment: Solvent exchange remediation

Pristine membrane permselectivity

Pressure [kPa]	Permeance [GPU]						Selectivity					
	N_2	CH_4	O_2	CO_2	H_2	He	CO_2/CH_4	CH_4/N_2	O_2/N_2	CO_2/N_2	H_2/N_2	He/N_2
300	1.33	1.54	8.63	50.3	109	113	32.6	1.16	6.49	37.9	81.8	84.8
700	1.29	1.56	8.56	51.4	102	113	32.9	1.22	6.66	40.0	79.4	88.2
1100	1.29	1.58	8.53	55.2	103	116	34.9	1.23	6.63	42.9	79.9	89.9
1500	1.27	1.58	8.42	54.9	106	115	34.8	1.24	6.64	43.3	83.9	90.3

Remediated membrane permselectivity

Pressure [kPa]	Permeance [GPU]						Selectivity					
	N_2	CH_4	O_2	CO_2	H_2	He	CO_2/CH_4	CH_4/N_2	O_2/N_2	CO_2/N_2	H_2/N_2	He/N_2
300	1.14	1.03	4.00	13.8	35.0	35.7	13.3	0.91	3.51	12.1	30.7	31.3
700	1.10	1.03	3.93	21.4	38.4	36.4	20.8	0.93	3.56	19.4	34.8	33.0
1100	1.07	1.03	3.93	23.7	38.8	36.3	23.0	0.97	3.69	22.2	36.4	34.1
1500	1.04	1.02	3.99	25.3	37.8	36.2	24.9	0.97	3.82	24.2	36.2	34.7

% Decrease in permeance of the remediated membrane as compared to the pristine membrane

Pressure [kPa]	N_2	CH_4	O_2	CO_2	H_2	He
300	14.2	33.1	53.6	72.6	67.8	68.3
700	14.1	34.3	54.1	58.3	62.4	67.9
1100	17.1	34.8	53.9	57.1	62.2	68.6
1500	17.7	35.5	52.6	53.9	64.5	68.4

Module: #6
Dimensions: 6 strands, 5.1cm long
Treatment: Lubricant contamination, cyclohexane remediation

Pristine membrane permselectivity

Pressure [kPa]	Permeance [GPU]						Selectivity					
	N_2	CH_4	O_2	CO_2	H_2	He	CO_2/CH_4	CH_4/N_2	O_2/N_2	CO_2/N_2	H_2/N_2	He/N_2
300	1.13	1.16	6.46	43.4	95.4	113	37.4	1.03	5.70	38.3	84.2	99.7
700	1.12	1.19	6.69	43.9	98.7	114	37.0	1.06	5.99	39.3	88.4	102
1100	1.10	1.17	6.66	46.3	102	116	39.6	1.06	6.03	41.9	92.1	105
1500	1.10	1.15	6.75	47.1	101	116	40.9	1.04	6.12	42.7	91.8	105

Contaminated membrane permselectivity

Pressure [kPa]	Permeance [GPU]						Selectivity					
	N_2	CH_4	O_2	CO_2	H_2	He	CO_2/CH_4	CH_4/N_2	O_2/N_2	CO_2/N_2	H_2/N_2	He/N_2
300	0.94	0.93	4.89	22.3	50.0	47.4	23.9	1.00	5.22	23.8	53.5	50.6
700	0.94	1.03	5.13	28.7	50.6	52.7	27.9	1.09	5.43	30.3	53.6	55.8
1100	0.97	1.08	5.20	32.4	52.2	55.0	30.1	1.11	5.36	33.4	53.7	56.7
1500	0.92	1.06	5.27	33.3	53.1	55.5	31.4	1.16	5.76	36.4	58.1	60.6

Remediated membrane permselectivity

Pressure [kPa]	Permeance [GPU]						Selectivity					
	N_2	CH_4	O_2	CO_2	H_2	He	CO_2/CH_4	CH_4/N_2	O_2/N_2	CO_2/N_2	H_2/N_2	He/N_2
300	1.32	1.25	7.13	44.9	97.1	113	35.8	0.95	5.41	34.1	73.7	86.0
700	1.88	1.33	7.61	47.6	101	121	35.7	0.71	4.05	25.3	53.8	64.5
1100	1.34	1.34	7.82	48.4	103	121	36.1	1.00	5.85	36.2	77.2	90.7
1500	1.29	1.31	7.82	52.0	103	122	39.6	1.02	6.05	40.2	79.8	94.2

% Decrease in permeance due to membrane contamination

Pressure [kPa]	N_2	CH_4	O_2	CO_2	H_2	He
300	17.4	19.7	24.3	48.7	47.6	58.1
700	15.4	13.3	23.3	34.7	48.7	53.5
1100	12.1	7.9	22.0	29.9	48.7	52.5
1500	17.1	8.0	21.9	29.3	47.5	52.3

% Decrease in permeance of the remediated membrane as compared to the pristine membrane

Pressure [kPa]	N_2	CH_4	O_2	CO_2	H_2	He
300	-16.2	-7.87	-10.3	-3.32	-1.73	-0.21
700	-68.2	-12.5	-13.6	-8.50	-2.45	-6.73
1100	-21.0	-14.8	-17.3	-4.59	-1.43	-4.78
1500	-17.2	-14.1	-15.9	-10.4	-1.96	-4.80

Resistance values [10^{10} s·Pa/mol] of pristine and contaminated membranes to gas permeation

Pressure [kPa]	Pristine						Contaminated					
	N_2	CH_4	O_2	CO_2	H_2	He	N_2	CH_4	O_2	CO_2	H_2	He
300	1.37×10^3	1.34×10^3	241	35.8	16.3	13.8	1.66×10^3	1.67×10^3	318	69.8	31.1	32.8
700	1.39×10^3	1.31×10^3	232	35.4	15.7	13.7	1.65×10^3	1.51×10^3	303	54.2	30.7	29.5
1100	1.41×10^3	1.33×10^3	233	33.6	15.3	13.4	1.60×10^3	1.45×10^3	299	47.9	29.8	28.3
1500	1.41×10^3	1.35×10^3	230	33.0	15.3	13.4	1.70×10^3	1.47×10^3	295	46.7	29.2	28.0

Gas permeance [GPU] of the lubricant layer

Pressure [kPa]	N_2	CH_4	O_2	CO_2	H_2	He
300	5.39	4.73	20.1	45.8	105	81.6
700	6.12	7.74	22.0	82.6	104	98.5
1100	8.04	13.59	23.7	108	107	105
1500	5.37	13.23	24.0	114	112	106

Module: #7
Dimensions: 6 strands, 4.9cm long
Treatment: Lubricant contamination, cyclohexane remediation

Pristine membrane permselectivity

Pressure [kPa]	Permeance [GPU]						Selectivity					
	N_2	CH_4	O_2	CO_2	H_2	He	CO_2/CH_4	CH_4/N_2	O_2/N_2	CO_2/N_2	H_2/N_2	He/N_2
300	1.40	1.39	7.43	47.5	97.9	116	34.1	0.99	5.30	33.9	69.8	82.5
700	1.41	1.49	7.64	48.0	96.3	112	32.3	1.05	5.41	33.9	68.1	79.4
1100	1.45	1.48	7.67	48.1	98.0	113	32.6	1.02	5.29	33.2	67.6	78.0
1500	1.46	1.41	7.59	50.2	101.6	116	35.5	0.97	5.21	34.4	69.7	79.4

Contaminated membrane permselectivity

Pressure [kPa]	Permeance [GPU]						Selectivity					
	N_2	CH_4	O_2	CO_2	H_2	He	CO_2/CH_4	CH_4/N_2	O_2/N_2	CO_2/N_2	H_2/N_2	He/N_2
300	1.17	1.25	6.14	38.9	57.9	56.5	31.1	1.07	5.23	33.2	49.3	48.1
700	1.14	1.33	5.63	37.8	57.5	58.3	28.4	1.17	4.94	33.2	50.4	51.1
1100	1.13	1.27	5.65	38.1	57.3	57.5	29.9	1.13	5.00	33.8	50.8	50.9
1500	1.10	1.22	5.68	39.3	58.1	58.4	32.1	1.11	5.15	35.6	52.7	53.0

Remediated membrane permselectivity

Pressure [kPa]	Permeance [GPU]						Selectivity					
	N_2	CH_4	O_2	CO_2	H_2	He	CO_2/CH_4	CH_4/N_2	O_2/N_2	CO_2/N_2	H_2/N_2	He/N_2
300	1.25	1.45	8.19	45.8	98.8	106	31.6	1.16	6.56	36.7	79.1	84.8
700	1.21	1.47	8.12	47.5	95.8	106	32.4	1.22	6.73	39.4	79.4	88.2
1100	1.21	1.48	8.09	49.9	96.4	109	33.6	1.23	6.70	41.3	79.9	89.9
1500	1.19	1.48	7.99	52.6	99.9	108	35.5	1.24	6.71	44.2	83.9	90.3

% Decrease in permeance due to membrane contamination

Pressure [kPa]	N_2	CH_4	O_2	CO_2	H_2	He
300	16.3	10.1	17.3	18.1	40.9	51.2
700	19.4	10.5	26.3	21.2	40.3	48.1
1100	22.2	13.7	26.4	20.8	41.5	49.2
1500	24.4	13.4	25.2	21.7	42.8	49.6

% Decrease in permeance of the remediated membrane as compared to the pristine membrane

Pressure [kPa]	N_2	CH_4	O_2	CO_2	H_2	He
300	11.0	-4.05	-10.3	3.60	-0.85	8.47
700	14.7	1.28	-6.31	0.89	0.59	5.16
1100	16.8	-0.41	-5.50	-3.74	1.62	4.08
1500	18.3	-4.78	-5.24	-4.77	1.71	7.09

Resistance values [10^{10} s·Pa/mol] of pristine and contaminated membranes to gas permeation

Pressure [kPa]	Pristine						Contaminated					
	N_2	CH_4	O_2	CO_2	H_2	He	N_2	CH_4	O_2	CO_2	H_2	He
300	1.15×10^3	1.16×10^3	218	34.0	16.5	14.0	1.38×10^3	1.29×10^3	263	41.5	28.0	28.6
700	1.14×10^3	1.09×10^3	212	33.7	16.8	14.4	1.42×10^3	1.22×10^3	287	42.8	28.1	27.8
1100	1.12×10^3	1.10×10^3	211	33.6	16.5	14.3	1.43×10^3	1.27×10^3	287	42.5	28.2	28.2
1500	1.11×10^3	1.15×10^3	213	32.2	15.9	14.0	1.47×10^3	1.32×10^3	285	41.2	27.8	27.7

Gas permeance [GPU] of the lubricant layer

Pressure [kPa]	N_2	CH_4	O_2	CO_2	H_2	He
300	7.22	12.4	35.6	215	141	110
700	5.87	12.7	21.4	179	143	121
1100	5.09	9.33	21.4	184	138	117
1500	4.52	9.13	22.6	181	136	118

Module: #8
Dimensions: 6 strands, 6.7cm long
Treatment: Cyclohexane remediation

Pristine membrane permselectivity

Pressure [kPa]	Permeance [GPU]						Selectivity					
	N_2	CH_4	O_2	CO_2	H_2	He	CO_2/CH_4	CH_4/N_2	O_2/N_2	CO_2/N_2	H_2/N_2	He/N_2
300	1.40	1.27	7.38	46.8	93.6	113	36.8	0.91	5.29	33.6	67.1	81.2
700	1.32	1.27	7.63	46.2	99.3	112	36.4	0.97	5.80	35.1	75.5	85.5
1100	1.34	1.28	7.72	45.4	99.3	114	35.5	0.96	5.77	34.0	74.2	85.6
1500	1.34	1.26	7.66	45.4	100	115	36.0	0.94	5.71	33.8	74.5	85.7

Remediated membrane permselectivity

Pressure [kPa]	Permeance [GPU]						Selectivity					
	N_2	CH_4	O_2	CO_2	H_2	He	CO_2/CH_4	CH_4/N_2	O_2/N_2	CO_2/N_2	H_2/N_2	He/N_2
300	1.36	1.44	7.66	38.9	99.5	111	27.1	1.05	5.62	28.5	73.0	81.4
700	1.34	1.55	7.86	41.0	99.1	113	26.5	1.15	5.86	30.5	73.9	84.2
1100	1.35	1.51	7.95	41.5	101	113	27.5	1.12	5.87	30.7	74.3	83.6
1500	1.37	1.50	7.97	42.3	98.7	113	28.3	1.09	5.80	30.8	71.8	82.0

% Decrease in permeance of the remediated membrane as compared to the pristine membrane

Pressure [kPa]	N_2	CH_4	O_2	CO_2	H_2	He
300	26.4	-15.5	-6.30	15.0	-8.92	-0.27
700	27.2	-19.4	-1.11	13.1	2.16	1.49
1100	22.5	-16.6	-1.67	9.66	-0.07	2.29
1500	21.4	-15.9	-1.53	8.91	3.63	4.28

Module: #9
Dimensions: 6 strands, 4.4cm long
Treatment: Cyclohexane remediation

Pristine membrane permselectivity

Pressure [kPa]	Permeance [GPU]						Selectivity					
	N_2	CH_4	O_2	CO_2	H_2	He	CO_2/CH_4	CH_4/N_2	O_2/N_2	CO_2/N_2	H_2/N_2	He/N_2
300	1.58	1.65	7.86	51.2	105	115	31.1	1.04	4.97	32.4	66.2	72.8
700	1.56	1.56	7.60	52.7	106	114	33.7	1.00	4.86	33.7	67.8	73.2
1100	1.57	1.56	7.54	52.5	106	117	33.6	0.99	4.80	33.4	67.5	74.1
1500	1.62	1.55	7.53	53.5	106	116	34.4	0.96	4.64	33.0	65.0	71.7

Remediated membrane permselectivity

Pressure [kPa]	Permeance [GPU]						Selectivity					
	N_2	CH_4	O_2	CO_2	H_2	He	CO_2/CH_4	CH_4/N_2	O_2/N_2	CO_2/N_2	H_2/N_2	He/N_2
300	1.48	1.65	8.22	58.6	106	127	35.4	1.11	5.55	39.5	71.7	85.9
700	1.55	1.64	8.38	60.4	107	131	36.9	1.06	5.41	39.0	69.3	84.3
1100	1.42	1.64	8.54	60.0	108	127	36.7	1.15	6.03	42.3	76.3	89.3
1500	1.48	1.64	8.55	62.6	109	130	38.2	1.11	5.79	42.4	74.0	88.2

% Decrease in permeance of the remediated membrane as compared to the pristine membrane

Pressure [kPa]	N_2	CH_4	O_2	CO_2	H_2	He
300	-14.1	-6.94	-11.6	-22.0	-8.26	-18.1
700	-9.44	-5.75	-11.4	-15.7	-2.24	-15.1
1100	-9.28	-15.9	-25.6	-26.7	-13.2	-20.5
1500	-11.0	-16.0	-25.0	-28.7	-13.7	-22.9

C.3 Raw Permeation Data at Different Operating Temperatures

Module: #1 **Dimensions:** 8 strands, 7.4cm long **Treatment:** Lubricant contamination
Pristine membrane; differential pressure held at 500kPa

Gas	Operating Temp. [K]	Barometric Pressure [kPa]	Ambient Temp. [K]	Volume [mL]	Time [s]		Average Flux [cm^3(STP)/cm^2·s]	Permeance [GPU]
N_2	303	103.2	296	0.20	112.00	113.47	4.48×10^{-4}	1.19
	308	103.1	296	0.20	90.69	91.03	5.56×10^{-4}	1.48
	313	102.9	296	0.20	76.40	74.97	6.66×10^{-4}	1.78
	318	102.9	296	0.20	63.50	63.31	7.94×10^{-4}	2.12
	323	102.9	296	0.20	56.22	56.28	8.96×10^{-4}	2.39
CH_4	303	102.3	296	0.20	91.07	95.07	5.38×10^{-4}	1.44
	308	102.3	296	0.20	78.50	77.47	6.43×10^{-4}	1.71
	313	102.3	296	0.20	68.41	68.35	7.33×10^{-4}	1.95
	318	102.3	296	0.20	61.37	61.32	8.17×10^{-4}	2.18
	323	102.3	296	0.20	51.87	51.84	9.66×10^{-4}	2.58
O_2	303	100.8	296	1.00	90.03	90.03	2.74×10^{-3}	7.31
	308	100.9	296	1.00	78.84	78.59	3.14×10^{-3}	8.37
	313	101.0	296	1.00	70.62	70.37	3.51×10^{-3}	9.35
	318	101.1	296	1.00	61.58	62.50	3.99×10^{-3}	10.6
	323	101.1	296	1.00	56.22	56.38	4.40×10^{-3}	11.7
CO_2	303	102.8	296	5.00	86.92	87.19	1.45×10^{-2}	38.5
	308	102.8	296	5.00	78.88	79.00	1.59×10^{-2}	42.5
	313	102.8	296	5.00	71.65	71.38	1.76×10^{-2}	46.9
	318	102.7	296	5.00	69.94	69.62	1.80×10^{-2}	48.0
	323	102.7	296	5.00	65.69	65.06	1.92×10^{-2}	51.3
H_2	303	102.2	296	10.0	70.56	70.25	3.56×10^{-2}	94.8
	308	102.2	296	10.0	59.38	59.28	4.22×10^{-2}	112
	313	102.2	296	10.0	53.97	53.91	4.64×10^{-2}	124
	318	102.3	296	10.0	50.19	49.15	5.04×10^{-2}	134
	323	102.2	296	10.0	46.31	46.94	5.37×10^{-2}	143
He	303	100.4	296	10.0	56.56	56.41	4.35×10^{-2}	116
	308	100.4	296	10.0	51.31	50.93	4.81×10^{-2}	128
	313	100.4	296	10.0	47.37	46.96	5.21×10^{-2}	139
	318	100.5	296	10.0	42.67	42.53	5.77×10^{-2}	154
	323	100.5	296	10.0	43.04	43.28	5.70×10^{-2}	152

Contaminated membrane; differential pressure held at 500kPa

Gas	Operating Temp. [kPa]	Barometric Pressure [kPa]	Ambient Temp. [K]	Volume [mL]	Time [s]		Average Flux [cm^3(STP)/cm^2·s]	Permeance [GPU]
N_2	303	101.3	296	0.10	84.60	83.66	2.95×10^{-4}	0.79
	308	101.4	296	0.10	68.18	67.62	3.66×10^{-4}	0.97
	313	101.4	296	0.20	115.53	114.22	4.32×10^{-4}	1.15
	318	101.5	296	0.20	104.22	106.09	4.72×10^{-4}	1.26
	323	101.5	296	0.20	84.53	83.25	5.92×10^{-4}	1.58
CH_4	303	101.6	296	0.10	74.12	73.78	3.36×10^{-4}	0.90
	308	101.6	296	0.10	60.97	61.06	4.08×10^{-4}	1.09
	313	101.7	296	0.10	47.06	47.93	5.24×10^{-4}	1.40
	318	101.7	296	0.20	82.91	83.32	5.99×10^{-4}	1.60
	323	101.7	296	0.20	71.03	71.85	6.97×10^{-4}	1.86
O_2	303	101.2	296	0.50	78.85	79.25	1.57×10^{-3}	4.18
	308	101.2	296	0.50	66.03	65.85	1.88×10^{-3}	5.01
	313	101.2	296	0.50	57.50	57.06	2.16×10^{-3}	5.77
	318	101.2	296	0.50	51.90	51.31	2.40×10^{-3}	6.40
	323	101.2	296	0.50	46.37	46.37	2.67×10^{-3}	7.13
CO_2	303	101.2	296	2.00	63.10	62.44	7.90×10^{-3}	21.1
	308	101.3	296	2.00	56.06	56.28	8.83×10^{-3}	23.6
	313	101.3	296	2.00	50.11	49.75	9.94×10^{-3}	26.5
	318	101.3	296	3.00	66.97	66.03	1.12×10^{-2}	29.8
	323	101.3	296	3.00	62.65	62.47	1.19×10^{-2}	31.7
H_2	303	100.8	296	5.00	89.87	89.47	1.38×10^{-2}	36.7
	308	100.8	296	5.00	77.53	76.94	1.60×10^{-2}	42.6
	313	100.8	296	5.00	67.37	66.66	1.84×10^{-2}	49.1
	318	100.7	296	5.00	59.09	58.72	2.09×10^{-2}	55.8
	323	100.7	296	5.00	53.28	53.24	2.32×10^{-2}	61.7
He	303	101.4	296	3.00	57.06	66.41	1.21×10^{-2}	32.2
	308	101.3	296	3.00	48.03	48.15	1.55×10^{-2}	41.3
	313	101.3	296	3.00	42.50	42.94	1.74×10^{-2}	46.5
	318	101.3	296	3.00	37.63	37.60	1.98×10^{-2}	52.7
	323	101.3	296	3.00	34.31	34.25	2.17×10^{-2}	57.9

Selectivity of pristine and contaminated membranes

Temp. [K]	Pristine						Contaminated					
	CO_2/CH_4	CH_4/N_2	O_2/N_2	CO_2/N_2	H_2/N_2	He/N_2	CO_2/CH_4	CH_4/N_2	O_2/N_2	CO_2/N_2	H_2/N_2	He/N_2
303	26.8	1.20	6.12	32.3	79.3	97.1	23.5	1.14	5.31	26.8	46.7	41.1
308	24.8	1.16	5.65	28.7	75.9	86.5	21.7	1.12	5.14	24.2	43.7	42.3
313	24.0	1.10	5.27	26.4	69.7	78.3	19.0	1.21	5.00	23.0	42.6	40.3
318	22.1	1.03	5.02	22.7	63.5	72.7	18.7	1.27	5.08	23.7	44.3	41.9
323	19.9	1.08	4.91	21.5	59.9	63.7	17.1	1.18	4.51	20.1	39.1	36.6

Activation energy of permeation [kJ/mol]

Measurement	N_2	CH_4	O_2	CO_2	H_2	He
Pristine	28.4	22.9	19.3	11.3	16.4	11.8
Contaminated	26.9	30.0	21.4	17.2	21.3	23.2

% Decrease in permeance due to membrane contamination

Temp. [K]	N_2	CH_4	O_2	CO_2	H_2	He
303	34.2	37.5	42.8	45.4	61.3	72.3
308	34.2	36.5	40.1	44.6	62.1	67.8
313	35.1	28.5	38.3	43.5	60.3	66.6
318	40.5	26.7	39.8	37.9	58.5	65.7
323	33.9	27.8	39.2	38.1	56.9	61.9

Resistance values [10^{10} s·Pa/mol] of pristine and contaminated membranes to gas permeation

Temp. [K]	Pristine						Contaminated					
	N_2	CH_4	O_2	CO_2	H_2	He	N_2	CH_4	O_2	CO_2	H_2	He
303	672	560	110	20.8	8.47	6.92	1.02×10^3	896	192	38.2	21.9	25.0
308	542	469	96.0	18.9	7.14	6.27	824	739	160	34.1	18.9	19.5
313	453	411	85.9	17.1	6.49	5.78	697	575	139	30.3	16.4	17.3
318	379	369	75.5	16.7	5.98	5.22	638	503	125	26.9	14.4	15.2
323	336	312	68.5	15.7	5.61	5.28	509	432	113	25.3	13.0	13.9

Gas permeance [GPU] of the lubricant layer

Temp. [K]	N_2	CH_4	O_2	CO_2	H_2	He
303	2.30	2.39	9.76	46.4	59.9	44.5
308	2.85	2.98	12.5	52.8	68.6	60.9
313	3.29	4.91	15.0	60.9	81.4	69.8
318	3.11	5.99	16.1	78.8	95.5	80.2
323	4.66	6.68	18.2	83.3	109	93.4

Module: #2
Dimensions: 6 strands, 5.2cm long
Treatment: Lubricant contamination, solvent exchange remediation

Pristine membrane permselectivity

Temp. [K]	Permeance [GPU]						Selectivity					
	N_2	CH_4	O_2	CO_2	H_2	He	CO_2/CH_4	CH_4/N_2	O_2/N_2	CO_2/N_2	H_2/N_2	He/N_2
303	1.69	1.58	9.89	44.5	106	125	28.1	0.94	5.86	26.3	63.0	73.9
308	2.03	1.94	10.95	48.2	117	137	24.8	0.96	5.39	23.7	57.4	67.7
313	2.40	2.27	12.2	52.1	130	153	23.0	0.94	5.07	21.7	54.1	63.6
318	2.90	2.72	14.2	57.2	150	164	21.0	0.94	4.87	19.7	51.8	56.4
323	3.16	3.27	15.4	62.2	164	177	19.0	1.03	4.88	19.7	51.8	56.0

Contaminated membrane permselectivity

Temp. [K]	Permeance [GPU]						Selectivity					
	N_2	CH_4	O_2	CO_2	H_2	He	CO_2/CH_4	CH_4/N_2	O_2/N_2	CO_2/N_2	H_2/N_2	He/N_2
303	1.19	1.40	5.14	30.2	53.4	56.6	21.6	1.17	4.31	25.3	44.8	47.4
308	1.38	1.41	6.21	32.3	60.2	65.6	22.8	1.02	4.49	23.3	43.5	47.4
313	1.64	1.82	7.55	34.9	67.3	72.5	19.1	1.11	4.61	21.3	41.1	44.3
318	1.96	2.19	8.98	37.8	78.5	80.1	17.3	1.12	4.58	19.3	40.0	40.8
323	2.23	2.52	9.95	41.9	86.7	89.7	16.6	1.13	4.46	18.8	38.8	40.2

Remediated membrane permselectivity

Temp. [K]	Permeance [GPU]						Selectivity					
	N_2	CH_4	O_2	CO_2	H_2	He	CO_2/CH_4	CH_4/N_2	O_2/N_2	CO_2/N_2	H_2/N_2	He/N_2
303	1.00	1.00	4.56	14.3	44.7	45.4	14.4	0.99	4.55	14.3	44.6	45.2
308	1.15	1.26	4.94	16.2	47.4	49.8	12.9	1.10	4.31	14.2	41.4	43.5
313	1.37	1.47	5.45	17.3	50.3	52.7	11.8	1.07	3.98	12.7	36.7	38.4
318	1.66	1.87	6.37	19.5	52.1	55.4	10.4	1.13	3.83	11.7	31.3	33.3
323	1.87	2.30	6.83	20.9	54.6	59.2	9.10	1.23	3.65	11.2	29.2	31.6

Activation energy of permeation [kJ/mol]

Measurement	N_2	CH_4	O_2	CO_2	H_2	He
Pristine	26.1	29.2	18.7	13.7	18.1	14.3
Contaminated	26.4	26.8	28.1	13.2	19.9	18.4
Remediated	26.1	33.5	17.6	15.9	8.13	10.4

% Decrease in permeance due to membrane contamination

Temp. [K]	N_2	CH_4	O_2	CO_2	H_2	He
303	29.4	11.6	48.0	32.1	49.8	54.7
308	31.8	27.3	43.2	33.0	48.3	52.3
313	31.9	19.7	38.1	33.1	48.2	52.5
318	32.4	19.5	36.5	33.9	47.8	51.1
323	29.5	23.0	35.6	32.6	47.2	49.4

% Decrease in permeance of the remediated membrane as compared to the pristine membrane

Temp. [K]	N_2	CH_4	O_2	CO_2	H_2	He
303	40.7	36.9	53.9	67.8	58.0	63.7
308	43.6	35.0	54.9	66.3	59.3	63.8
313	42.9	35.2	55.3	66.7	61.3	65.5
318	42.8	31.1	55.0	65.9	65.3	66.1
323	40.9	29.9	55.8	66.4	66.7	66.6

Resistance values [10^{10} s·Pa/mol] of pristine and contaminated membranes to gas permeation

Temp. [K]	Pristine						Contaminated					
	N_2	CH_4	O_2	CO_2	H_2	He	N_2	CH_4	O_2	CO_2	H_2	He
303	902	964	154	34.3	14.3	12.2	375	127	142	16.2	14.2	14.7
308	751	785	139	31.6	13.1	11.1	351	295	106	15.6	12.2	12.1
313	635	672	125	29.3	11.7	9.98	297	165	76.9	14.5	10.9	11.0
318	525	561	108	26.6	10.1	9.31	252	135	62.0	13.7	9.27	9.73
323	482	465	98.7	24.5	9.30	8.60	201	139	54.6	11.8	8.29	8.40

Gas permeance [GPU] of the lubricant layer

Temp. [K]	N_2	CH_4	O_2	CO_2	H_2	He
303	4.06	12.0	10.7	94.1	107	104
308	4.35	5.17	14.4	97.7	125	126
313	5.13	9.24	19.8	105	139	138
318	6.05	11.3	24.6	111	164	157
323	7.58	10.9	27.9	129	184	181

Module: #4
Dimensions: 6 strands, 6.4cm long
Treatment: Solvent exchange remediation

Pristine membrane permselectivity

Temp. [K]	Permeance [GPU]						Selectivity					
	N_2	CH_4	O_2	CO_2	H_2	He	CO_2/CH_4	CH_4/N_2	O_2/N_2	CO_2/N_2	H_2/N_2	He/N_2
303	1.77	2.12	8.46	44.0	108	118	20.8	1.19	4.77	24.8	61.2	66.8
308	2.05	2.38	10.1	46.9	118	130	19.7	1.16	4.95	22.9	57.5	63.5
313	2.45	2.86	11.6	51.1	131	142	17.8	1.17	4.74	20.9	53.7	57.9
318	2.90	3.31	13.4	54.6	142	153	16.5	1.14	4.64	18.9	49.2	53.0
323	3.43	3.69	14.1	59.2	158	163	16.1	1.07	4.10	17.2	46.0	47.6

Remediated membrane permselectivity

Temp. [K]	Permeance [GPU]						Selectivity					
	N_2	CH_4	O_2	CO_2	H_2	He	CO_2/CH_4	CH_4/N_2	O_2/N_2	CO_2/N_2	H_2/N_2	He/N_2
303	1.51	1.40	6.73	32.0	57.7	56.5	22.9	0.92	4.45	21.1	38.2	37.3
308	1.76	1.78	7.66	35.2	64.3	62.3	19.8	1.01	4.36	20.1	36.6	35.5
313	1.97	1.91	8.63	36.4	71.0	68.5	19.0	0.97	4.38	18.5	36.0	34.8
318	2.30	2.33	9.59	39.6	79.0	75.7	17.0	1.01	4.17	17.2	34.4	33.0
323	2.56	2.78	10.7	41.9	90.3	82.0	15.1	1.08	4.16	16.4	35.2	32.0

Activation energy of permeation [kJ/mol]

Measurement	N_2	CH_4	O_2	CO_2	H_2	He
Pristine	27.2	23.5	20.9	12.12	15.3	13.2
Remediated	21.6	26.8	18.7	10.64	17.9	15.3

% Decrease in permeance of the remediated membrane as compared to the pristine membrane

Temp. [K]	N_2	CH_4	O_2	CO_2	H_2	He
303	14.7	34.0	20.5	27.3	46.8	52.3
308	14.2	25.5	24.4	24.9	45.4	52.1
313	19.5	33.1	25.7	28.7	46.0	51.7
318	20.6	29.8	28.6	27.6	44.5	50.6
323	25.4	24.7	24.2	29.1	42.8	49.8

Module: #6
Dimensions: 6 strands, 5.1cm long
Treatment: Lubricant contamination, cyclohexane remediation

Pristine membrane permselectivity

Temp. [K]	Permeance [GPU]						Selectivity					
	N_2	CH_4	O_2	CO_2	H_2	He	CO_2/CH_4	CH_4/N_2	O_2/N_2	CO_2/N_2	H_2/N_2	He/N_2
303	1.48	1.45	9.13	48.3	102	118	33.2	0.98	6.18	32.7	68.9	79.5
308	1.74	1.70	10.2	51.5	110	131	30.2	0.98	5.86	29.7	63.4	75.2
313	2.13	2.16	11.5	56.2	125	153	26.1	1.01	5.39	26.3	58.8	71.6
318	2.43	2.70	12.7	62.5	146	164	23.1	1.11	5.22	25.7	60.0	67.5
323	2.81	3.01	14.0	64.0	156	160	21.2	1.07	4.99	22.7	55.6	56.8

Contaminated membrane permselectivity

Temp. [K]	Permeance [GPU]						Selectivity					
	N_2	CH_4	O_2	CO_2	H_2	He	CO_2/CH_4	CH_4/N_2	O_2/N_2	CO_2/N_2	H_2/N_2	He/N_2
303	0.83	1.11	5.15	22.2	53.2	54.6	20.1	1.33	6.20	26.8	64.0	65.6
308	1.07	1.43	6.24	28.2	59.7	62.1	19.8	1.34	5.84	26.4	55.9	58.2
313	1.37	1.76	7.68	30.8	66.4	70.1	17.5	1.28	5.59	22.4	48.3	51.0
318	1.66	2.20	8.65	35.8	75.1	79.6	16.3	1.33	5.22	21.6	45.3	48.0
323	1.87	2.49	9.35	36.5	79.8	81.7	14.6	1.34	5.01	19.6	42.8	43.8

Remediated membrane permselectivity

Temp. [K]	Permeance [GPU]						Selectivity					
	N_2	CH_4	O_2	CO_2	H_2	He	CO_2/CH_4	CH_4/N_2	O_2/N_2	CO_2/N_2	H_2/N_2	He/N_2
303	1.53	1.66	9.29	46.4	108	111	28.0	1.09	6.09	30.4	70.9	72.8
308	1.91	2.39	10.4	51.0	124	128	21.3	1.25	5.44	26.7	64.9	67.1
313	2.21	2.53	11.6	55.6	136	140	22.0	1.15	5.26	25.2	61.6	63.5
318	2.64	2.74	13.6	59.7	151	155	21.8	1.04	5.15	22.6	57.1	58.5
323	3.09	3.36	14.7	63.4	162	165	18.9	1.09	4.77	20.5	52.3	53.5

Activation energy of permeation [kJ/mol]

Measurement	N_2	CH_4	O_2	CO_2	H_2	He
Pristine	26.4	31.2	17.6	12.32	18.6	13.7
Contaminated	33.6	34.2	25.0	19.8	17.0	17.0
Remediated	28.3	26.7	19.4	12.7	16.5	16.1

% Decrease in permeance due to membrane contamination

Temp. [K]	N_2	CH_4	O_2	CO_2	H_2	He
303	43.8	24.0	43.6	53.9	47.7	53.6
308	38.6	16.25	38.7	45.2	45.8	52.5
313	35.6	18.3	33.2	45.2	47.0	54.1
318	31.8	18.7	31.8	42.8	48.5	51.5
323	33.7	17.2	33.3	42.9	49.0	48.8

% Decrease in permeance of the remediated membrane as compared to the pristine membrane

Temp. [K]	N_2	CH_4	O_2	CO_2	H_2	He
303	-3.23	-14.2	-1.74	3.80	-6.36	5.46
308	-9.78	-40.3	-1.88	0.99	-12.5	2.05
313	-3.39	-17.2	-0.87	1.00	-8.34	8.30
318	-8.76	-1.47	-7.27	4.46	-3.35	5.76
323	-9.86	-11.5	-4.94	0.88	-3.36	-3.65

Resistance values [10^{10} s·Pa/mol] of pristine and contaminated membranes to gas permeation

Temp. [K]	Pristine						Contaminated					
	N_2	CH_4	O_2	CO_2	H_2	He	N_2	CH_4	O_2	CO_2	H_2	He
303	1.05×10^3	1.07×10^3	170	32.2	15.3	13.2	819	337	132	37.7	13.9	15.3
308	895	912	153	30.2	14.1	11.9	562	177	96.5	24.9	11.9	13.1
313	729	721	135	27.7	12.4	10.2	403	162	67.2	22.9	11.0	12.0
318	640	575	123	24.9	10.7	9.48	298	133	57.1	18.6	10.0	10.1
323	553	516	111	24.3	9.94	9.74	281	107	55.4	18.2	9.53	9.29

Gas permeance [GPU] of the lubricant layer

Temp. [K]	N_2	CH_4	O_2	CO_2	H_2	He
303	1.90	4.62	11.8	41.2	112	102
308	2.77	8.78	16.1	62.4	130	118
313	3.86	9.62	23.1	68.0	141	130
318	5.22	11.7	27.2	83.6	155	155
323	5.54	14.5	28.1	85.2	163	167

Module: #8
Dimensions: 6 strands, 6.7cm long
Treatment: Cyclohexane remediation

Pristine membrane permselectivity

Temp. [K]	Permeance [GPU]						Selectivity					
	N_2	CH_4	O_2	CO_2	H_2	He	CO_2/CH_4	CH_4/N_2	O_2/N_2	CO_2/N_2	H_2/N_2	He/N_2
303	1.78	1.62	9.35	38.6	109	123	23.8	0.91	5.25	21.7	61.4	69.0
308	2.01	2.00	10.5	42.0	117	133	21.0	1.00	5.19	20.9	58.1	65.9
313	2.25	2.27	11.2	44.6	131	140	19.6	1.01	4.96	19.8	58.4	62.5
318	2.71	2.73	12.5	49.0	142	143	17.9	1.01	4.60	18.1	52.3	52.8
323	2.94	3.19	13.6	52.3	148	172	16.4	1.08	4.62	17.8	50.4	58.4

Remediated membrane permselectivity

Temp. [K]	Permeance [GPU]						Selectivity					
	N_2	CH_4	O_2	CO_2	H_2	He	CO_2/CH_4	CH_4/N_2	O_2/N_2	CO_2/N_2	H_2/N_2	He/N_2
303	1.69	2.02	8.08	42.0	104	113	20.8	1.19	4.77	24.8	61.2	66.8
308	1.96	2.28	9.68	44.8	112	124	19.7	1.16	4.95	22.9	57.5	63.5
313	2.34	2.74	11.1	48.8	126	135	17.8	1.17	4.74	20.9	53.7	57.9
318	2.77	3.17	12.8	52.2	136	147	16.5	1.14	4.64	18.9	49.2	53.0
323	3.28	3.52	13.4	56.5	150	156	16.1	1.07	4.10	17.2	45.7	47.6

Activation energy of permeation [kJ/mol]

Measurement	N_2	CH_4	O_2	CO_2	H_2	He
Pristine	20.9	27.1	15.3	12.6	13.0	12.3
Remediated	27.2	23.5	21.2	12.1	15.2	13.2

% Decrease in permeance of the remediated membrane as compared to the pristine membrane

Temp. [K]	N_2	CH_4	O_2	CO_2	H_2	He
303	4.98	-24.7	13.6	-8.75	5.20	8.08
308	2.86	-13.5	7.42	-6.63	3.95	6.41
313	-4.10	-20.3	0.55	-9.47	4.26	3.59
318	-2.16	-15.8	-3.07	-6.61	3.95	-2.59
323	-11.6	-10.4	1.07	-8.07	-1.37	9.08